SEDIMENTOLOGY AND STRATIGRAPHY OF THE NANUSHUK FORMATION AND RELATED FORELAND BASIN DEPOSITS, CENTRAL BROOKS RANGE FOOTHILLS, ALASKA

By

Grant Shimer

RECOMMENDED:

_____
Dr. Catherine Hanks

_____
Dr. Michael Whalen

_____
Dr. Paul Layer

_____
Mr. Marwan Wartes

_____
Dr. Paul McCarthy
Advisory Committee Chair

_____
Dr. Paul McCarthy
Chair, Department of Geology and Geophysics

APPROVED:

_____
Dr. Paul Layer
Dean, College of Natural Science and Mathematics

_____
Dr. John Eichelberger
Dean of the Graduate School

_____
Date

SEDIMENTOLOGY AND STRATIGRAPHY OF THE NANUSHUK FORMATION AND RELATED FORELAND BASIN DEPOSITS, CENTRAL BROOKS RANGE FOOTHILLS, ALASKA

A
DISSERTATION

Presented to the Faculty
of the University of Alaska Fairbanks

in Partial Fulfillment of the Requirements
for the Degree of

DOCTOR OF PHILOSOPHY

By
Grant Shimer, B.A., M.S.

Fairbanks, Alaska

August 2013

Abstract

I interpret sedimentary facies and depositional environments from the Albian-Cenomanian Nanushuk Formation of Alaska's North Slope from sedimentary structures observed in core samples and in outcrop in the National Petroleum Reserve – Alaska (NPRA) and surrounding areas, and support these interpretations with supplemental analyses of geophysical well logs and $^{40}Ar/^{39}Ar$ dating of volcanogenic deposits. The results have implications for the reservoir characterization of a shallow, frozen oil field at Umiat, Alaska, and for interpretations of the Colville foreland basin.

In the central Brooks Range foothills the Nanushuk Formation comprises shallow marine and non-marine facies associations that can be grouped into marine-distributive and river-distributive systems. In wells at Umiat, Alaska, shoreface and wave-influenced deltaic sandstones (marine-distributive systems) occur at the base of the Nanushuk Formation, followed by a marine transgression and subsequent progradation of a delta complex (river-distributive system).

The shift from marine-distributive to river-distributive systems is related to shelf building processes during the Albian-Cenomanian. Marine-distributive systems occurred at or near the shelf edge in a high-energy coastal environment, whereas river-distributive systems rapidly prograded over the shallow Nanushuk shelf following transgression. Marine-distributive conditions resumed when rapidly progradational river-distributive systems reached the shelf edge. This pattern occurs in the Umiat, Wolf Creek, and Grandstand No. 1 subsurface wells.

The reservoir quality of the Nanushuk Formation varies strongly with facies. Well-sorted sandstones at the top of upward-coarsening successions in both marine- and river-distributive units have the highest permeabilities within the Nanushuk Formation. Marine-distributive units have low permeability anisotropy in contrast to river-distributive units due to better sorting in wave-influenced environments and the higher frequency of impermeable lamination surfaces in deltaic sandstones. Despite coarser

grain size and similar depositional environments as lower Nanushuk Formation sandstones, transgressive units at the top of the Nanushuk Formation have low permeability, probably due to the presence of calcite cement. These results suggest hat the highest quality Nanushuk Formation reservoirs most likely occur in time-transgressive, regionally extensive marine-distributive sandstones of the lower Nanushuk Formation.

Table of Contents

Page

Page

Page

Page

Page

List of Figures

Page

Page

List of Tables

Page

Acknowledgements

I received financial and logistical support from U.S. Department of Energy contract DE-FC26-08NT0005641, the Alaska Division of Geological and Geophysical Surveys (AKDGGS), and Renaissance Alaska, LLC. Individual thanks to my committee; specifically Paul McCarthy for advice and guidance, and bringing me on to the DOE contract in the first place, and to Cathy Hanks for continued financial support and teaching opportunities. I received thoughtful and insightful advice from Marwan Wartes, and I must also thank Dave LePain for the knowledge he shared with me while he was in Alaska. I appreciate the guidance of Paul Layer concerning geochronology in a less exciting environment than the sides of volcanoes. Thanks to Mike Whalen for being available and interested, and to Sam Van Langingham for a brief period of inspiration.

This project started at the Geologic Materials Center (GMC) in Eagle River, Alaska. Ken Papp and the staff of the GMC were extremely helpful, providing space for core analysis and photography, and releasing samples for me to analyze.

Sincerest thanks to all of the Geology and Geophysics community at UAF. Open doors and smiling faces made a big difference in my years at UAF. I learned a lot from the entire faculty, as a student, a teaching assistant, and an advisee. Particular thanks go to Sarah and Rainer for inspiring me to teach with creativity, energy, and flexibility. Jeff, Ken, and Maciej made a big difference at the end of this project with their expertise in the geochronology and advanced instrument labs, fellow students made for good conversation that kept me at least partially socialized. Anything I achieved here was easier because of the people who keep the department running, especially those who do the paperwork, keep the printers running, and make sure the paychecks come in on time.

Finally, to the friends and adoptive family of Fairbanks, thanks for all the adventures, and for helping me live a life I always wanted. You helped make Fairbanks my home for many years, and a place I truly love. I do not know if I can ever find such an honestly and unapologetically weird place to live, but I hope I can always come back to visit.

Chapter 1: Introduction

1.1 Motivation

The initial purpose of this project was to investigate the sedimentology and stratigraphy of an unconventional frozen petroleum reservoir in sandstones of the Nanushuk Formation at Umiat, Alaska. This research was one component of an interdisciplinary University of Alaska Fairbanks (UAF) study funded by the United States Department of Energy (DOE) to improve reservoir characterization of Umiat Field, which is located in the southeastern corner of the National Petroleum Reserve – Alaska (NPRA). Umiat is fairly unusual as an unconventional reservoir in that the petroleum reservoirs are found in permafrost. It was my responsibility to interpret the sedimentary facies present in the subsurface through core description, identify reservoir intervals in the Nanushuk Formation, and describe the geometry and permeability characteristics of the reservoir intervals so petroleum engineers could refine their models and simulations. The three chapters presented in this dissertation represent my work on the Umiat project and subsequent research I undertook to investigate questions about the timing of deposition and the controls on facies distribution in the Colville foreland basin. The following discussion introduces the geologic background of the Colville foreland basin and Nanushuk Formation and presents some of the scientific problems I address in my research.

1.2 Geologic Background

The Colville foreland basin formed in response to the stacking of thrust sheets and loading along the Brooks Range orogenic front (Coakley and Watts, 1991). Foreland basins are classified as *peripheral*, where basin load accumulates on the under-riding slab, or *retroarc*, where the basin occupies space on the over-riding slab adjacent to a magmatic arc (DeCelles and Giles, 1996). The Colville foreland basin is a peripheral foreland basin, as it lies on the Arctic Alaska microplate (Hubbard et al., 1987), which

dips below the thrust sheets of the Brooks Range without generating a magmatic arc (Nunn et al., 1987; Coakley and Watts, 1991; Coglan et al., 1993; Cole et al., 1997).

Foreland basin sedimentary fill generally occurs in several major depozones: the wedge-top, foredeep, and forebulge (DeCelles and Giles, 1996). Umiat is located in the Brooks Range foothills, along the axis of the foreland basin foredeep. Basin fill in a foredeep, which is the deepest part of the basin in a foreland basin system, typically consists of a combination of transverse alluvial deposits and longitudinal, structure-parallel rivers (Clevis et al., 2004). This is true of the Colville foreland basin and the Nanushuk Formation, which advanced from west to east along the axis of the foredeep but also has a south to north component along the thrust front (Molenaar, 1985; LePain et al., 2009). The Colville foreland basin foredeep is somewhat unusual in that it was exceptionally deep (Houseknecht et al., 2009; Houseknecht and Wartes, 2013), creating significant accommodation for deposition of "Brookian" sediment derived from the Brooks Range and Herald Arch (Moore et al., 1994; Mull et al., 2003). The Nanushuk Formation is the non-marine to shallow marine component of Torok-Nanushuk depositional sequences (Mull et al., 2003; Decker, 2007; Houseknecht et al., 2009) that constitute up to 2000 m of sediment deposited in the foreland basin during the mid-Cretaceous Albian-Cenomanian (Houseknecht et al., 2009).

The Nanushuk Formation has been studied extensively since federal exploration of the NPRA began in 1944, when numerous exploratory wells were drilled to target petroleum reservoirs in Brookian deposits (Schindler, 1988). During the 1970s and 1980s, a second generation of studies on the Nanushuk Formation accumulated a vast amount of data on what was then known as the Nanushuk Group (Ahlbrandt et al., 1979; Fox et al., 1979; Molenaar, 1982; Huffman, 1985). The Nanushuk Group was composed of numerous formations defined by facies and depositional environments (Detterman, 1956) but was revised and downgraded to the Nanushuk Formation, with former formation names discarded (Mull et al., 2003). The now informal formation names appear in Chapters 1 and 3 because they were extensively used in NPRA well reports from the 1950s and they

remain in common use in subsurface work. Despite significant early research on the Nanushuk Formation most of the reservoirs in the Brooks Range foothills, apart from Umiat, are undeveloped gas accumulations, so little work has been done on reservoir characterization of the Nanushuk Formation at any site.

More recent studies of the Nanushuk Formation have emphasized sedimentary facies and sequence stratigraphic interpretations (LePain and Kirkham, 2001; Houseknecht and Schenk, 2005; LePain et al., 2009). I also applied modern facies analysis to the Nanushuk Formation through a re-investigation of the NPRA wells and new investigations of local outcrop exposures. The NPRA wells are an invaluable resource and I used data from the original drilling reports to supplement my own observations throughout the dissertation. The facies interpretations, permeability data, radioisotopic ages and geochemistry I compiled from the NPRA wells allowed me to address significant questions at Umiat field (Chapter 2), investigate the timing of Brookian events (Chapter 3), and interpret the interplay between sedimentary facies and bathymetry in a high-accommodation foreland basin (Chapter 4).

1.3 Umiat Field

A better understanding of shallow, frozen reservoirs has larger implications for petroleum exploration in the Arctic, an emerging frontier. The major petroleum reservoirs at Umiat are located in structural traps in the hanging wall of a thrust-faulted anticline (Molenaar, 1982; Hanks et al., in press). The high quality, light oil found in the Nanushuk Formation sandstones is thought to be sourced from the underlying Torok Formation, the overlying Seabee Formation or even deeper sources such as the Pebble Shale, with migration pathways along local faults (Ahlbrandt, 1979; Magoon and Claypool, 1979). Despite known accumulations of valuable light oil, Umiat remains undeveloped because the petroleum reservoirs are located at shallow, permafrost-affected depths. Resulting complications include ice bridging and collapse in boreholes (Collins, 1958), pressure maintenance issues (Watt et al., 2010), and pore-clogging ice (Baptist, 1960; Hanks et al., in press). Pore ice, in particular, has been the source of recent study by petroleum

engineers in the UAF Umiat group (Godabrelidze, 2010; Venepalli, 2011), as the presence of ice severely reduces the relative permeability of the oil (Hanks et al., in press).

The many complications present in an unconventional reservoir such as Umiat make it difficult to produce oil economically and creates an interesting scientific challenge for geologists and engineers. The Umiat group undertook this challenge with the ultimate goal of producing accurate models of Umiat field for use in predicting the volume, flow characteristics, and producibility of the oil field. This task required the identification of reservoir intervals with high permeability, detailed permeability characteristics of the reservoir interval, and description of the geometry of the reservoir intervals in the subsurface. The basic question was: "How does the sedimentology affect the reservoir characteristics of the Nanushuk Formation?" Through the description of cores from the Umiat wells I developed the sedimentary framework for Umiat field, which is the subject of Chapter 2. The insights gained in that process led to subsequent research on geochronology and basin evolution in Chapters 3 and 4.

1.4 Bentonite Geochronology and Geochemistry

The sedimentology and stratigraphy of a foreland basin can be used to reconstruct the evolution of the basin over time (Vail et al., 1991; Catuneanu et al., 2009) but this requires some form of chronostratigraphic control. A rough chronostratigraphic framework exists for Brookian formations of the Colville basin, based largely on biostratigraphy. The biostratigraphic zones of the Nanushuk Formation, for instance, are defined by megafossils, including bivalves, cephalopods, and gastropods (Jones and Gryc, 1960; Imlay, 1961; Elder et al., 1989) and by micropaleontology, including foraminifera, pollen, spores, and acritarchs (Tappan, 1960; May and Shane, 1985). The ranges of the Cretaceous Age boundaries, based on biostratigraphic constraints, are broad, however, and often span several million years. Furthermore, the "dates" of Cretaceous Age boundaries are defined on the basis of global data and are frequently

revised. In this project I use the most recently published Age boundaries defined by the International Commission on Stratigraphy (Cohen et al., 2013).

One method for securing more precise dates for a sedimentary deposit is radioisotopic dating of volcanogenic material. Published radioisotopic ages from the Colville foreland basin are rare (Lanphere and Tailleur, 1983; Conrad et al., 1990; Flaig, 2010), partly due to the challenges of producing reliable ages from altered volcanic ash found in the basin (Wartes, pers. comm.). Chapter 3 is my attempt to generate geologically accurate dates from altered volcanic ashes (bentonites) recovered from five wells in the central Brooks Range foothills. I used the $^{40}Ar/^{39}Ar$ geochronology method, which is based on the decay of potassium (K) to argon (Ar). The $^{40}Ar/^{39}Ar$ method uses ^{39}Ar produced from mineral separates in a nuclear reactor as a proxy for parent ^{39}K content, which allows for analyses of smaller samples (McDougall and Harrison, 1999). This is crucial when dealing with limited sample sizes from cores. I obtained dates from various mineral phases (biotite, plagioclase, sanidine) preserved in bentonites from the Nanushuk, Seabee, Tuluvak, and Schrader Bluff formations. The goal of this research was to compare dates within and between wells and to bracket major stratigraphic surfaces. I hypothesized that there would be age variation from west to east that could be used to better understand the timing of migration of Brookian deposits along the axis of the foreland basin and correlate changes in facies with known tectonic events.

Another outstanding question about bentonites within the Colville foreland basin is the provenance of the volcanic material. Elemental concentrations can be used to classify igneous rocks so I processed any remaining portions of bentonite samples from the Umiat wells for X-ray fluorescence spectroscopy (XRF). Both major and trace element geochemistry were used to classify the bentonites in terms of rock type and tectonic setting. I chose samples exclusively from Umiat wells 2 and 11 in order to evaluate changes in bulk composition over time.

1.5 The High Accommodation Colville Foreland Basin

The sedimentary record of any foreland basin is affected by tectonic setting, orogenic history, eustatic sea level, and climatic variables (Van Wagoner and Bertram, 1995), which affect bathymetry and relative accommodation. As previously mentioned, the Colville foreland basin is unusual in that it has clinoform-sequences with thicknesses of up to 2000 m (Houseknecht et al., 2009) and slope heights of up to 700 m (Houseknecht and Wartes, 2013). The great height of the clinoforms is related to inherited structural relief and high accommodation created in the Early Cretaceous (Houseknecht and Wartes, 2013). The purpose of Chapter 4 was to investigate the relationship between observed distribution of wave-influenced and river-dominated facies within the Nanushuk Formation and the progradation of Torok-Nanushuk clinoforms into the high accommodation foreland basin. The implications of this part of the study are important for the development of high-angle clinoforms and prediction of facies throughout foreland basins.

Though the larger sequence stratigraphic framework of the Nanushuk Formation has been described (Decker, 2007; Houseknecht et al., 2009), local sequence stratigraphic surfaces and systems tracts are difficult to identify and correlate both in outcrop and in the subsurface (LePain et al., 2009). Trajectory analysis can be used to interpret lateral and vertical migration of facies and is particularly useful in well-based, subsurface studies because established models can be applied using available one-dimensional lithological data (Helland-Hansen and Hampson, 2009). I used facies successions observed in the NPRA wells to interpret stacking patterns, sequence stratigraphic surfaces, and shoreline trajectories in the Nanushuk Formation in the central Brooks Range foothills. I was particularly interested in the relationship between wave-influenced and river-dominated facies and the relative position of the shelf margin. My hypothesis was that high-energy, high accommodation conditions prevalent at or near the shelf edge contributed to the presence of wave-influenced sediments in the lower Nanushuk Formation. I was also interested in the relative position of facies with respect to flooding surfaces or

transgressive surfaces of erosion, and how transgressive events change relative accommodation and facies distribution. Furthermore, I investigated both west-to-east and south-to-north subsurface cross-sections of the Nanushuk Formation to compare changes in progradation history. Not only are these results relevant for reconstructing the evolution of the Colville foreland basin and the related tectonic history of the Arctic but the observed patterns are likely relevant to other peripheral foreland basins elsewhere.

1.6 Dissertation Format

This dissertation comprises three distinct chapters which represent manuscripts submitted or prepared for submission to peer-reviewed journals. All three chapters are directly related to the Nanushuk Formation in the central Brooks Range foothills in the vicinity of Umiat, Alaska. Chapter 2 was submitted in December 2012 to the American Association of Petroleum Geologists Bulletin (AAPG Bulletin). The paper was accepted, pending revision, on June 10, 2013.

Chapter 3 is planned for submission to Cretaceous Research, which publishes all aspects of research on the Cretaceous. The formatting guidelines for Cretaceous Research also require numbered headings, so the structure of Chapters 3 and 4 follow the format used in Chapter 2. The reference styles are subtly different, however, and the reference sections in the dissertation reflect this. I conducted the majority of work on Chapter 3, with co-authors that include Drs. Layer and Benowitz of the UAF Geochronology Lab, and Dr. Sliwinski of the Advanced Instrumentation Laboratory. Drs. Benowitz and Layer conducted instrumental analyses and determined plateau ages used in the paper. Additional co-authors include Drs. McCarthy and Hanks, who provided funding and assisted in manuscript preparation.

Chapter 4 is also planned for submission to Cretaceous Research, as it touches on several aspects of stratigraphy and basin development and is well suited for a broad international journal. It is the only manuscript on which I will be the sole author.

All interpretations presented in this dissertation are based on my analysis of cores, core photos, well logs, and on data mining from existing literature. This study builds upon published reports and publicly available data; these sources are cited and referenced accordingly. New data discussed in the dissertation includes sedimentological core descriptions, petrography, sandstone permeability collected by fellow graduate students working on the Umiat project (Chapter 2), $^{40}Ar/^{39}Ar$ ages (Chapter 3), and tephra geochemistry (Chapter 3). Though I did not collect it, I processed the permeability data and created the plots used in Chapter 2 and compiled the results in the supplemental data.

Distance and depth measurements in all chapters are presented in feet and miles to conform with well measurements and petroleum industry terminology. Metric or SI (système international) units are included in parentheses. In some cases metric units are presented first, where values and figures are cited or modified from existing publications. Those values, which are often rounded to the nearest hundred meters or kilometer, do not convert well to English units, but I nevertheless include the conversions in parentheses.

1.7 References

Ahlbrandt, T.S., 1979, Introduction to geologic studies of the Nanushuk Group, North Slope, Alaska, *in* T.S. Ahlbrandt, ed., Preliminary Geologic, Petrologic, and Paleontologic Results of the Study of Nanushuk Group Rocks, North Slope Alaska, U.S. Geological Survey Circular 794,p. 1-4.

Ahlbrandt, T.S., Huffman, A.C., Fox, J.E., and Pasternack, I., 1979, Depositional Framework and reservoir quality studies of selected Nanushuk Group outcrops, *in* T.S. Ahlbrandt, ed., Preliminary Geologic, Petrologic, and Paleontologic Results of the Study of Nanushuk Group Rocks, North Slope Alaska, U.S. Geological Survey Circular 794, p. 14-31.

Baptist, O.C., 1960, Oil recovery and formation damage in permafrost, Umiat field, Alaska. U.S. Bureau of Mines Report of Investigations 5642, 27 p.

Catuneanu, O., Abreu, V., Bhattacharya, J.P., Blum, M.D., Dalrymple, R.W., Eriksson, P.G., Fielding, C.R., Fisher, W.L., Galloway, W.E., Gibling, M.R., Giles, K.A., Holbrook, J.M., Jordan, R., Kendall, C.G.St.C., Macurda, B., Martinson, O.J., Miall, A.D., Neal., J.E., Nummedal, D., Pomar, L., Posamentier, H.W., Pratt, B.R., Sarg, J.F., Shanley, K.W., Steel, R.J., Strasser, A., Tucker, M.E., and Winker, C., 2009, Towards the standardization of sequence stratigraphy: Earth-Science Reviews, v. 92, p. 1-33.

Clevis, Q., De Boer, P.L., and Nijman, W., 2004, Differentiating the effect of episodic tectonism and eustatic sea-level fluctuations in foreland basins filled by alluvial fans and axial deltaic systems: insights from a three-dimensional stratigraphic forward model: Sedimentology, v. 51, p. 809-835.

Coakley, B.J., and Watts, A.B., 1991, Tectonic controls on the development of unconformities: the North Slope, Alaska: Tectonics, v. 10, p. 101-130.

Coglan, J., Lerche, I., and Russell, B., 1993, Inverse elastic flexural modelling of sedimentary basins: a case study from the Colville Trough, National Petroleum Reserve, Alaska: *in* A.G., Doré, ed., Basin Modelling: Advances and Applications: Norwegian Petroleum Society Special Publication 3, p. 609-621.

Cohen, K.M., Finney, S., and Gibbard, P.L., 2013, International Chronostratigraphic Chart: International Commission on Stratigraphy. http://www.stratigraphy.org/ICSchart/ChronostratChart2013-01.pdf.

Cole, F., Bird, K.J., Toro, J., Roure, F., O'Sullivan, P.B., Pawlewicz, M., and Howell, D.G., 1997, An integrated model for the tectonic development of the frontal Brooks Range and Colville Basin 250 km west of the Trans-Alaska Crustal Transect: Journal of Geophysical Research, v. 102, p. 20685-20708.

Collins, F.R., 1958, Test Wells, Umiat Area Alaska: U.S. Geological Survey Professional Paper 305-B, 206 p.

Conrad, J.E., McKee, E.H., and Turrin, B.D., 1990, Age of tephra beds at the Ocean Point dinosaur locality, North Slope, Alaska, based on K-Ar and $^{40}Ar/^{39}Ar$ analyses: Evolution of Sedimentary Basins-North Slope Basin, U.S. Geological Survey Bulletin 1990, 14 p.

DeCelles, P.G., and Giles, K.A., 1996, Foreland basin systems: Basin Reseaerch, v. 8, p.105-123.

Decker, P.L., 2007 Brookian sequence stratigraphic correlations, Umiat field to Milne Point field, west-central North Slope, Alaska: Preliminary Interpretive Report, Alaska Division of Geological and Geophysical Surveys 2007-2, 21 p.

Detterman, R.L., 1956, New and redefined nomenclature of the Nanushuk group, *in* G. Gryc, and others, eds., Mesozoic Sequence in Colville River Region, Northern Alaska: American Association of Petroleum Geologists Bulletin, v. 40, p. 233-244.

Elder, W.P., Miller, J.W., and Adam, D.P., 1989, Maps showing fossil localities and checklists of Jurassic and Cretaceous macrofauna of the North Slope of Alaska: U.S. Geological Survey Open-File Report 89-556, 7 p. 12 sheets.

Flaig, P.P., 2010, Depositional environments of the Late Cretaceous (Maastrichtian) dinosaur-bearing Prince Creek Formation: Colville River region, North Slope, Alaska. Ph.D. Dissertation, University of Alaska, 311 p.

Fox, J.E., Lambert, P.W., Pitman, J.K., and Wu, C.H., 1979, A study of reservoir characteristics of the Nanushuk and Colville Groups, Umiat Test Well 11, National Petroleum Reserve in Alaska: U.S. Geological Survey Circular 820, 47 p.

Godabrelidze, V., 2010, Characterization and fluid flow properties of frozen rock systems of Umiat oil field, Alaska: MS. Thesis, University of Alaska Fairbanks, 116 p.

Hanks, C., Shimer, G., Oraki-Kohshour, I., Ahmadi, M., McCarthy, P., and Dandekar, A., in press, Integrated reservoir characterization and simulation of a shallow, light oil, low temperature reservoir: Umiat Field, National Petroleum Reserve, Alaska: AAPG Bulletin.

Helland-Hansen, W., and Hampson, G.J., 2009, Trajectory analysis: concepts and applications: Basin Research, v. 21, p. 451-483.

Houseknecht, D.W., and Schenk, C.J., 2005, Sedimentology and sequence stratigraphy of the Cretaceous Nanushuk, Seabee, and Tuluvak formations exposed on Umiat Mountain, North-Central Alaska: U.S. Geological Survey Professional Paper 1709-B, 18 p.

Houseknecht, D.W., and Wartes, M.A., 2013, Clinoform deposition across a boundary between orogenic front and foredeep – an example from the Lower Cretaceous in Arctic Alaska: Terra Nova, v. 25, p. 206-211.

Houseknecht, D.W., Bird, K.J., and Schenk, C.J., 2009, Seismic analysis of clinoforms depositional sequences and shelf-margin trajectories in Lower Cretaceous (Albian) strata, Alaska North Slope: Basin Research, v. 21, p. 644-654.

Hubbard, R.J., Edrich, SP., and Rattey, .P., 1987, Geologic evolution and hydrocarbon habitat of the 'Arctic Alaska microplate': Marine and Petroleum Geology, v. 4, p. 2-34.

Huffman Jr., A.C., ed., 1985, Geology of the Nanushuk Group and Related Rocks, North Slope, Alaska: U.S. Geological Survey Bulletin 1614, 129 p.

Imlay, R.W., 1961, Characteristic Lower Cretaceous megafossils from northern Alaska: U.S. Geological Survey Professional Paper 335, 74 p.

Jones, D.L., and Gryc, G., 1960, Upper Cretaceous Pelycycpods of the genus *Inoceramus* from northern Alaska: U.S. Geological Survey Professional Paper 334-E, 164 p.

Lanphere, M.A. and Tailleur, I.L., 1983, K-Ar ages of bentonites in the Seabee Formation, Northern Alaska: A Late Cretaceous (Turonian) time-scale point: Cretaceous Research, v. 4, 361-370.

LePain, D.L., McCarthy, P.J., and Kirkham, R., 2009, Sedimentology, stacking patterns, and depositional systems in the middle Albian-Cenomanian Nanushuk Formation in outcrop, Central North Slope, Alaska: Alaska Division of Geological and Geophysical Surveys Report on Investigations 2009-1, 86 p.

LePain, D.L., and Kirkham, R., 2001, Potential reservoir facies in the Nanushuk Formation (Albian-Cenomanian), central North Slope, Alaska: examples from outcrop and core, *in* D.W., Houseknecht, ed., NPRA Core Workshop Petroleum Plays and Systems in the National Petroleum Reserve – Alaska: SEPM Core Workshop No. 21, Denver Colorado, June 7-8, p., 19-36.

Magoon, L.B., and Claypool, G.E., 1979, Hydrocarbon source potential of the Nanushuk Group and the Torok Formation, a preliminary report, *in* T.S. Ahlbrandt, ed., Preliminary Geologic, Petrologic, and Paleontologic Results of the Study of Nanushuk Group Rocks, North Slope Alaska, U.S. Geological Survey Circular 794,, p. 54-60.

May, F.E., and Shane, J.D., 1985, An analysis of the Umiat delta using palynologic and other data, North Slope, Alaska, *in* A.C. Huffman, ed., Geology of the Nanushuk Group and Related Rocks, North Slope, Alaska: U.S. Geological Survey Bulletin 1614, p. 97-120.

McDougall I., and Harrison, T.M., 1999, Geochronology and the Thermochronology by the $^{40}Ar/^{39}Ar$ Method: Oxford University Press, New York. 269 p.

Molenaar, C.M., 1982, Umiat Field, an oil accumulation in a thrust-faulted anticline, North Slope of Alaska, *in,* R.B. Powers, ed., Geologic Studies of the Cordilleran Thrust Belt: Rocky Mountain Association of Geologists, v. 2, p. 537-548.

Molenaar, C.M., 1985, Subsurface correlations and depositional history of the Nanushuk Group and related strata, North Slope, Alaska, *in* A.C. Huffman, Jr., ed., Geology of the Nanushuk Group and Related Rocks, North Slope, Alaska: U.S. Geological Survey Bulletin 1614, p., 37-60.

Moore, T.E., Wallace, W.K., Bird, K.J., Karl, S.M., Mull, C.G., and Dillon, J.T., 1994, Geology of Northern Alaska, *in* The Geology of North America, v. G-1, The Geology of Alaska: Geological Society of America, p. 49-140.

Mull, C.G., Houseknecht, D.W., and Bird, K.J., 2003, Revised Cretaceous and Tertiary stratigraphic nomenclature in the Colville Basin, northern Alaska: U.S. Geological Survey Professional Paper 173, 51 p.

Nunn, J.A., Czerniak, M., and Pilger Jr., R.H., 1987, Constraints on the structure of Brooks Range and Colville basin, northern Alaska, from flexure and gravity analysis: Tectonics, v. 6, p. 603-617.

Schindler, J.F., 1988, History of exploration in the National Petroleum Reserve in Alaska, with emphasis on the period from 1975-1982, *in* G. Gryc, ed., Geology and Exploration of the National Petroleum Reserve in Alaska, 1974-1982: U.S. Geological Survey Professional Paper 1399, p. 13-76.

Tappan, H.N., 1960, Cretaceous biostratigraphy of northern Alaska: AAPG Bulletin, v. 44, p. 273-297.

Vail, P.R., Audemard, F., Bowman, S.A., Eisner, P.N., and Pere-Cruz, C., 1991, The stratigraphic signatures of tectonics, eustasy and sedimentology-an overview, *in*, G. Einsele and A. Seilacher, eds., Cyclic and Event Stratification, Springer-Verlag, Berlin, p. 617-659.

Van Wagoner, J.C., and Bertram, G.T., 1995, Introduction, *in* J.C Van Wagoner and G.T. Bertram, Sequence Stratigraphy of Foreland Basin Deposits, American Association of Petroleum Geologists Memoir 64: Sequence Stratigraphy of Foreland Basin Deposits, American Association of Petroleum Geologists Memoir 64, p. ix-xxi.

Venepalli, K., 2011, Implications of pore-scale distribution of frozen water for the production of hydrocarbon reservoirs located in permafrost: M.S. theis, University of Alaska Fairbanks, 101 p.

Watt, J., Huckabay, A., and Landt, M.R., 2010, Umiat: a North Slope giant primed for oil development: Oil and Gas Journal, v. 108, p. 30-38.

Chapter 2: Sedimentology, stratigraphy, and reservoir properties of an unconventional reservoir in the Cretaceous Nanushuk Formation at Umiat Field, North Slope, Alaska[1]

2.1 Abstract

There are numerous oil and gas accumulations in the Brooks Range foothills of the National Petroleum Reserve–Alaska (NPRA). We use cores and well logs from twelve abandoned legacy wells at Umiat Field, near the southeastern boundary of the NPRA, to characterize the sedimentology and stratigraphy of an unconventional shallow frozen reservoir in sandstones of the Cretaceous (Albian-Cenomanian) Nanushuk Formation. There are five facies associations in the Nanushuk Formation at Umiat: offshore and pro-delta, lower shoreface, upper shoreface, delta front, and delta plain.

Three stratigraphically distinct, regionally extensive Nanushuk Formation depositional systems at Umiat contain several potential petroleum reservoirs. The lower Nanushuk Formation, including a reservoir interval known informally as the Lower Grandstand, primarily consists of marine mudstone and shoreface sandstones. The middle Nanushuk Formation is dominantly deltaic, and contains a second major reservoir interval in the informal Upper Grandstand sandstone. Both the Upper and Lower Grandstand are regressive. The transgressive upper Nanushuk Formation contains an additional potential reservoir interval in shoreface sandstones of the informal Ninuluk interval, but the primary reservoir intervals at Umiat Field are upper shoreface and delta front sandstones in the Lower and Upper Grandstand, where increased sorting and decreased bioturbation in high-energy depositional environments affect overall permeability and permeability anisotropy.

[1] Shimer, G.T., McCarthy, P.J, and Hanks, C.L., 2013, Sedimentology, stratigraphy, and reservoir properties of an unconventional reservoir in the Cretaceous Nanushuk Formation at Umiat Field, North Slope, Alaska: AAPG Bulletin, in press.

2.2 Introduction

Umiat Field is an undeveloped petroleum accumulation in the Brooks Range foothills of the National Petroleum Reserve–Alaska (NPRA: Fig. 2.1). The field consists of clastic deposits of the Albian-Cenomanian Nanushuk Formation deformed in a thrust-faulted anticline (Fig. 2.2: Collins, 1958; Molenaar, 1982). Previous studies established the presence of two sandstone reservoir intervals with oil-water contacts at 450 ft. (173 m) and 640 ft. (195 m) below sea level, almost entirely within deep permafrost found from 770-1055 ft. (235-322 m) below the ground surface (Molenaar, 1982). The shallow depth and presence of deep permafrost make Umiat an unconventional reservoir and the field remains undeveloped, in part due to low reservoir pressures and the permeability-reducing effects of pore ice (Hanks et al., in press). The site also lies at a distant location from existing pipeline infrastructure, approximately 100 miles southwest of Prudhoe Bay and 80 miles west of the Trans-Alaska Pipeline System (TAPS). Though early estimates of recoverable oil ranged from 30-100 million barrels depending on recovery factors chosen (Molenaar, 1982), there may be up to 1.4 billion barrels of oil in place (Levi-Johnson, 2010). Despite known engineering challenges, advances in horizontal drilling technology and high oil prices created renewed interest in Umiat Field and justified a reassessment of the field.

Several previous generations of research focused on the Nanushuk Formation at Umiat Field. The field was discovered during federal investigations of Naval Petroleum Reserve No. 4 (NPR-4) between 1944-1953, when eleven wells were drilled at the site to investigate oil seeps at the base of Umiat Mountain (Fig. 2.2B: Collins, 1958). The Umiat wells are now considered “legacy” wells that are abandoned and shut-in. Over 4000 ft. of core was recovered during initial investigations to better characterize the subsurface. The cores and cuttings are stored at the Alaska Geologic Materials Center (GMC) in Eagle River, Alaska, with additional samples at the United States Geological Survey (USGS) Core Research Center in Lakewood, Colorado.

The original report on Umiat drilling operations (Collins, 1958) includes core and cuttings descriptions, micro faunal analyses, well logs (resistivity and spontaneous potential) and a summary of reservoir characteristics. Seven of the eleven Umiat wells produced oil from sandstones in the Nanushuk Formation (individual sandstone beds were not tested), while there was no recovery from an additional well (Umiat No. 2) because of interactions between the rock, permafrost, and freshwater drilling fluids (Collins, 1958). Though approximately 40,000 barrels of oil were recovered before 1953, the recovery factor estimates for this time ranged from 8-32.5% in the permafrost-affected reservoir (Molenaar, 1982). All eleven Umiat wells have not been studied and reported on in detail in public domain literature since the original drilling reports (Collins, 1958) and they represent a valuable resource for the evaluation of the Nanushuk Formation in the subsurface.

A federal reinvestigation of the petroleum resources of the NPR-4 began in 1974 and in 1977 the National Petroleum Reserves Production Act transferred the NPR-4 from the U.S. Navy to the Department of the Interior, when it became the NPRA (Schindler, 1988). New reservoir quality assessments of the Nanushuk Formation during this time included core description, biostratigraphy, petrographic analyses, and 2-D seismic interpretations (Ahlbrandt et al., 1979; Fox et al., 1979). In 1978 the Seabee No. 1 well was also drilled at Umiat to sample deep strata below the Nanushuk Formation. The Seabee No. 1 well lies below the oil-water contact in the Lower Grandstand, based on geophysical well log analysis, and lacks any core samples from the Nanushuk Formation (Fig. 2.2B). The well does contain a modern suite of geophysical well logs through the Nanushuk Formation (Legg and Brockway, 1983) and a check-shot survey, which are both valuable for subsurface interpretations.

The second generation of summary reports and reviews of Umiat and the Nanushuk Formation was completed in the 1980's (Molenaar, 1982; Huffman, 1985; Gryc, 1988). Following years of inactivity, recent studies of the Nanushuk Formation at various locations on the North Slope utilized modern facies analysis (LePain and Kirkham, 2001;

Houseknecht and Schenk, 2005; LePain et al., 2009) and sequence stratigraphic interpretations (Decker, 2007; Houseknecht and Schenk, 2005) to establish the Nanushuk Formation as a spatially and chronostratigraphically variable mix of wave-, river-, and tide-influenced facies deposited in a largely deltaic setting (LePain et al., 2009).

The purpose of this study is to assess facies variability within the Nanushuk Formation at Umiat Field, characterize the reservoir-scale stratigraphic architecture, and investigate how facies variability affects potential reservoir distribution. Five facies associations within three distinct depositional systems are defined on the basis of cores and well logs from all eleven Umiat wells and the nearby Seabee No. 1 well (Fig. 2.2b). Four broadly distributed reservoir intervals correspond to informal units of the Nanushuk Formation. Different sedimentary processes are responsible for each reservoir interval but three of the intervals have similar characteristic permeability profiles and degrees of heterogeneity. The fourth interval is distinct in character, but poorly represented in the subsurface. The results of this evaluation of the sedimentology and stratigraphy of the Nanushuk Formation at Umiat Field are important for evolving production models and have implications for broader interpretations of Nanushuk Formation depositional environments on the east-central North Slope. Other potential permeable intervals likely exist in upward-coarsening topset sandstones deposited in both wave- and river-dominated environments of the fold-and-thrust belt in the Brooks Range foothills.

2.3 Geologic Setting

Umiat Field, Alaska (N 69º 22'12", W 152º 8'10") is located in the northern Brooks Range foothills along the southeastern boundary of the NPRA (Fig. 2.1). Most of the infrastructure at Umiat, including some of the original well sites, sits on Quaternary sediments of the Colville River floodplain on the southern limb of an asymmetric, northward-vergent, thrust-faulted anticline (Fig. 2.2A-C). The anticline deforms Lower Cretaceous to Tertiary sediments derived from the ancestral Brooks Range to the south

(Mull et al., 2004). These "Brookian" strata are part of a thick package of clastic sediments that filled the Colville foreland basin starting in the Early Cretaceous (Fig. 2.3: Mull et al., 2003). The four relevant Brookian formations at Umiat are the Albian-Cenomanian Torok and Nanushuk formations and the overlying Cenomanian-Turonian Seabee and Tuluvak formations. These formation pairs make up two distinct depositional megasequences (Mull, 1985; Hubbard et al., 1987; Decker, 2007). Cenomanian-Turonian strata, including the upper portion of the Nanushuk Formation, are exposed on the eastern limb of the Umiat anticline in bluffs at Umiat Mountain (Houseknecht and Schenk, 2005) but the Upper Grandstand and Lower Grandstand intervals of the Nanushuk Formation are not exposed at the surface.

The Nanushuk Formation prograded from west-to-east along the axis of the Colville Basin, with an additional south-to-north component in the area that now makes up the east-central Brooks Range foothills (Houseknecht and Schenk, 2005; Decker, 2007; Houseknecht et al., 2009; LePain et al., 2009). The formation has been described as fluvial, deltaic and shallow marine, with major deltaic depocenters in the west and central North Slope (Ahlbrandt et al., 1979; Mull, 1985), but there is considerable west-to-east variation in Nanushuk Formation depositional environments across the North Slope. In the Umiat area the Nanushuk Formation is slightly younger and more sand-rich than in the west, possibly due to contributions from source areas from multiple, shorter rivers draining the northern flank of the ancestral Brooks Range and/or due to greater wave-influence and reworking (Molenaar, 1985; LePain and Kirkham, 2001; Houseknecht and Schenk, 2005; LePain et al., 2009).

Originally defined as the Nanushuk Group (Detterman, 1956), with numerous shallow marine and non-marine formations, the Nanushuk was lowered to formation status to comply with international guidelines (Mull et al., 2003). Though now informal units, the formations of the former Nanushuk Group remain in common use in the subsurface (Fig. 2.3B). At Umiat Field these units include the marine Tuktu, shallow marine to deltaic Grandstand, marginal marine to non-marine Killik tongue of the Chandler, and the

shallow marine Ninuluk "*formations*". Killik is used here instead of Chandler to emphasize the local character of the former formation. Furthermore, in the subsurface at Umiat the Grandstand contains two distinct, sand-rich intervals (Upper and Lower Grandstand) separated by a tongue of marine mudstone of the Tuktu, commonly referred to as the Shale Barrier.

Umiat reservoir tests during the 1944-1953 drilling period produced oil primarily from the Upper Grandstand, with minor production from the Ninuluk and oil shows in the other "formations" (Molenaar, 1982). In Umiat No. 11, the Grandstand and Killik have higher average porosity and permeability than the Ninuluk, probably due to changes in depositional environment and possible changes in provenance (Fox et al., 1979). This relationship has been assumed to be consistent in the subsurface throughout the reservoir, but it is important to note that Umiat No. 11 was a dry well that lies in the footwall of the thrust structure and outside the limits of the known petroleum trap.

2.4 Regional Context

The Colville basin formed in flexural response to tectonic loading along the ancestral Brooks Range and Herald Arch (Fig. 2.1: Nunn et al., 1987; Coakley and Watts, 1991; Moore et al., 1994). The earliest sedimentary evidence for initiation of the Brookian orogeny is Hauterivian in age (Bird and Molenaar, 1992) but the Albian-Cenomanian (113-100.5 Ma; Cohen et al., 2013) Torok and Nanushuk formations were deposited during a period of extension and exhumation on the south side of the Brooks Range that started ~113 Ma (Blythe et al., 1996; O'Sullivan et al., 1997). By the late Albian, the high volume of sediment represented by the Torok and Nanushuk formations filled much of the Colville Basin and overtopped the Barrow Arch (Molenaar, 1985; LePain et al., 2009), and cooling and exhumation slowed by ~95 Ma (O'Sullivan et al., 1997)

2.5 Methods

4218 ft. of cores were photographed, described, and logged from the eleven Umiat wells in collections at the Alaska Geologic Materials Center (GMC). Most of the available core was from Umiat wells 1, 2, 3, 9, 10, and 11 (Fig. 2.4). The condition and size of the cores varies between wells. Wells 1 and 2 have 1.5-inch (4 cm) diameter cores, while wells 9, 10, and 11 have 2.5–inch (6 cm) diameter cores. Many of the cores were still coated in drilling mud, and Umiat No. 11 was the only well with significant slabbed intervals. With the permission of the GMC we slabbed much of the core from Umiat No. 9.

New interpretations were cross-referenced with the original core and cuttings descriptions (Collins, 1958). The thicknesses of sandstone and mudstone intervals in all of the Umiat wells were quantified using core descriptions and published cuttings data (Collins, 1958), and a sand:mud ratio was calculated for the mudstone-dominated intervals in the subsurface. Where resistivity and spontaneous potential (SP) well logs were available, we used the data to interpret gaps between cored intervals and to correlate between the Umiat wells. The Seabee No. 1 well also has a gamma ray log, used for further correlation. Though the oil-water contacts are thought to be at 450 ft. and 640 ft. below sea level, the contact was not directly observed in core. Bioturbation intensities, which are used to assess the degree of burrowing, were determined using a scale of 0-6 (Bann et al., 2004).

Air-permeability data were collected using a New England Research Tiny Perm II mini-permeameter. Horizontal permeability (K_h) was recorded at 1-ft. intervals from slabbed sandstone cores. The rough surfaces of unslabbed cores prevented the formation of an adequate seal for permeameter readings. Vertical permeability (K_v) measurements were made on relatively flat, unlaminated surfaces at more irregular intervals. For ease of interpretation, individual permeability values (K_h and K_v) were log transformed:

Eq. 1: $\log(K) = \log_{permeability}$

Log transformed values range from 0 (log1 md) to 3 (log1000 md). 10 md was used as the lower cut-off for defining reservoir sandstones. We also calculated permeability anisotropy (K_v/K_h) and present this data as averages for reservoir intervals. Any ratio over 2.0 was considered an outlier caused by instrumental or operator error, and was not included in the average values.

2.6 Facies Associations

Facies are distinguished on the basis of grain size, sedimentary structures, and biological features (Table 2.1; Fig. 2.5). Individual facies are grouped into facies associations (Table 2.2) on the basis of bedding relationships observed in core, upward-coarsening or upward-fining trends from lithologic logs and well logs, and observed trace fossils (Fig. 2.6). Five facies associations are defined (Fig. 2.7-2.9) with additional subdivision of facies associations to differentiate sub-environments (i.e.: distal and proximal lower shoreface).

2.6.1 Facies Association 1: Offshore

Description: FA-1 (Figs. 2.7-2.8; Table 2.2) comprises successions of silty shale (F-1), massive mudstone (F-2) and wavy or lenticular bedded mudstone (F-3). Highly bioturbated (BI 4-6) mudstones contain abundant *Phycosiphon* and *Schaubcylindrichnus freyi* (Fig. 2.6). *Paleophycus* and *Planolites* are associated with increasing sand content and the transition to FA-2a. Lenticular or wavy-bedded mudstones (F-3) have lower bioturbation intensities (BI 0-3). Both F-2 and F-3 mudstones contain arenaceous and calcareous foraminifera of the Albian *Verneuilinoides borealis* faunal zone (Bergquist, 1958) and have the highest percentage of dinoflagellates in the Nanushuk Formation (May and Shane, 1985).

Interpretation: Published faunal and palynological analyses establish the marine character of FA-1 mudstones. The *Verneuilinoides borealis* faunal zone consists of

shallow marine fauna (Bergquist, 1958), while the palynological assemblage of dinoflagellates, acritarchs, and spores is typical of a near shore, shallow marine setting (May and Shane, 1985). Furthermore, the trace fossil assemblage closely resembles the *Cruziana* ichnofacies, which is associated with both offshore marine and prodelta settings (MacEachern et al., 2005).

This paper follows the convention of LePain et al. (2009) and groups prodelta and non-deltaic shelf mudstones of the Nanushuk Formation into a single offshore facies association deposited below storm wave base (*sensu* Van Wagoner et al., 1990; Hampson and Storms, 2003). Thin sandy laminations or wavy and lenticular bedding found in FA-1 may be the distal expression of storm-wave, surge, or river flood-derived turbidity flows that bring sand onto the inner shelf (Nelson, 1982; Myrow and Southard, 1996; Myrow et al., 2002; Pattison, 2005; Lamb et al., 2008). These features genetically link FA-1 with overlying shallow marine and deltaic facies associations in progradational systems (Figs. 2.7-2.8).

2.6.2 Facies Association 2a: Distal Lower Shoreface

Description: FA-2a is a heterolithic facies association composed of bioturbated mudstone (F-2) interbedded with thin beds (1-10 ft.) of low-angle, cross-laminated very-fine sand (F-5) or ripple cross-laminated very-fine sand (F-6). Sandy beds typically coarsen upward, and increase in number, thickness and degree of amalgamation up core. Beds of mudstone may contain laminations or lenticular bedding disturbed by bioturbation (BI 1-4). Mud drapes and thin (<1 ft.) beds of mudstone that occur between the sandy beds are heavily bioturbated (BI > 4). Some thin sandstone beds are heavily bioturbated (BI > 4), resulting in sand-rich mudstones associated with *Phycosiphon*, but most sandstone beds are not (BI < 3). The trace fossil assemblage in sand-rich mudstones and sandstones also includes *Schaubcylindrichnus freyi*, *Planolites* and, rarely, *Conichnus*, *Diplocraterion*, and *Ophiomorpha* (Fig. 2.6).

Interpretation: Beds of very-fine sandstone with low-angle cross-lamination (F-5) and ripple cross-lamination (F-6) interbedded with laminated or massive mudstone (F-2) beds are interpreted to represent hummocky cross-stratification formed by the oscillatory energy of storm waves in the distal lower shoreface (Dott and Bourgeois, 1982; Dumas and Arnott, 2006). The storm wave-derived hummocky cross-strata in the distal lower shoreface represent discontinuities that punctuate periods of deposition dominated by suspension settling (*sensu* Hampson, 2000). These beds coarsen upward (Fig. 2.7), suggesting a regressive character of the shoreface environment and a gradual transition to the proximal lower shoreface (FA-2b). Similar wave-derived facies successions have been described in shoreface settings from the Cretaceous Western Interior Seaway (Pattison, 1995; Hampson and Storms, 2003) and in modern and ancient asymmetric wave-dominated deltas, where wave energy concentrates sand on the up-drift side of a river (Bhattacharya and Giosan, 2003; Li et al., 2011). The trace fossil assemblage includes *Phycosiphon*, *Planolites*, and *Schaubcylindrichnus freyi*, components of the *Cruziana* ichnofacies found in both distal shoreface and wave-influenced deltaic environments (Buatois et al., 2008; Dafoe et al., 2010; Gingras et al., 2011).

2.6.3 Facies Association 2b: Proximal Lower Shoreface

Description: FA-2b consists of amalgamated beds of very fine- to fine-grained sandstone. Sedimentary structures include low angle (F-5), parallel laminated (F-8) and ripple cross-laminated sandstones (F-6), which are occasionally lined with plant debris. Well-sorted, apparently massive sandstone (F-4) intervals increase in frequency up-well from more clearly laminated or bioturbated sandstones with higher concentrations of organic matter. The trend of upward-coarsening, increasingly amalgamated sandstone beds continues up-well into FA-3. Isolated siderite rip-up clasts also increase in frequency up-well. Bioturbation is common and trace fossils are more visible where organic matter is abundant. Trace fossils include *Paleophycus*, *Ophiomorpha*, *Diplocraterion*, *Rosselia*, and *Schaubcylindrichnus freyi* (Fig. 2.6).

Interpretation: The distinction between the distal lower shoreface (FA-2a) and proximal lower shoreface (FA-2b) is largely based on amalgamation of sandstone beds (Fig. 2.7: *sensu* Van Wagoner et al., 1990; Hampson, 2000; Hampson and Storms, 2003). Outside of wells No. 9 and No. 2, core samples are sparse or of poor quality and the boundary between distal and proximal lower shoreface is indistinct. Bioturbation intensity decreases in this facies association but beds that appear well-sorted and massive may contain extensive cryptobioturbation as in other storm- or wave-influenced environments (MacEachern et al., 2005).

2.6.4 Facies Association 3: Upper Shoreface

Description: Trough-cross laminated (F-9), massive (F-4), and parallel-laminated fine-grained sandstones (F-8) are the most common facies in FA-3. The vertical distribution of these facies is not systematic. Sets of amalgamated beds are 50 to 60 ft. thick. Bioturbation intensity and trace fossil diversity are both low (Fig. 2.7). Rare trace fossils include *Skolithos*.

Interpretation: Amalgamated sandstones in FA-3 (Fig. 2.7) are interpreted to reflect deposition at or above fair-weather wave base where wave energy is constant (*sensu* Hampson, 2000). Higher energy corresponds with an increase in grain size from very fine-sandstone in the lower shoreface to fine-grained sandstone in the upper shoreface (Fig. 2.7). In the upper shoreface, trough cross-lamination is interpreted as the result of sub-aqueous longshore dune migration (Flint, 1988; Hampson and Storms, 2003; Clifton, 2006). High-energy conditions in shoreface and foreshore settings prohibit bioturbation or inhibit preservation (Li et al., 2011) and are responsible for low bioturbation intensity and diversity.

2.6.5 Facies Association 4: Delta Front

Description: Significant lenticular to wavy bedding (F-3) transitions up-well to ripple cross-laminated (F-6a), parallel laminated (F-8) and trough cross-laminated (F-9) sandstone. Sets of amalgamated beds are 60 to 70 ft. thick. Occasional beds of mud-

draped, ripple cross-laminated sandstones are also present (Fig. 2.5). Gravel lag deposits (F-13) consisting of single pebble layers comprised of mudstone rip-up clasts are rare. Bioturbation intensity is low (BI 0-3) in sandstones and lenticular or wavy-bedded mudstones (F-3) but soft sediment deformation occurs in muddy facies and may obscure traces.

Interpretation: A delta front generally encompasses shoreline and seaward dipping subaqueous topset and foreset beds of coarse sediment (Bhattacharya, 2006). Major depositional environments in a river-dominated delta front are derived from terminal distributary channels and include subaqueous levees, distributary mouth bars, and distributary channels (Coleman and Gagliano, 1965). In the Umiat wells, parallel-laminated, ripple cross-laminated, and trough cross-laminated sandstones are attributed to distributary mouth bars or distributary channel bars that rapidly prograded out over distal delta front mudstones, as indicated by soft sediment deformation (Fig. 2.8). Sparse bioturbation is also typical of delta front deposits, where high water turbidity, high sedimentation rate, and salinity fluctuations can inhibit burrowing organisms (MacEachern et al., 2005). The gravel lag deposits are interpreted as evidence for channelization. The lack of additional evidence for channels is not surprising, given the limited amount of core available, as well as the propensity for delta distributary channels to be actively filled by distributary mouth bars (Olariu and Bhattacharya, 2006). The rare occurrence of mud-draped ripples is interpreted as minimal evidence for tidal influence in the distributary system. Though commonly associated with fluctuations in energy in tidal systems (Bhattacharya, 2006), mud drapes are not always tidal in origin (Clifton, 2006).

2.6.6 Facies Association 5a: Delta Plain

Description: FA-5a includes dark grey to black mudstones, typically carbonaceous, both laminated (F-1) and massive (F-2), with lenticular or wavy bedded mudstones (F-3) that have rare syneresis cracks. Other characteristic features are layers of oxidized siltstone or claystone, Corbiculid bivalves, plant fossils, root traces, coal (F-11), and bentonites (F-12). Coal deposits are thin (<1 ft.). *Teichichnus* and *Skolithos* trace fossils are found in

interbedded mudstone and sandstone intervals. *Teichichnus* in particular is more common in FA-5a than in other facies associations. In Umiat wells 1 and 11 there is a mix of dinoflagellates and acritarchs, spores, and gymnosperm pollen (May and Shane, 1985) in associated intervals.

Interpretation: Mudstones in FA-5a are interpreted as marginal marine to non-marine lagoon, interdistributary bay, and lake deposits on the basis of several factors. Corbiculid bivalve beds, abundant plant fragments, spores, gymnosperm pollen, and thin beds of coal distinguish FA-5 from marine mudstones of FA-1. Corbiculid bivalves are found in brackish or hypoxic water conditions (May and Shane, 1985; Holmes and Miller, 2006), and the palynological assemblage of dinoflagellates, acritarchs, spores, and gymnosperm pollen suggests brackish conditions as well (May and Shane, 1985). Syneresis cracks also occur in settings with mixed salinity, such as brackish water bays (Pratt, 1998). The trace fossil assemblage also supports a brackish delta plain interpretation. Though not exclusive to brackish conditions, *Teichichnus* is typically one of the dominant trace fossils in brackish interdistributary bays and is frequently found in association with syneresis cracks (Buatois et al., 2008). A similar set of facies occurs in brackish to non-marine shallow water deposits of the Dunvegan Formation in northwestern Alberta (Bhattacharya and Walker, 1991). These facies are typical of deltas comprised of numerous mud-dominated sub-environments, including swamps, marshes, tidal flats, lagoons, and interdistributary bays, which can be difficult to distinguish in ancient settings (Bhattacharya, 2006). Interdistributary bay or lagoon environments are also important down-drift components of asymmetric wave-dominated deltas (Bhattacharya and Giosan, 2003) and in wave-dominated shoreface successions (Flint, 1988). A delta plain or coastal plain interpretation is preferred based on the stratigraphic position of FA-5 above upper shoreface (FA-3) or delta front (FA-4) deposits (Fig. 2.7-2.8).

2.6.7 Facies Association 5b: Crevasse Sands

Description: Wavy bedded mudstones (F-3) grade up into thin (5-10 ft.) flaser bedded and asymmetrical ripple cross-laminated sandstone (F-6a) and mud-draped, ripple cross-

laminated sandstone (F-7). Mud drapes are frequently sideritized, especially in Umiat No. 11. In isolated instances a gravel lag of mudstone rip-up clasts, a thin sandstone, and a subsequent upward-fining succession interrupt upward coarsening flaser bedding (F-7). Underlying interbedded mudstone intervals (FA-5a) commonly exhibit soft sediment deformation (probably convolute bedding or ball and pillow structures, but core samples are too small to definitively determine the origin of soft sediment deformation structures). *Skolithos* and *Teichichnus* are common, and the palynological assemblage is the same as FA-5a. Plant fragments are preserved on lamination surfaces in ripple cross-laminated sandstones.

Interpretation: FA-5b represents sandstones and mudstone rip-up lag deposits found in association with mudstones and coals of FA-5a (Fig. 2.9). These deposits are interpreted as overbank sandstones and mudstones or avulsion-derived influxes of sand into interdistributary bays and lagoons on the delta plain. Specific process interpretations vary based on grain size trends observed in core or inferred from well logs, and follow deltaic facies interpretations (Elliot, 1974; Bhattacharya and Walker, 1991). Where beds coarsen upward, a crevasse-splay or crevasse delta interpretation is preferred. Rarer upward-fining successions with mudstone rip-up lags are interpreted as passively filled crevasse channels.

2.7 Permeability Facies Distribution

Permeability profiles for different facies associations illustrate the relationship between permeability and depositional processes in the Nanushuk Formation at Umiat (Figs. 2.7-2.9). Though sandstone reservoir intervals reach up to 120 ft. in total thickness, only a small percentage of each sandstone interval has air permeability values greater than 10 md (log permeability >1). Permeable zones are restricted to sandstones from upper shoreface (FA-3) and delta front (FA-4) facies associations (Figs. 2.7-2.8). Both K_h and K_v are associated with the coarsest and most well-sorted portions of upper shoreface and

deltaic deposits. In most cases these deposits coarsen upward (Figs. 2.7-2.8), except near the top of the Nanushuk Formation (Fig. 2.9).

Permeability anisotropy varies depending on facies and facies association (Table 2.3). The lowest anisotropy (values near 1.0) occurs in upper shoreface deposits. This presumably occurs due to increased sorting, and is associated with apparently massive sand (F-4) and a decrease in visible trace fossils (BI <2) related to high energy, increased water turbidity, and substrate instability (MacEachern et al., 2005; Li et al., 2011). Anisotropy is higher in delta front (FA-4) sandstones, which are comprised of ripple cross-laminated (F6), trough cross-laminated (F-9), and massive sandstone (F-4), and contain more frequent laminations defined by thin mudstone layers or carbonaceous debris. Bioturbation intensity is low (BI <2) and mud deposition rates are high, in contrast to shoreface environments where wave energy transports suspended sediment offshore (MacEachern et al., 2005). Well-preserved mud drapes and carbonaceous laminations reduce vertical permeability and are the likely cause of higher anisotropy.

2.8 Reservoir Scale Stratigraphic Architecture

The commonly used informal subsurface units of the Nanushuk Formation (Fig. 2.3b) are effective for describing the stratigraphic architecture of shallow marine and deltaic sandstones at Umiat Field. Each of these informal units (Tuktu, Lower Grandstand, Shale Barrier, Upper Grandstand, Killik, Ninuluk) generally corresponds to a unique depositional environment that determines reservoir distribution and quality.

2.8.1 Tuktu

The Tuktu consists of marine mudstone (FA-1) that underlies and intertongues with shallow marine (FA-2, FA-3) and deltaic (FA-4) sandstones of the Lower Grandstand and Upper Grandstand. Tongues of the Tuktu are present beneath the Lower Grandstand, particularly in the west at Umiat No. 1 (Figs. 2.10 and 2.11). Elsewhere on the North

Slope and below the depths studied in the Umiat wells, Tuktu mudstones at the base of the Nanushuk Formation transition downward into the Torok Formation, which consists of mudstones and turbidites deposited in marine slope and basin-floor settings (Mull et al., 2003). Another thick tongue of the Tuktu separates the Lower Grandstand from the Upper Grandstand (Fig. 2.10). This tongue is known informally as the Shale Barrier at Umiat Field, and is best discussed with the Upper Grandstand (see below).

2.8.2 Lower Grandstand

In previous studies, the Lower Grandstand was considered a single reservoir interval (Watt et al., 2010). Core interpretation and permeability profiles, however, show that the Lower Grandstand actually consists of at least two upward-coarsening sand bodies separated by a regionally extensive flooding surface (Figs. 2.7 and 2.10). Resistivity and spontaneous potential logs are funnel-shaped or blocky in character (Fig. 2.11). The flooding surface and associated impermeable mudstones and sandstones represent a major flow barrier within the Lower Grandstand. The widespread distribution of the flooding surface, allows us to divide the Lower Grandstand into a basal reservoir interval (Lower Grandstand A) and upper reservoir interval (Lower Grandstand B; Fig. 2.11). The median thickness of the Lower Grandstand A is 150 ft. (Table 2.4). Positive kicks in SP logs and drops in resistivity indicate further compartmentalization of Lower Grandstand A in Umiat No. 1, Umiat No. 2, and Seabee No. 1 (Figs. 2.10 and 2.11). The Lower Grandstand B is typically much thinner (~90 ft. thick in the central reservoir). There is more between-well variation in Lower Grandstand B, which is very thin in Umiat No. 1 (50 ft.) and much thicker in Umiat No. 11 (140 ft.), but the well log character is more uniform (Fig. 2.10).

The top of Lower Grandstand B occurs at an abrupt transition from a fine-grained upper shoreface sandstone (FA-3) to a carbonaceous mudstone (FA-5a) deposited in interdistributary bays or lagoons. In most wells the carbonaceous mudstone layer is ~20-50 ft.-thick and is part of a regressive succession associated with the Lower Grandstand B. In Umiat No. 1 mudstones of FA-5 are 70 ft.-thick, suggesting increased back-barrier

accommodation to the west. In most of the wells a thin (10-20 ft.-thick) sandstone truncates the carbonaceous mudstone (Fig. 2.11). The sandstone is interpreted as a transgressive lag deposit at the base of the "Shale Barrier".

2.8.3 Shale Barrier (Tuktu) and Upper Grandstand

The Shale Barrier is 290-335 ft.-thick with an average thickness of 310 ft. (Table 2.4). The interval consists of marine mudstone (FA-1) and distal shoreface sandstones (FA-2a). Sandstones are typically very fine-grained, with sand:mud ratios from 0.05-0.76 (Table 2.5). The maximum sand:mud estimate comes from Umiat No. 1, where the Shale Barrier is ~43% sand. However, Umiat No. 1 is located approximately five miles (8 km) west of centrally-located wells, which have a relatively consistent sand:mud ratio of 0.10-0.30. A thick sandstone body in the middle of the Shale Barrier in Umiat No. 1 illustrates the reduction in sand content from west to east. The sand thins from 50 ft. in Umiat No. 1 in the west to 20 ft. in Umiat No. 9 and it is nearly absent in Umiat No. 2 (Fig. 2.10).

The Upper Grandstand is a regionally extensive, river-dominated deltaic sandstone (FA-4) found in all of the Umiat wells. The interval varies from 35 to 80 ft.-thick, with an average thickness of 52 ft. Well logs are funnel-shaped or serrated (Fig. 2.12). The Upper Grandstand lacks internal flooding surfaces that can be correlated, but it does thin towards the northeast where it becomes more heterolithic (Table 2.4). The top of the Upper Grandstand is an abrupt, easily distinguished boundary between fine- or medium-grained sandstone of the Upper Grandstand and carbonaceous mudstone of the overlying Killik (Fig. 2.12).

2.8.4 Killik

The Killik is a marginal-marine to non-marine delta plain (FA-5) genetically related to the underlying Upper Grandstand. It is difficult to correlate sandstone layers within the Killik between wells (Fig. 2.10), and the sand:mud ratio varies considerably in each well

(Table 2.5). It is also difficult to correlate thin coal layers, which are interpreted as localized accumulations of organic matter-rich swamps or marshes on the delta plain.

The irregular distribution of sandstone layers within the Killik are crevasse channel and crevasse splay deposits on the delta plain (FA-5b). Crevasse channel and splay deposits are found elsewhere in the Nanushuk Formation (LePain et al., 2009), and are a typical component of the delta plain environment (Elliot, 1974; Bhattacharya and Walker, 1991). The geometry and extent of the crevasse splay sands, which can be tenuously correlated between Umiat wells in some instances (Fig. 2.10), is similar to modern crevasse splays that cover up to 7.5-9.5 mi2 (12-15 km2) in deltaic environments (Coleman, 1988).

2.8.5 Ninuluk

The Ninuluk is poorly represented in the Umiat wells due to erosion on the southern limb of the Umiat anticline. Facies variability within the Ninuluk is difficult to interpret because the primary data source for interpretation is the original cuttings descriptions (Collins, 1958). The best core data are from Umiat No. 11, in which there are two thick sandstone intervals defined as Ninuluk A and Ninuluk B. Ninuluk A is the lower interval, and is ~35 ft.-thick (Table 2.4). A similarly thick sandstoneinterval can be found in wells No. 6, No. 7, and No. 10. The upper interval, Ninuluk B, averages 40 ft.-thick (Table 2.4), though it is much thicker in wells No. 9 and No. 11. In Umiat No. 8 the Ninuluk is an apparently amalgamated sandstone nearly 100 ft.-thick. Unfortunately, these sandstone intervals are missing in much of the field due to erosion.

2.9 Nanushuk Formation Depositional Systems

In the Umiat area, the informal units of the Nanushuk Formation can be grouped together to describe two distinct deltaic systems: an upward-coarsening, progradational wave-dominated deltaic system comprised of the Tuktu and Lower Grandstand, and an upward-coarsening, progradational river-dominated deltaic system comprised of the Shale

Barrier, Upper Grandstand and Killik. These two major upward-coarsening, regressive systems are capped by the Ninuluk, which is interpreted as a back-stepping, transgressive system.

2.9.1 The Tuktu and Lower Grandstand: Wave-Dominated Deltaic System

The facies successions described in the Tuktu and Lower Grandstand resemble the deposits of regressive wave-dominated shorefaces and wave-influenced deltas, where wave energy disperses sediment brought to the coast by distributary systems (Hampson and Storms, 2003; Bhattacharya and Giosan, 2003; Hampson and Howell, 2005; Fig. 2.13A). The wave-dominated shoreface successions coarsen upward from offshore mudstones (FA-1) of the Tuktu into lower shoreface (FA-2) and upper shoreface (FA-3) sandstones of the Lower Grandstand (Fig. 2.11). The type examples for the shoreface succession are from Umiat No. 9 (860-940 ft., 965-1085 ft.: Fig. 2.7), which closely resembles the characteristic profile of a wave-dominated shoreface (Bhattacharya and Walker, 1991; Van Wagoner et al., 1990; Hampson, 2000; Hampson and Storms, 2003). The trace fossil assemblage of both *Cruziana* and *Skolithos* type ichnofacies further supports a shoreface interpretation (Frey, 1990; Pemberton and MacEachern, 1995).

In the Lower Grandstand A at both Umiat No. 2 (910-1050 ft.) and No. 11 (2960-3090 ft.: Fig. 2.11), thin lags marked by rip-up clasts interrupt hummocky cross-strata. These features can be found in both shoreface and wave-influenced deltaic environments (Bhattacharya and Walker, 1991; Hampson and Howell, 2005). Though it is possible to distinguish non-deltaic shoreface deposits from wave-influenced deltas in core using physical and biogenic indicators of fluvial discharge (Dafoe et al., 2010), there are not characteristic features that would permit this distinction in the Umiat wells.

The upper part of the Lower Grandstand A shows limited evidence for subaerial exposure beneath a minor flooding surface. There are root traces at the top of Lower Grandstand A in Umiat No. 9 (Fig. 2.7). Immediately above this layer are mudstones of FA-1 with

trace fossils of the *Cruziana* ichnofacies including *Phycosiphon*, *Paleophycus*, and *Planolites* (Fig. 2.6). The abrupt deepening interpreted from facies present above Lower Grandstand A marks the beginning of a second wave-dominated shoreface facies succession in all of the Umiat wells (Fig. 2.11). This second succession, which is capped by brackish water facies of the delta plain or coastal plain environments (FA-5a), comprises Lower Grandstand B.

The top of Lower Grandstand B lies beneath a ~20 ft.-thick sandstone in multiple wells (Fig. 2.11). The base of this sandstone, which consists of distal lower shoreface deposits (FA-2a) with trace fossils of the *Cruziana* ichnofacies, is interpreted to be a transgressive surface of erosion. Transgressive surfaces of erosion cap progradational parasequences and displace changes in bioturbation intensity and character (Gani et al., 2008). The ~20 ft.-thick sandstone represents wave reworking of the shelf during a slow rise in relative sea level associated with a back-stepping shoreline trajectory. The overlying offshore mudstones (FA-1) are part of the Shale Barrier and represent a major flooding surface at the top of the Lower Grandstand.

2.9.2 The Shale Barrier, Upper Grandstand, and Killik: River-Dominated Deltaic System

The Shale Barrier consists of offshore marine mudstone (FA-1) with thin beds of distal lower shoreface sandstone (FA-2a). The abrupt deepening of facies from the Lower Grandstand into the Shale Barrier is interpreted as a maximum flooding surface that represents a rise in relative sea level and an increase in accommodation. In this interpretation, the Shale Barrier, Upper Grandstand, and Killik are genetically linked marine shelf/prodelta (FA-1), delta front (FA-4), and delta plain (FA-5) components of a prograding deltaic system (Fig. 2.13B) that advanced out over the Lower Grandstand. Unlike the Lower Grandstand, the Upper Grandstand sandstone is a single-storey interval, and has a facies succession (Fig. 2.12) consistent with a river-dominated delta interpretation (*sensu* Bhattacharya and Walker, 1991) with no evidence of wave influence. The overlying delta plain mudstones of the Killik are over 300 ft.-thick,

suggesting significant accommodation landward of the delta front. The dominance of brackish water conditions throughout the Killik (May and Shane, 1985) favors a broad, low-angle delta plain subject to influxes of marine water. Improved well control could be used to interpret minor transgressions within the Killik preceding the major transgression described below.

2.9.3 The Ninuluk: Back-Stepping Deltaic System

The Ninuluk-Killik boundary is defined by a shift from mud-dominated delta plain deposits with non-marine microfossil assemblages to sandstones with marine microfossils similar to those found in the Lower and Upper Grandstand (Collins, 1958). In Umiat No. 11 the Ninuluk consists of two, thick sandstone intervals separated by a thin mudstone (Fig 2.9). The two intervals bear many similarities to a pair of sandstone intervals described in outcrop at Umiat Mountain (Houseknecht and Schenk, 2005), though the Ninuluk intervals in the Umiat wells are nearly twice as thick as those described in outcrop. In Umiat No. 11 the ~30 ft.-thick lower Ninuluk sandstoneis interpreted as coalesced, tidally-influenced distributary mouth bar deposits (FA-4: Fig. 2.13C). This interval is similar to the lower Ninuluk sandstone in outcrop that Houseknecht and Schenk (2005) interpreted as an estuary or flood-tidal inlet in a transgressive setting. The basis of their interpretation was the presence of possible herringbone cross-bedding. The decreasing frequency of spores and gymnosperm pollen and increasing frequency of dinoflagellates and acritarchs in the Ninuluk also supports a transgressive interpretation (May and Shane, 1985). The lower Ninuluk in Umiat No. 11 has trough cross-stratification, with sideritized mud drapes, though there is no evidence for herringbone cross-bedding in core. It is also relatively coarse-grained compared to the rest of the Nanushuk Formation. Consequently, the proximal distributary mouth bar deposits in the lower Ninuluk sandstone at Umiat Field are interpreted as part of a back-stepping delta system (Fig. 2.13C).

The upper Ninuluk sandstone interval in the Umiat No. 11 is 50 ft.-thick (Fig. 2.9), with massive, trough-cross laminated, and parallel laminated sandstones (Fig. 2.13C). A

similar wave-influenced upper interval is exposed at Umiat Mountain (Houseknecht and Schenk, 2005). The facies succession in the upper Ninuluk sandstone is most similar to upper shoreface (FA-3) deposits, but may also be deltaic in origin (e.g. delta front). Unlike the other Nanushuk Formation sandstones, the upper Ninuluk contains detrital and authigenic calcite (Collins, 1958; Fox et al., 1979), a possible sign of its transgressive shoreface origin. Calcareous cement can be associated with marine flooding surfaces and transgressive events at the top of highstand systems tracts (Taylor et al., 1995; Ketzer et al., 2002). The upper Ninuluk is a transgressive upper shoreface sandstone with lag deposits at the base, capped by a flooding surface. The thickness of the Ninuluk supports a relatively slow relative sea level rise and corresponding transgressive event, where significant accommodation developed at the same pace as sediment supply. This contrasts with thinner (<20 ft.) transgressive sandstones at the top of the Lower Grandstand.

2.10 Reservoir Potential of Informal Units

The major reservoir intervals at Umiat are the Lower Grandstand and Upper Grandstand sandstones, with additional potential petroleum accumulations in the sandstones of the Killik and Ninuluk. Both the Upper and Lower Grandstand are regionally extensive in the subsurface (Fig. 2.10). The Ninuluk is also extensive, but is eroded from the top of the Umiat anticline structure and is only found on the southern flank and in the footwall (Fig. 2.2). In contrast, sandstones in the Killik are not laterally extensive and are difficult to correlate between wells. Consequently, the Upper and Lower Grandstand are considered the primary reservoirs at Umiat.

Due to the regional extent of the Upper and Lower Grandstand (Fig. 2.10), and the similar thickness for the intervals within the predicted trap limits, it is likely that permeability trends are consistent across the site within each reservoir interval. The upward increase in permeability toward the top of reservoir intervals is apparent in both

vertical and horizontal air permeability results. These trends suggest that permeabilities greater than 10 md are limited to the upper 20-40 ft. of the Upper Grandstand and Lower Grandstand reservoir intervals (Figs. 2.7-2.8).

Permeability trends in both intervals of the Lower Grandstand and in the Upper Grandstand are consistent with increasing porosity related to improved sorting in increasingly high-energy deposits of regressive, upward-coarsening shoreface and deltaic sandstones (Figs. 2.7-2.8). Previous authors hypothesized that winnowing of ductile phyllitic grains by high-energy shoreface deposits was responsible for an increase in porosity at the top of Grandstand sandstones (Bartsch-Winkler, 1985; Huffman et al., 1985; Fox et al., 1979). This increase in permeability may also be related to a decrease in bioturbation intensity in upper shoreface settings (Fig. 2.7) and the lack of bioturbation in deltaic settings (Fig. 2.8). A similar relationship between energy and bioturbation intensity was observed in sandy deposits of the Cretaceous Ferron delta in southern Utah (Li et al., 2011). The trends in the Upper and Lower Grandstand contrast directly with the Ninuluk, a transgressive interval with upward decreasing permeability (Fig. 2.9).

Most of the oil produced from the Nanushuk Formation at Umiat during the 1944-1953 drilling period came from the Upper Grandstand (Molenaar, 1982) but recent studies have revised reservoir estimates for Umiat Field due, in part, to an improved understanding of the Lower Grandstand. Several of the wells crucial to original estimates did reach the Lower Grandstand, including the discovery well (Umiat No. 3). Ice formation and hole caving also prevented drillers from reaching the Lower Grandstand in Umiat No. 6 (Collins, 1958), which is important because the interpreted oil-water contact in the Upper Grandstand lies at 450 ft. below sea level between Umiat No. 6 and Umiat No. 7 (Molenaar, 1982: Fig. 2.2B). New estimates that include the reservoir potential of the Lower Grandstand should increase the amount of producible oil from 70 million bbl (Molenaar, 1982) to 12-15% of the >1.2 billion barrels of oil in place (OOIP) reported in recent assessments of the Umiat Field (Watt et al., 2010; Levi-Johnson, 2010; Hanks et al., in press). This is a range of 180-225 million barrels. Furthermore, separation of the

Lower Grandstand into two intervals adds to the complexity of the reservoir, though both Lower Grandstand A and B can be found in all the wells within the oil-water contact boundaries.

The Ninuluk is a low priority reservoir target, due to its absence by erosion over most of the field and postulated biodegraded oil in the areas where it is present. Contrary to the Grandstand, the upper Ninuluk has an upward decreasing permeability profile (Fig. 2.9) interpreted as an upward-deepening succession of less-winnowed shoreface sandstone. The presence of calcite cement is a likely inhibitor of porosity, further reducing the reservoir quality of the Ninuluk sandstones.

2.11 Conclusions

Umiat, first discovered in 1946, remains undeveloped due to engineering challenges present in a remotely located, shallow, frozen, light-oil field. There is renewed interest in Umiat, however, due to higher oil prices, improvements in technology, and recent gas discoveries in the region. Though the eleven Umiat wells lack modern suites of geophysical well logs, the thousands of feet of core from the wells that are available for examination at the Alaska Geologic Materials Center make it possible to re-interpret Umiat Field using modern facies analysis and stratigraphic concepts. New interpretations of the sedimentology, stratigraphy, and permeability characteristics of the Nanushuk Formation at Umiat Field inidcate a field characterized by laterally extensive shoreface and deltaic sandstones. There are four primary potential reservoir intervals at Umiat: two in the vertically compartmentalized, multi-storey shoreface sandstones of the Lower Grandstand, a river-dominated deltaic reservoir in the Upper Grandstand, and a limited transgressive deltaic/shoreface reservoir in the Ninuluk.

The results of this study have several implications for the development of Umiat Field. Facies-controlled permeability characteristics allowed for improved reservoir simulations, and newly quantified reservoir interval geometries were used to revise and

increase estimates of original oil in place. Despite differences in depositional environments, the Lower Grandstand and Upper Grandstand reservoir intervals both have similar air permeability profiles, and the laterally continuous nature of the intervals make them good targets for horizontal drilling techniques. As the field undergoes a new wave of exploration and further testing of production methods in the coming years, modern subsurface studies should shed further light on the nature of the Nanushuk Formation reservoirs at Umiat.

2.12 Acknowledgements

U.S. Department of Energy contract DE-FC26-08NT0005641 funded this research. The Alaska Division of Geological and Geophysical Surveys (AKDGGS) and Renaissance Alaska, LLC provided additional travel and equipment. This submission benefited from helpful comments and suggestions from Denise Stone and Alan Huckabay. We also thank Ken Papp and the staff of the Alaska Geological Materials Center (a division of AKDGGS), and David LePain and Marwan Wartes of the AKDGGS for their time and expertise. Significant thanks also go to Jeremy Davis, Raelene Wentz, Diudonné Agboada, and Iman Oraki Koshour for research assistance.

2.13 References

Ahlbrandt, T. S., A. C. Huffman Jr., J. E. Fox, and I. Pasternack, 1979, Depositional framework and reservoir-quality studies of selected Nanushuk group outcrops, North Slope, Alaska, *in,* T.S. Ahlbrandt, ed., Preliminary geologic, petrologic, and paleontologic results of the study of Nanushuk Group rocks, North Slope, Alaska: U.S. Geological Survey Circular 794, p. 14-31.

Anderson, D. M., and R. C. Reynolds, 1966, Umiat Bentonite: An Unusual Montmorillonite from Umiat Alaska: American Mineralogist, v. 51, 1443-1455.

Bann, K. L., C. R. Fielding, J. A. MacEachern, and S. C. Tye, 2004, Differentiation of estuarine and offshore marine deposits using integrated ichnology and sedimentology: Permian Pebbly Beach Formation, Sydney Basin, Australia, *in*, D. McIlroy, ed., The Application of Ichnology to Palaeoenvironmental and Stratigraphic Analysis: Lyell Meeting 2003, The Geological Society of London, Special Publication 228, p. 179-211.

Bartsch-Winkler, S. B., 1985, Petrography of sandstones of the Nanushuk Group from four measured sections, central North Slope, Alaska, *in* A. C. Huffman, ed., Geology of the Nanushuk Group and Related Rocks, North Slope, Alaska: U.S. Geological Survey Bulletin 1614, p. 75-97.

Bergquist, H. R., 1958, Micropaleontologic study of the Umiat Field, Northern Alaska, *in* F. R. Collins, ed., Test Wells, Umiat Area Alaska: U.S. Geological Survey Professional Paper 305-B, p. 199-204.

Bhattachaya, J., 2006, Deltas, *in* H. W. Posamentier, and R. G. Walker, eds., Facies Models Revisited: SEPM Special Publication No. 84, p. 237-292.

Bhattacharya, J., and L. Giosan, 2003, Wave-influenced deltas: geomorphological implications for facies reconstruction: Sedimentology, v. 50, p. 187-210.

Bhattacharya, J., and R. G. Walker, 1991, River- and wave-dominated depositional systems of the Upper Cretaceous Dunvegan Formation, northwestern Alberta: Bulletin of Canadian Petroleum Geology, v. 39, p. 165-191.

Bird, K. J., and C. M. Molenaar, 1992, The North Slope foreland basin, Alaska, *in* R. W. Macqueen and D. A. Leckie, eds., Foreland Fold and Thrust Belts: AAPG Memoir 55, p. 363-393.

Blythe, A. E., J. M. Bird, and G. I. Omar, 1996, Deformational history of the central Brooks Range, Alaska: Results from fission-track and $^{40}Ar/^{39}Ar$ analyses: Tectonics, v. 15, p. 440-455.

Buatois, L. A., N. Santiago, K. Parra, and R. Steel, 2008, Animal-substrate interactions in an Early Miocene wave-dominated tropical delta: delineating environmental stresses and depositional dynamics (Tácata field, eastern Venezuela): Journal of Sedimentary Research, v. 78, p. 458-479.

Clifton, H. E., 2006, A reexamination of facies models for clastic shorelines, *in* H. W. Posamentier, and R. G. Walker, eds., Facies Models Revisited: SEPM Special Publication No. 84, p. 293-337

Coakley, B. J., and A. B. Watts, 1991, Tectonic controls on the development of unconformities: the North Slope, Alaska: Tectonics, v. 10, p. 101-130.

Cohen, K. M., S. Finney, and P. L. Gibbard, 2013, International Chronostratigraphic Chart: International Commission on Stratigraphy. http://www.stratigraphy.org/ICSchart/ChronostratChart2013-01.pdf.

Coleman, J. M., 1988, Dynamic changes and processes in the Mississippi River delta: Geological Society of America Bulletin, v. 100, p. 999-1015.

Coleman, J. M., and S. M. Gagliano, 1965, Sedimentary structures, Mississippi River deltaic plain: Trans Gulf-Coast Ass. Geol. Socs., v. 14, p. 67-80.

Collins, F. R., 1958, Test Wells, Umiat Area Alaska: U.S. Geological Survey Professional Paper 305-B, 206 p.

Dafoe, L. T., M. K. Gingras, and S. G. Pemberton, 2010, Wave-influenced deltaic sandstone bodies and offshore deposits in the Viking Formation, Hamilton Lake area, south-central Alberta, Canada: Bulletin of Canadian Petroleum Geology, b. 58, p. 173-201.

Decker, P. L., 2007, Brookian sequence stratigraphic correlations, Umiat Field to Milne Point field, west-central North Slope, Alaska: Alaska Division of Geological and Geophysical Surveys Preliminary Interpretive Report 2007-2, 21 p.

Detterman, R. L., 1956, New and redefined nomenclature of the Nanushuk group, *in,* G. Gryc, and others, eds., Mesozoic Sequence in Colville River Region, Northern Alaska: American Association of Petroleum Geologists Bulletin v. 40, p. 233-244.

Dott Jr., R. H. and J. Bourgeois, 1982, Hummocky stratification: significance of its variable bedding sequences: Geological Society of America Bulletin, v. 93, p. 663-680.

Dumas, S., and R. W. C. Arnott, 2006, Origin of hummocky and swaley cross-stratification–the controlling influence of unidirectional current strength and aggradation rate: Geology, v. 34, p. 1073-1076.

Elliot, T., 1974, Interdistributary bay sequences and their genesis: Sedimentology, v. 21, p. 611-622.

Flint, A. G., 1988, Sharp-based shoreface sequences and "offshore bars" in the Cardium Formation of Alberta: Their relationship to relative changes in sea level, *in* Sea-Level Changes-An Integrated Approach: SEPM Special Publication No. 42, p. 357-370.

Fox, J. E., P. W. Lambert, J. K. Pitman, and C. H. Wu, 1979, A study of reservoir characteristics of the Nanushuk and Colville Groups, Umiat Test Well 11, National Petroleum Reserve in Alaska: U.S. Geological Survey Circular 820, 47 p.

Frey, R. W., 1990, Trace fossils and hummocky cross-stratification, Upper Cretaceous of Utah: PALAIOS, v.5, p. 203-218.

Gani, M. R., J. P. Bhattacharya, and J. A. MacEachern, 2008, Using ichnology to determine relative influence of waves, storms, tides, and rivers in deltaic deposits: Examples from Cretaceous Western Interior Seaway, U.S.A., *in*, J. A. MacEachern, K. L. Bann, M. K. Gingras, and S. G. Pemberton, eds., Applied Ichnology, SEPM Short Course Notes No. 52, p. 209-225.

Gingras, M. K., J. A. MacEachern, and S. E. Dashtgard, 2011, Process ichnology and the elucidation of physico-chemical stress: Sedimentary Geology, v. 237, p. 115-134.

Gryc, G., ed., 1988, Geology and Exploration of the National Petroleum Reserve in Alaska, 1974-1982: U.S. Geological Survey Professional Paper 1399, 940 p.

Hampson, G. J. 2000, Discontinuity surfaces, clinoforms, and facies architecture in a wave-dominated, shoreface-shelf parasequence: Journal of Sedimentary Research, v. 70, p. 325-340.

Hampson, G. J., and J. A. Howell, 2005, Sedimentologic and geomorphic characterization of ancient wave-dominated deltaic shorelines: Upper Cretaceous Blackhawk Formation, Book Cliffs, Utah, U.S.A., *in* L. Giosan and J.P. Bhattacharya, eds., River Deltas—Concepts, Models, and Examples: SEPM Special Publication No. 83, p. 133-154.

Hampson, G. J., and J. E. A. Storms, 2003, Geomorphological and sequence stratigraphic variability in wave-dominated, shoreface-shelf parasequences: Sedimentology, v. 50, p. 667-701.

Hanks, C., G. Shimer, I. Oraki-Kohshour, R. Wentz, M. Ahmadi, P. McCarthy, and A. Dandekar, Integrated reservoir characterization and simulation of a shallow, light oil, low temperature reservoir: Umiat Field, National Petroleum Reserve, Alaska: AAPG Bulletin, in press.

Holmes, S. P., and N. Miller, 2006, Aspects of the ecology and population genetics of the bivalve *Corbula gibba*: Marine Ecology Progress Series, v. 315, p. 129-140.

Houseknecht, D. W., and C. J. Schenk, 2005, Sedimentology and sequence stratigraphy of the Cretaceous Nanushuk, Seabee, and Tuluvak formations exposed on Umiat Mountain, North-Central Alaska: U.S. Geological Survey Professional Paper 1709-B, 18 p.

Houseknecht, D. W., K. J. Bird, and C. J. Schenk, 2009, Seismic analysis of clinoform depositional sequences and shelf-margin trajectories in Lower Cretaceous (Albian) strata, Alaska North Slope: Basin Research, v. 21, p. 644-654.

Hubbard, R. J., S. P. Edrich, and P. Rattey, 1987, Geologic evolution and hydrocarbon habitat of the 'Arctic Alaska microplate': Marine and Petroleum Geology, v. 4, p. 2-34.

Huffman Jr., A. C., ed., 1985, Geology of the Nanushuk Group and Related Rocks, North Slope, Alaska: U.S. Geological Survey Bulletin 1614, 129 p.

Huffman Jr., A. C., T. S. Ahlbrandt, I. Pasternack, G. D. Stricker, and J. E. Fox, 1985, Depositional and sedimentologic factors affecting the reservoir potential of the Cretaceous Nanushuk Group, central North Slope, Alaska, *in* A. C. Huffman, ed., Geology of the Nanushuk Group and Related Rocks, North Slope, Alaska: U.S. Geological Survey Bulletin 1614, p. 61-74.

Ketzer, J. M., S. Morad, R. Evans, and I. S. Al-Aasm, 2002, Distribution of diagenetic alterations in fluvial, deltaic, and shallow marine sandstones within a sequence stratigraphic framework: evidence from the Mullaghmore Formation (Carboniferous), NW Ireland: Journal of Sedimentary Research, v. 72, p. 760-774.

Lamb, M. P., P. M. Myrow, C. Lukens, K. Houck, and J. Strauss, 2008, Deposits from wave-influenced turbidity currents: Pennsylvanian Miniturn Formation, Colorado, U.S.A.: Journal of Sedimentary Research, v. 78, p. 480-498.

Legg, G. W., and R. Brockway, 1983, Geological Report Seabee Test Well No. 1: U.S. Geological Survey Report, 79 p.

LePain, D. L., and R. Kirkham, 2001, Potential reservoir facies in the Nanushuk Formation (Albian-Cenomanian), central North Slope, Alaska: Examples from outcrop and core, *in,* D.W. Houseknecht, ed., NPRA Core Workshop - Petroleum Plays and Systems in the National Petroleum Reserve – Alaska: SEPM Core Workshop No. 21, p. 19-36

LePain, D. L., P. J. McCarthy, and R. Kirkham, 2009, Sedimentology, stacking patterns, and depositional systems in the middle Albian-Cenomanian Nanushuk Formation in outcrop, Central North Slope, Alaska: Alaska Division of Geological and Geophysical Surveys Report on Investigations 2009-1, 86 p.

Levi-Johnson, I. O., 2010, Petrophysical Property Modeling of Umiat Field, a Frozen Oil Reservoir, Master's Thesis, University of Alaska Fairbanks, 144 p.

Li, W., J. P. Bhattacharya, Y. Zhu, D. Garza, and E. Blankenship, 2011, Evaluating delta asymmetry using three-dimensional facies architecture and ichnological analysis, Ferron 'Notom Delta', Capital Reef, Utah, USA: Sedimentology, v. 58, p. 478-507.

MacEachern, J. A., K. L. Bann, J. P. Bhattacharya, and C. D. Howell, 2005, Ichnology of Deltas: Organism response to the dynamic interplay of rivers, waves, storms and tides, *in* L. Giosan, and J. P. Bhattacharya, eds., River Deltas—Concepts, Models, and Examples, SEPM Special Publication No. 83, p. 49-85.

May, F. E., and J. D. Shane, 1985, An analysis of the Umiat delta using palynologic and other data, North Slope, Alaska, *in* A. C. Huffman, ed., Geology of the Nanushuk Group and Related Rocks, North Slope, Alaska: U.S. Geological Survey Bulletin 1614, p. 97-120.

Molenaar, C. M., 1982, Umiat Field, an oil accumulation in a thrust-faulted anticline, North Slope of Alaska, *in,* R. B. Powers, ed., Geologic Studies of the Cordilleran Thrust Belt: Rocky Mountain Association of Geologists, v. 2, p. 537-548.

Molenaar, C. M., 1985, Subsurface correlations and depositional history of the Nanushuk Group and related strata, North Slope, Alaska, *in* A. C. Huffman, ed., Geology of the Nanushuk Group and Related Rocks, North Slope, Alaska: U.S. Geological Survey Bulletin 1614, p. 37-60.

Moore, T. E., W. K. Wallace, K. J. Bird, S. M. Karl, C. G. Mull, and J. T. Dillon, 1994, Geology of Northern Alaska, *in* The Geology of North America, v. G-1, The Geology of Alaska: Geological Society of America, p. 49-140.

Mull, C. G., 1985, Cretaceous tectonics, depositional cycles, and the Nanushuk group, Brooks Range and Arctic Slope, Alaska, *in* A. C. Huffman, ed., Geology of the Nanushuk Group and Related Rocks North Slope, Alaska: U.S. Geological Survey Bulletin 1614, p. 7-36.

Mull, C. G., D. W. Houseknecht, and K. J. Bird, 2003, Revised Cretaceous and Tertiary stratigraphic nomenclature in the Colville Basin, northern Alaska: U.S. Geological Survey Professional Paper 173, 51 p.

Mull, C. G., D. W. Houseknecht, G. H. Pessel, and C. P. Garrity, 2004, Geologic map of the Umiat quadrangle, Alaska: U.S. Geological Survey Scientific Investigations Map 2817-A, scale 1:250,000.

Myrow, P. M., W. Fischer, and J. W. Goodge, 2002, Wave-modified turbidites: combined flow shoreline and shelf deposits, Cambrian, Antarctica: Journal of Sedimentary Research, v. 72, p. 641-656.

Myrow, P. M., and J. B. Southard, 1996, Tempestite deposition: Journal of Sedimentary Research, v. 66, p. 875-887.

Nelson, C. H., 1982, Modern shallow-water graded sand layers from storm surges, Bering Shelf: a mimic of Bouma sequences and turbidite systems: Journal of Sedimentary Petrology, v., 52, p. 537-545.

Nunn, J. A., M. Czerniak, and R. H. Pilger Jr., 1987, Constraints on the structure of Brooks Range and Colville Basin, northern Alaska, from flexure and gravity analysis: Tectonics, v. 6, p. 603-617.

Olariu, C., and J. P. Bhattacharya, 2006, Terminal distributary channels and delta front architecture of river-dominated delta systems: Journal of Sedimentary Research, v. 76, p. 212-233.

O'Sullivan, P. B., J. M. Murphy, and A. E. Blythe, 1997, Late Mesozoic and Cenozoic thermotectonic evolution of the central Brooks Range and adjacent North Slope foreland basin, Alaska: Including fission track results from the Trans-Alaska Crustal Transect (TACT): Tectonics, v. 102, p. 20,821-20,845.

Paola, C. S. M. Wiele, and M. A. Reinhart, 1989, Upper-regime parallel lamination as the result of turbulent sediment transport and low-amplitude bed forms: Sedimentology, v. 36, p. 47-59.

Pattison, S. A. J., 2005, Storm-influenced prodelta turbidite complex in the Lower Kenilworth Member at Hatch Mesa, Book Cliffs, Utah, U.S.A.: Implications for shallow marine facies models: Journal of Sedimentary Research, v. 75, p. 420-439.

Pattison, S. A. J., 1995, Sequence stratigraphic significance of sharp-based lowstand shoreface deposits, Kenilworth Member, Book Cliffs, Utah: AAPG Bulletin v. 79, p. 444-462.

Pemberton, S. G., and J. A. MacEachern, 1995, The sequence stratigraphic significance of trace fossils: examples from the Cretaceous foreland basin of Alberta, Canada, *in* J. C. Van Wagoner and G. T. Bertram, eds., Sequence Stratigraphy of Foreland Basin Deposits: Outcrop and Subsurface Examples from the Cretaceous of North America: American Association of Petroleum Geologists, Memoir 64, p. 429-475.

Pratt, B. R., 1998, Syneresis cracks: subaqueous shrinkage in argillaceous sediments caused by earthquake-induced dewatering: Sedimentary Geology, v. 117, p. 1-10.

Schindler, J. F., 1988, History of exploration in the National Petroleum Reserve in Alaska, with emphasis on the period from 1975-1982, *in* G. Gryc, ed., Geology and Exploration of the National Petroleum Reserve in Alaska, 1974-1982: U.S. Geological Survey Professional Paper 1399, p. 13-76.

Taylor, K. G., R. L. Gawthorpe, and J. C. Van Wagoner, 1995, Stratigraphic control on laterally persistent cementation, Book Cliffs, Utah, Journal of the Geological Society, v. 152, p. 225-228.

Van Wagoner, J. C., R. M. Mitchum, K. M. Campion, and V. D. Rahmanian, 1990, Siliciclastic sequence stratigraphy in well logs, cores, and outcrops: AAPG Methods in Exploration 7, 55 p.

Watt, J., A. Huckabay, and M. R. Landt, 2010, Umiat: a North Slope giant primed for oil development: Oil and Gas Journal, v. 108, p. 30-38.

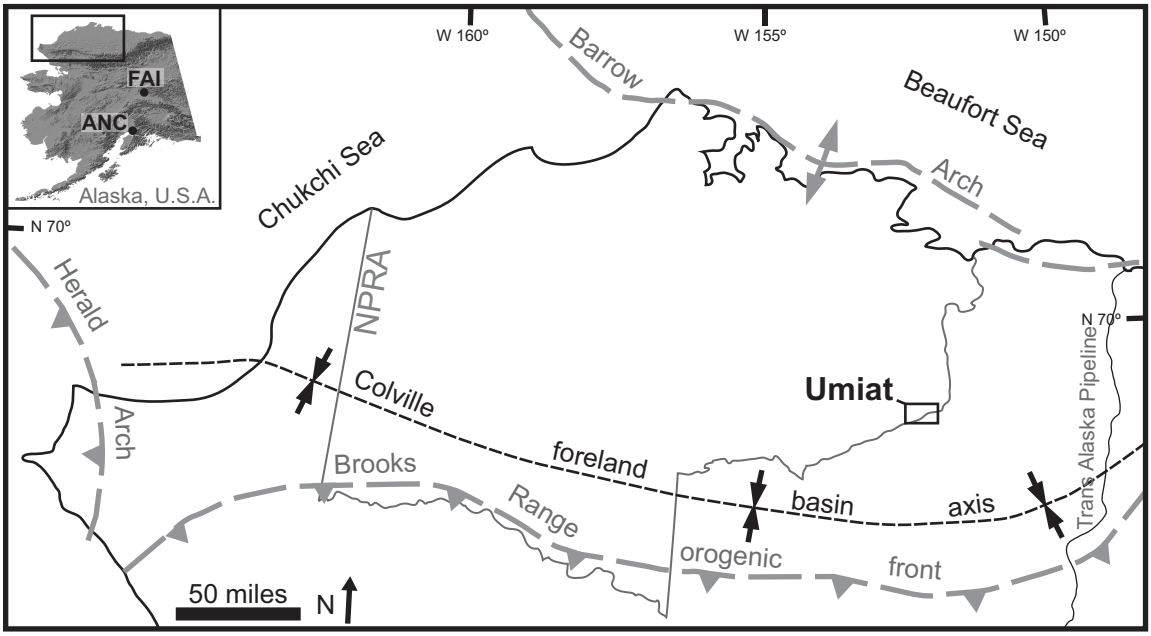

Figure 2.1 Map of the North Slope of Alaska Depicting Major Geologic Features
Location of Umiat Field (black rectangle) in relation to the axis of the Colville foreland basin, the thrust front of the Brooks Range, and the Herald and Barrow arches (modified from Decker, 2007). The Colville River forms the eastern boundary of the National Petroleum Reserve–Alaska (NPRA). Inset (upper left): digital elevation model of Alaska with the study area outlined in black and Fairbanks (FAI) and Anchorage (ANC) for reference.

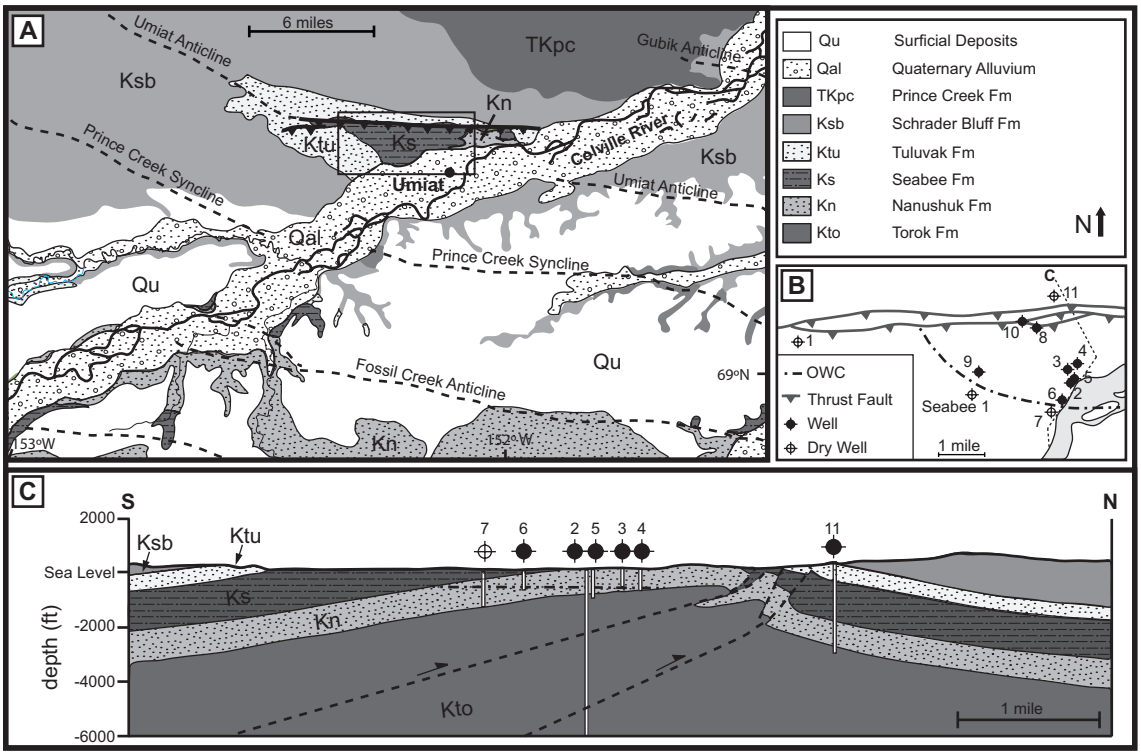

Figure 2.2. Regional Geologic Map and Structure of the Umiat Area.
(A) Geologic map of the Umiat area (modified from Mull et al., 2004). Surface exposure of the Nanushuk Formation is limited. Note the orientation of major anticlines and synclines, indicative of the fold-and-thrust origin of the Brooks Range foothills. The black rectangle shows the location of Figure 2.2B For the location of 2.2A see Figure 2.1 The north arrow in the legend is for 2.2A and 2.2B. (B) Locations of the eleven Umiat wells and the Seabee No. 1 well. Dash-dot line indicates oil-water contact on the south side of the Umiat anticline, while dashed line marks the trace of the cross section in Figure 2C. (C) North-south cross-section of Umiat anticline with basic stratigraphy, major thrust faults (dashed lines), and well locations (modified from Molenaar 1982). Dash-dot line indicates the Nanushuk Formation (Kn) oil-water contact.

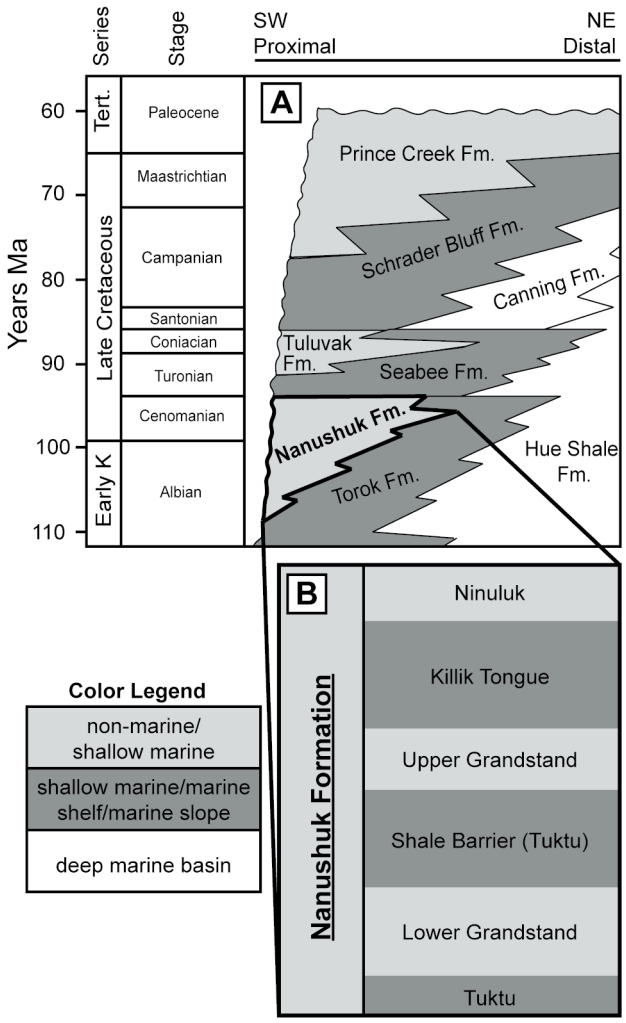

Figure 2.3 Stratigraphic Column of Brookian Formations in the Colville Basin.
(A) Brookian stratigraphic units of the Colville Basin relevant to this study. Nanushuk Formation outlined in bold (modified from Mull et al., 2003). A shaded legend refers to the generalized depositional environments for each formation. (B) Informal subsurface stratigraphy of the Nanushuk Formation in common usage at Umiat Field.

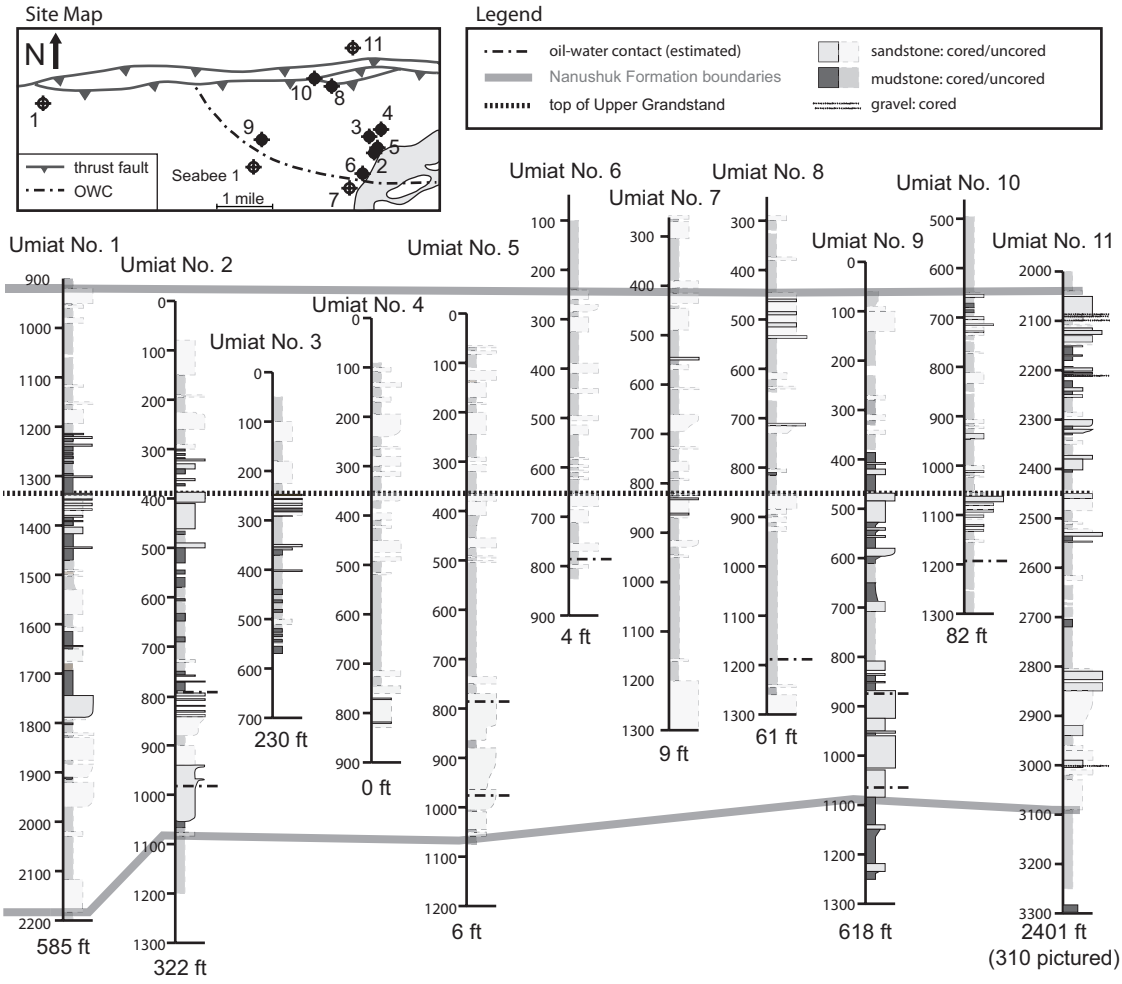

Figure 2.4 Summary of Wells and Cores
Stratigraphic sections the eleven wells at Umiat Field (Figs. 2.1 and 2.2), illustrating the Nanushuk Formation. The inset map shows the location of each well. In the stratigraphic sections cored intervals are darkened, while un-cored intervals are lightly shaded. Totals at the bottom of each well indicate the amount of core described for each well. Not all of the described core is illustrated; some is from outside of the Nanushuk Formation (Torok, Seabee, and Tuluvak formations). The estimated position of the oil-water contact in wells with oil shows that reached sufficient depth is also shown. The stratigraphic sections are "hung" on the top of the Upper Grandstand sandstone.

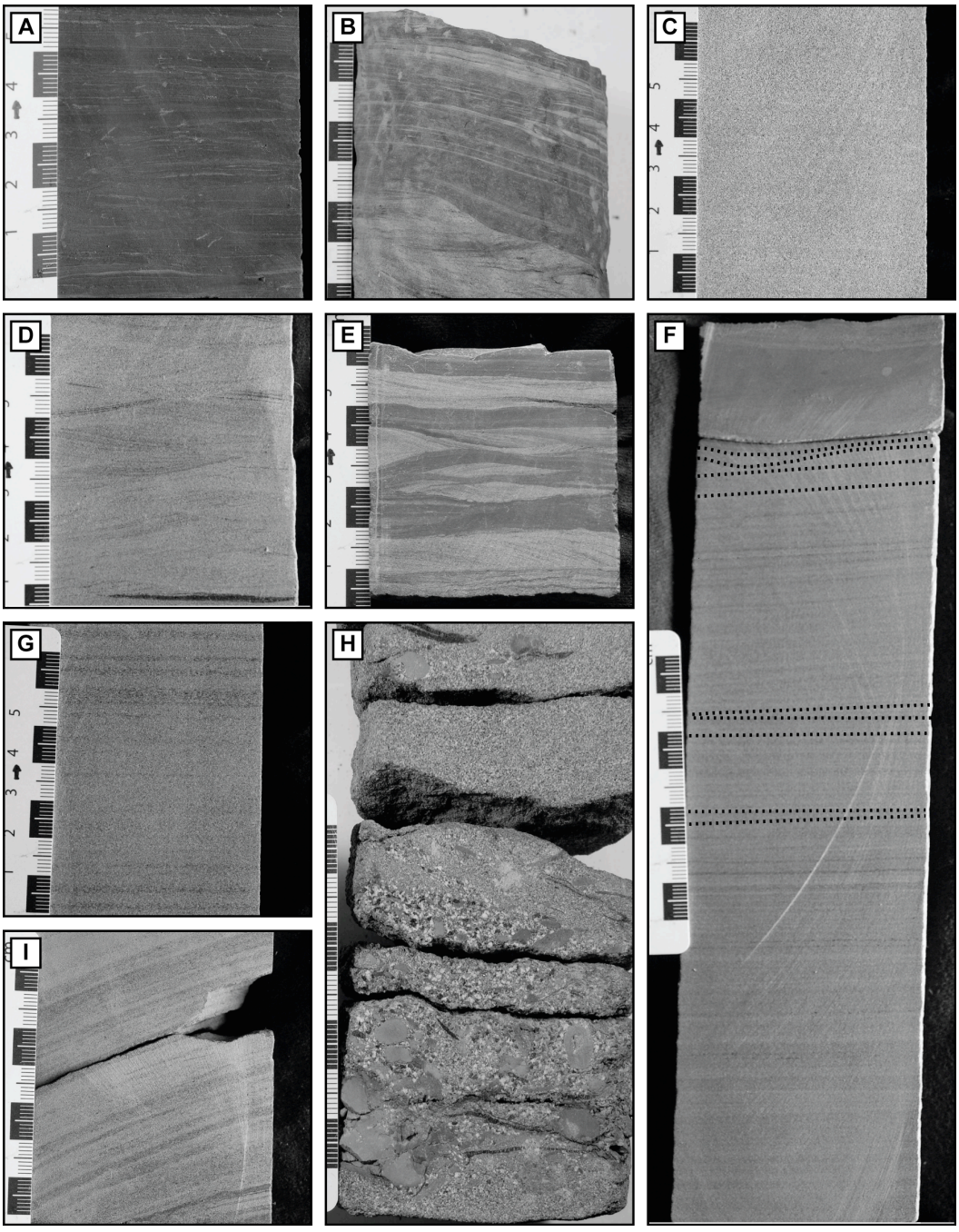

Figure 2.5 Photographs of Sedimentary Facies.
Core photographs from the Nanushuk Formation at Umiat field showing selected sedimentary facies described in the text. (A) F-1, laminated mudstone (B) F-3, wavy/lenticular bedded mudstone (C) F-4, apparently massive sandstone, with possible faint parallel bedding (D) F-6, ripple cross-laminated sandstone (E) F-7, mud-draped ripple cross-laminated sandstone (F) F-5, low-angle cross-laminated sandstone, with dotted lines to highlight lamination surfaces (G) F-8, parallel laminated sandstone (H) F-10, poorly-sorted, normally-graded sand and gravel (I) F-9, trough cross-bedded sandstone with foreset dips >15º. Not pictured: F-2 mudstone; F-11 coal; F-12 bentonite; F-13 lag deposits.

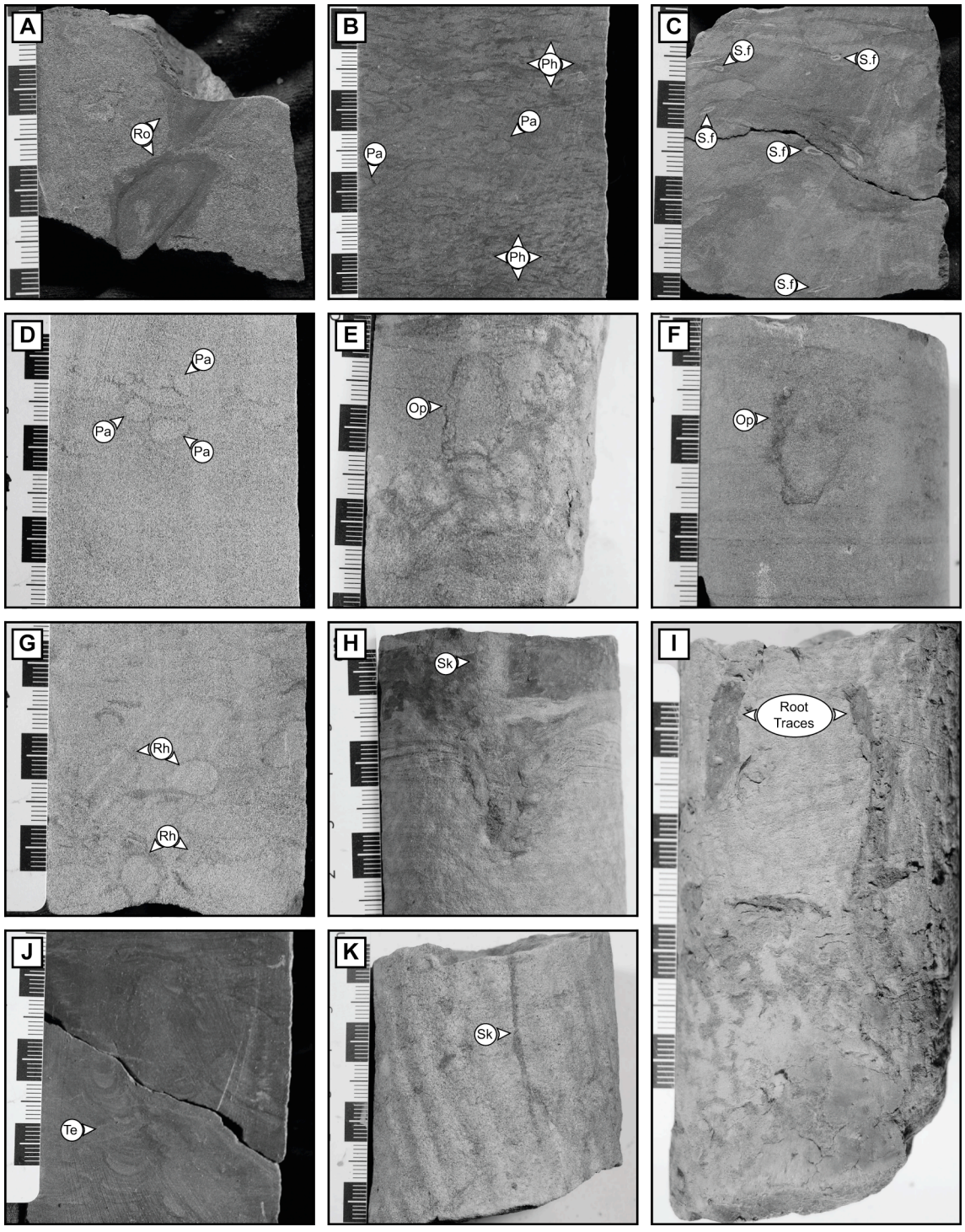

Figure 2.6 Photographs of Trace Fossils (Ichnology)
Examples of trace fossils observed in core. (A) *Rosselia* (B) *Phycosiphon* and *Paleophycus* (C) *Schaubcylindrichnus freyi* (D) *Paleophycus* (E) *Ophiomorpha* (F) *Ophiomorpha* (G) *Rhizocorallium* (H) *Skolithos* (I) Root traces (J) faint *Teichichnus* (K) *Skolithos*.

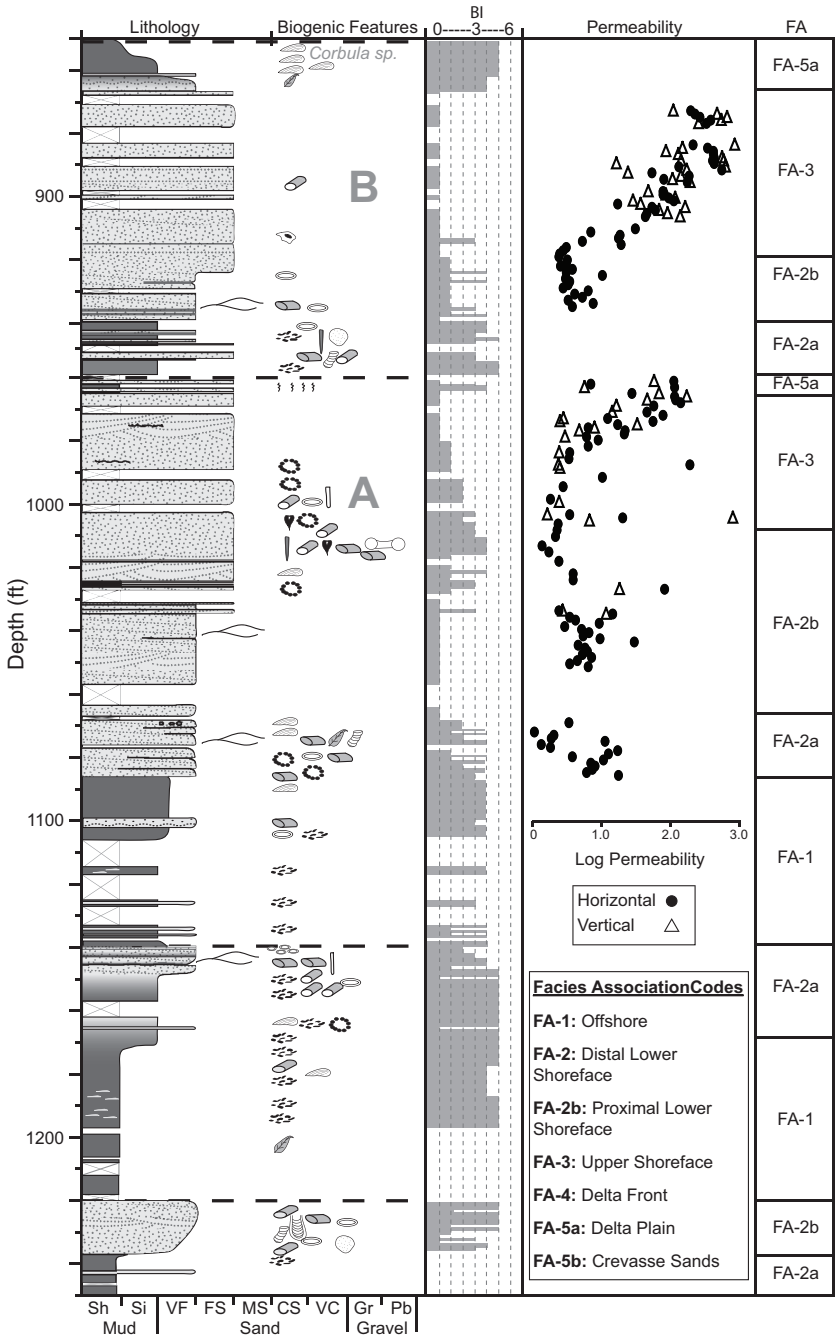

Figure 2.7 Facies Associations 1, 2 and 3, Umiat No. 9.
Four upward-coarsening successions (bounded by dashed lines) consist of offshore (FA-1), distal lower shoreface (FA-2a), proximal lower shoreface (FA-2b), and upper shoreface (FA-3) deposits in Umiat No. 9. This multi-storey shoreface succession is typical of the Lower Grandstand in the Umiat wells. Thin delta plain (FA-5a) mudstones occur at the top of the two uppermost shoreface sandstones. Bioturbation intensity is highest in muddy or heterolithic deposits, and decreases as sand beds become amalgamated from 1020-970 ft. and 920-870 ft. Permeability, in contrast, increases towards the top of shoreface successions (990-970 ft. and 930-870 ft.). A and B refer to reservoir units. See Figure 7 for complete symbol legend.

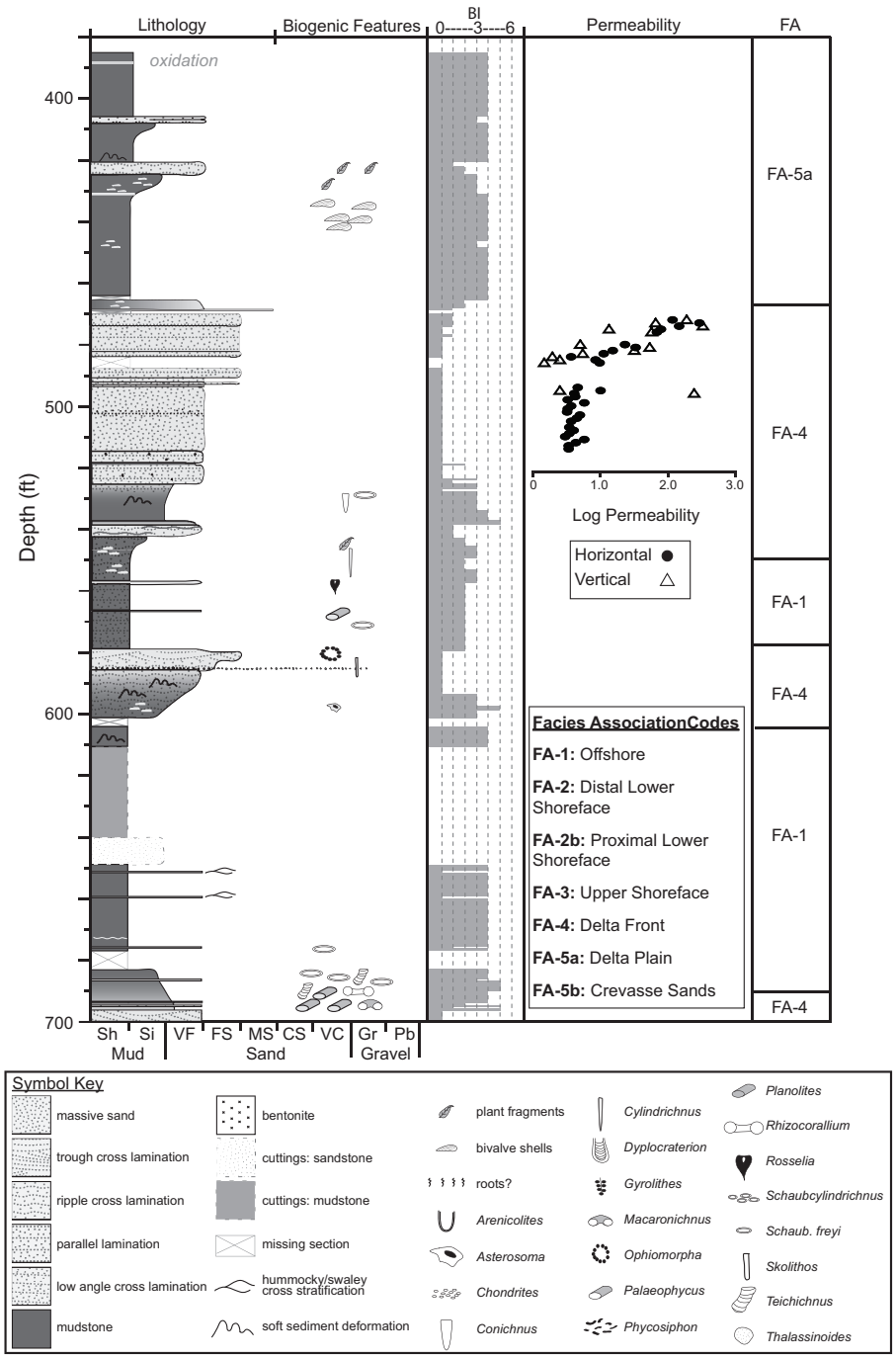

Figure 2.8 Facies Associations 1, 3, and 4, Umiat No. 9.
An upward-coarsening delta-front succession from 580-470 ft. in Umiat No. 9 consists of prodelta (FA-1), delta front (FA-4), and delta plain (FA-5) deposits. The single-storey delta front succession is typical of the Upper Grandstand in the Umiat wells. Bioturbation intensity is low, even in prodelta or distal delta front deposits (580-530 ft.). Permeability increases towards the top of the delta front sands (490-470 ft.). The lighter shaded areas with dashed lines (610-650 ft.) are interpretations based on original cuttings data (Collins, 1958).

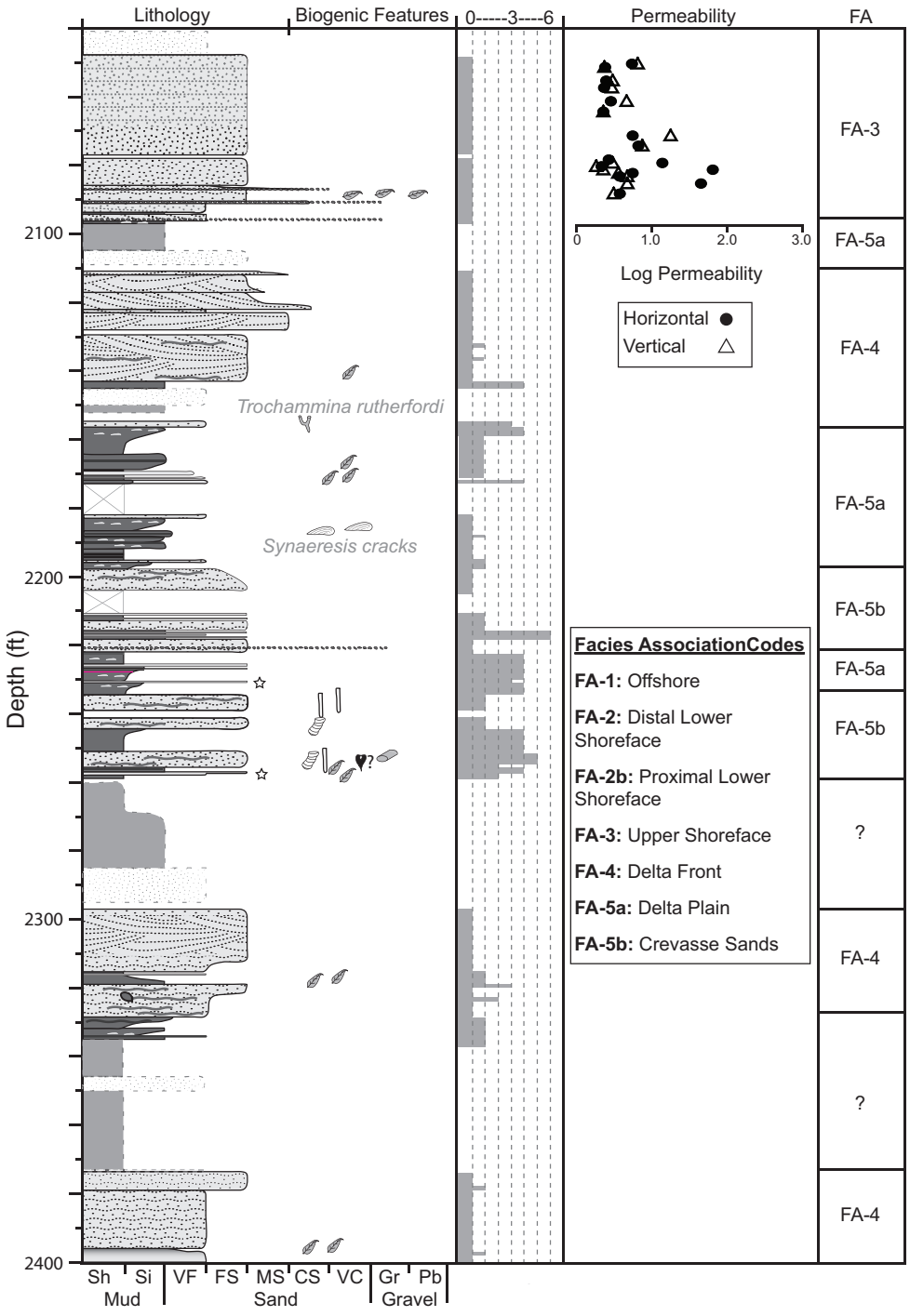

Figure 2.9 Facies Associations 3, 4, and 5, Umiat No. 11.
Umiat No. 11 is the only well with a complete succession of delta plain deposits in core, including interdistributary bay (FA-5a) and crevasse splay (FA-5b) facies associations. A thick sandstone at the top of the delta plain succession (2095-2040 ft.) is transgressive in origin and shows a reverse trend in permeability compared to lower sandstones (Figs. 2.7 and 2.8). Lighter shaded areas with dashed lines are interpretations based on original cuttings data (Collins, 1958). See Figure 7 for complete symbol legend.

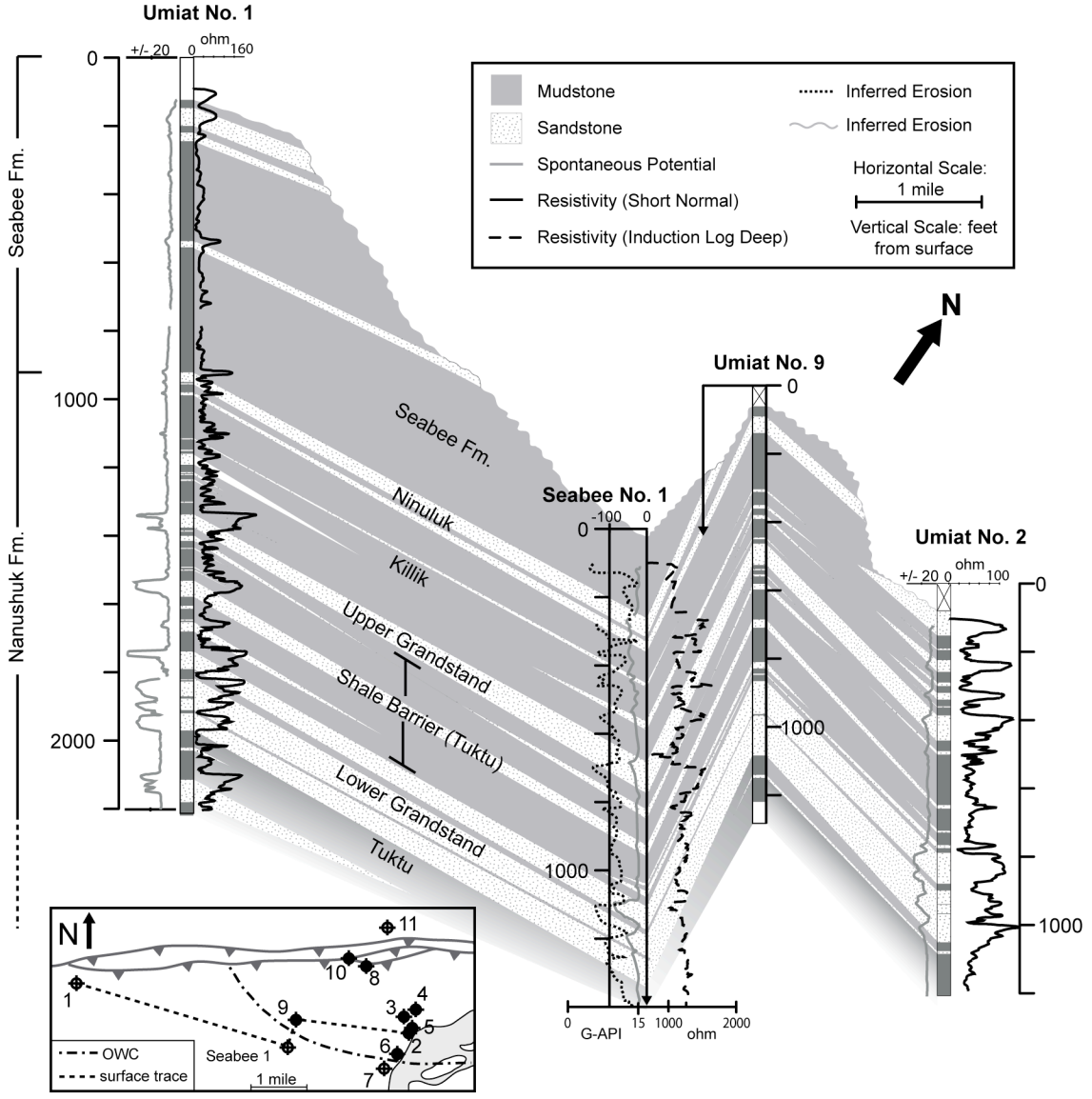

Figure 2.10 Fence Diagram of Umiat No. 1, 9, and 2, and Seabee No. 1.
Interpretations based on core description (this paper), cuttings (Collins, 1958), and well logs (Collins, 1958; Legg and Brockway, 1983). Umiat No. 9 is shifted slightly to the north in diagram to distinguish it from Seabee No. 1 well. The base of the Nanushuk Formation (Tuktu) is undetermined. The Lower Grandstand (shoreface), Upper Grandstand (delta-front), and Ninuluk sandstone reservoir units are laterally extensive, though the Ninuluk is largely eroded in the eastern part of Umiat field. It is difficult to correlate sandstones in the Killik and Shale Barrier (Tuktu) portions of the Nanushuk Formation, but some thin sands may represent the same surface. Inset map shows surface trace of fence diagram (dashed line). Oil-water contact in Upper Grandstand passes between Umiat No. 9 and Seabee No. 1, as shown in the inset map (dash-dot line).

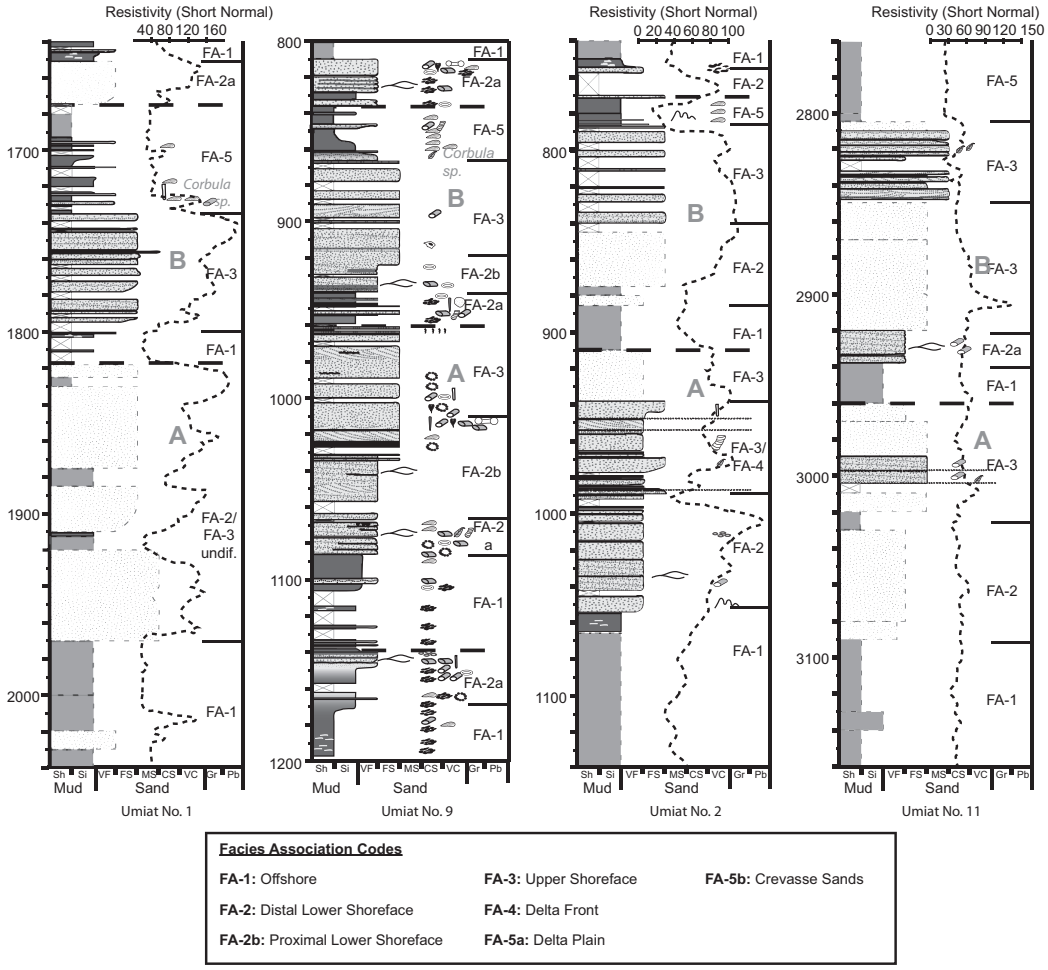

Figure 2.11 The Lower Grandstand
Segments of measured sections from Umiat wells 1, 9, 2 and 11 showing multi-storey shoreface deposits of the Lower Grandstand. Wells arranged in rough west-to-east order from left-to-right. A flooding surface separates reservoir units Lower Grandstand A and B (thick dashed line). The top of the Lower Grandstand includes delta plain mudstones and is capped by a transgressive sandstone in each well except Umiat No. 11. Lighter shaded areas with dashed lines are interpretations based on original cuttings data (Collins, 1958). See Figure 7 for symbol legend.

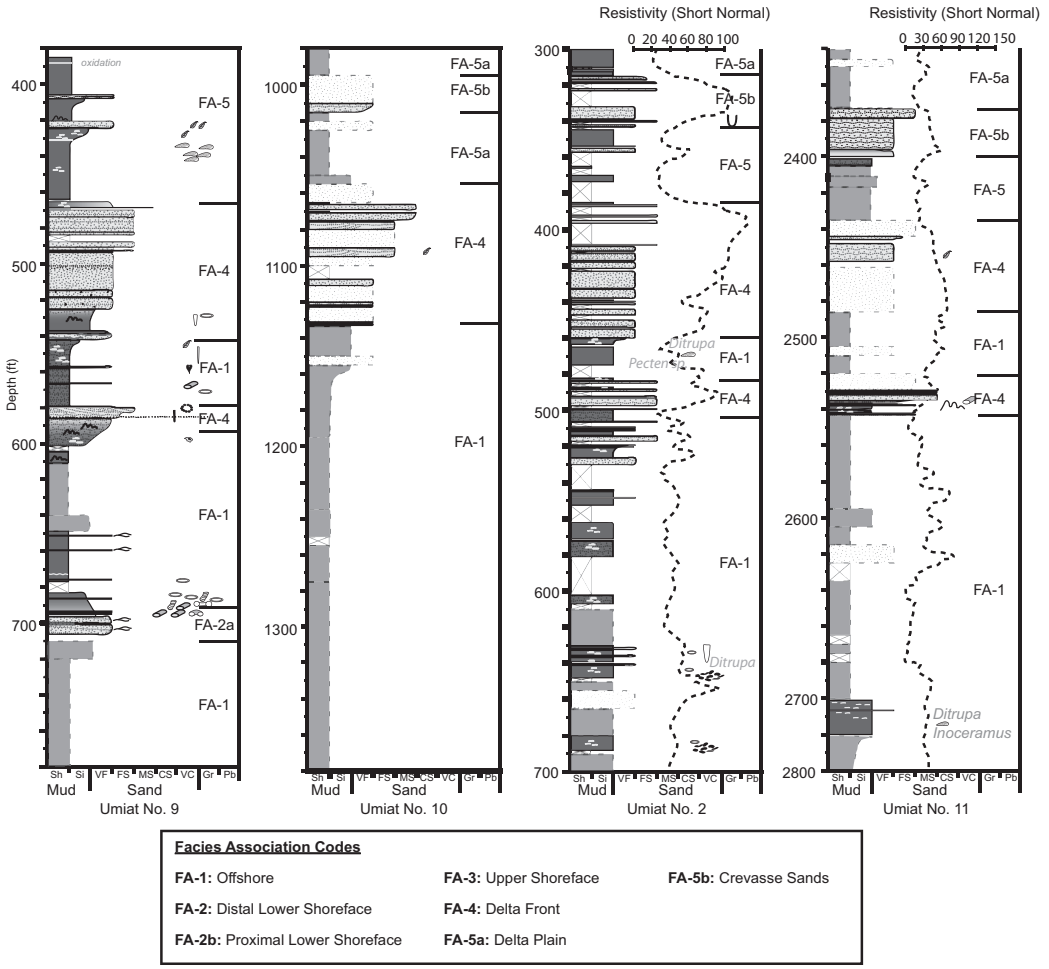

Figure 2.12 The Upper Grandstand
Segments of measured sections from Umiat wells 9, 10, 2 and 11 showing ~60-70 ft.-thick Upper Grandstand of the Nanushuk Formation. Wells arranged in rough west-to-east order from left-to-right. The Upper Grandstand is interpreted as distributary mouth bar deposits of a river-dominated delta. Lighter shaded areas with dashed lines are interpretations based on original cuttings data (Collins, 1958). See Figure 7 for symbol legend.

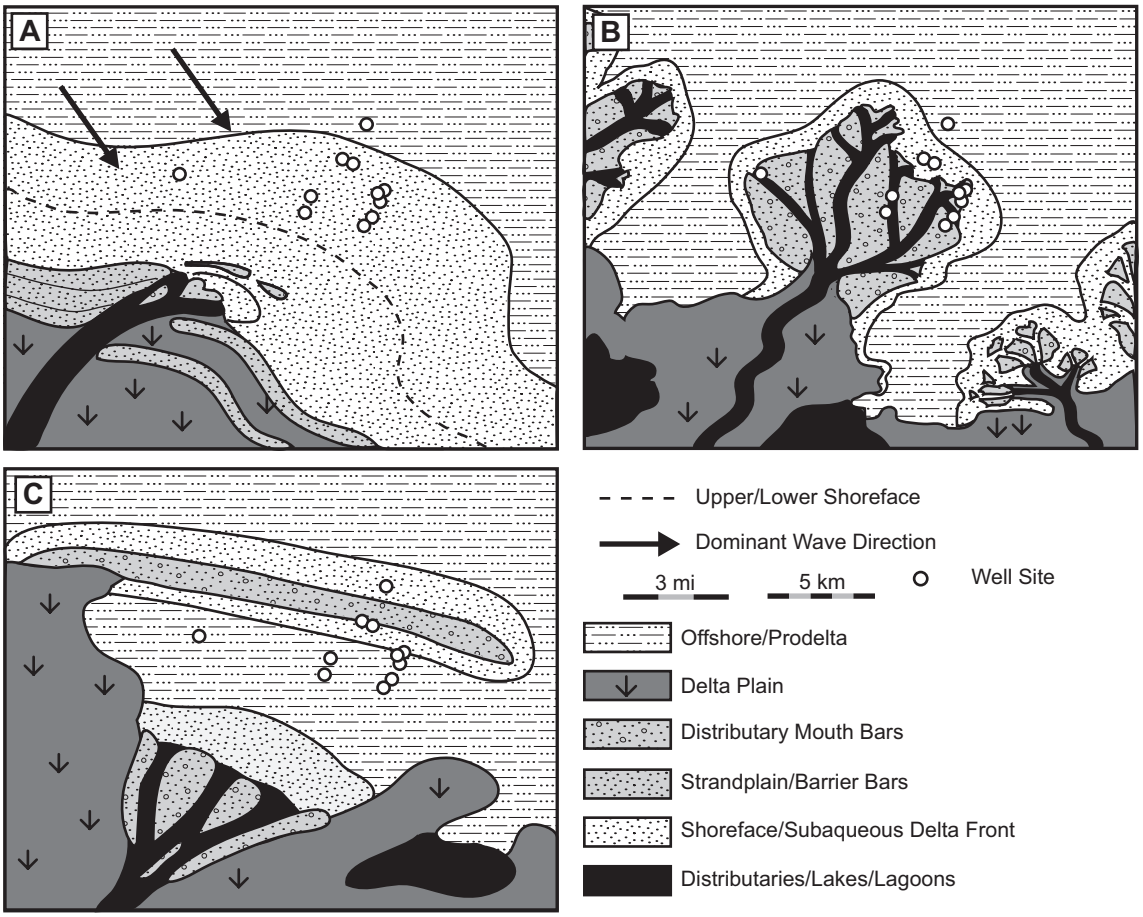

Figure 2.13 Nanushuk Formation Depositional Environments
Schematic cartoons illustrating interpretations for Lower Grandstand (A), Upper Grandstand/Killik Tongue (B), and Killik/Ninuluk (C) depositional environments, with the locations of the Umiat wells for reference. The Lower Grandstand consists of shoreface sandstones, interpreted as being deposited in a wave-influenced deltaic setting. The inferred wave direction is based on modern shoreline currents. The Upper Grandstand and Killik were deposited in a river-dominated deltaic setting by delta front (Upper Grandstand) and delta plain (Killik) processes. The Ninuluk includes both tidally influenced delta front sandstones and overlying transgressive shoreface sandstones.

Table 2.1 Facies Defined from Core at Umiat Field.

Facies	Diagnostic Features	Process Interpretation
F-1: Silty Shale	Laminated silty mudstone with color dependent on both grain size and organic matter content. Laminations are parallel/subparallel. Grades up into F-3 in some settings. BI of 3 or less.	Suspension settling in low energy settings. Well-preserved laminations may indicate low oxygen (dysoxic) conditions that inhibit biogenic activity.
F-2: Mudstone	a. Dark grey to black shale to sandy silt, with color dependent on both grain size and organic matter content. Some red-orange staining is present. Either massive, or with a BI of 4 or greater: individual traces are discernable, but bedding features are indistinct. Includes a wide range of trace fossils. Bivalve and gastropod shells present.	Suspension settling in an environment that supports significant biogenic activity. Red-orange staining may indicate exposure to the atmosphere or diagenetic alteration.
	b. carbonaceous mudstone, with common plant fossils and bivalve fossils.	Accumulation of organic matter and mud in water-saturated and poorly oxygenated lake or bay environments.
F-3: Lenticular-Wavy Bedded Mudstone	Dark grey lenticular to wavy bedded mudstone. Very fine to fine-grained sand or silty laminations (1-5 cm thick) have internal ripple cross-laminations.	Suspension settling interrupted by rare unidirectional currents.
F-4: Apparently Massive Sandstone	Light grey, well-sorted, very fine- to fine-grained sandstone with rare beds of medium sandstone. No visible structures, but rare carbonaceous partings.	Lack of visible structure due to rapid deposition, high degree of sorting, dewatering, or cryptobioturbation.
F-5: Low Angle Cross-Laminated Sandstone	Light grey, well-sorted very fine- to fine-grained sandstone. Low angle laminations dip <15º and show changes in thickness. Beds 0.5-2 m thick. Associated features include mudstone rip-up clasts and shell lags.	Hummocky to swaley cross-stratification deposited by oscillatory currents. (Dott and Bourgeois, 1982)
F-6: Ripple Cross-Laminated Sandstone	a. Light grey very fine- to fine-grained asymmetrical ripple cross-laminated sandstone. Mudstone laminations are common.	Ripple migration under unidirectional currents as part of larger, subaqueous bar-forming processes.
	b. Light grey very fine- to fine-grained symmetrical ripple cross-laminated sandstone. Mudstone laminations are common.	Ripple formation under oscillatory currents.
F-7: Mud Draped Ripple Cross-Laminated Sandstone	Light grey to tan, fine- to medium-grained ripple cross-laminated sandstones with cm-thick, oxidized mud drapes.	Mixed energy conditions, with suspension settling during low energy slack water conditions.
F-8: Parallel Laminated Sandstone	Light grey, well-sorted very fine- to medium-grained plane parallel laminated sandstone. Larger laminations show normal grading. Lamination surfaces are often associated with carbonaceous partings.	Upper flow regime plane bed conditions, or swash zone conditions (Paola et al., 1989)
F-9: Trough Cross-Laminated Sandstone	Grey to tan very fine- to medium-grained sandstone with high angle (>15º) laminations.	Subaqueous dunes formed by unidirectional currents in the distributary system or by cross-shore and longshore currents along the coast.
F-10: Poorly Sorted Sandstone and Gravelly Sandstone	Grey to tan poorly sorted very fine- to coarse-grained sand. Sand is always the dominant grain size, with pebble-sized clasts that include mudstone rip-ups, coal fragments, and rare lithics. Pebbles occur as lag deposits or mixed into a poorly sorted matrix.	Channel lag and bar formed by unidirectional currents. Coal fragments point to terrestrial origin.
F-11: Coal	Black coal deposits from 5-10 cm thick, Often found in association with F12.	Accumulation of organic matter in low-lying, water-saturated, and poorly oxygenated terrestrial environments.
F-12: Bentonite	Yellow and light grey beds of clay (montmorillonite; Anderson and Reynolds, 1966), some biotite-rich. Occasionally with root traces. Commonly found with F11.	Altered volcanic air fall deposits preserved in low energy terrestrial settings.
F-13 Lag Deposits	Layers of mudstone rip-up or disarticulated bivalve shells. Typical layer only as thick as a single clast.	Coarse-grained deposits associated with high-energy deposition of storm beds.

Table 2.2 Summary of Facies Associations at Umiat Field.

Facies Association	Facies	Diagnostic Features	Environmental Interpretation	Depositional Processes
FA-1	F-1, F-2	Laminated shale or bioturbated mudstone (*Cruziana* ichnofacies)	Offshore/Prodelta	Suspension settling in the prodelta or the marine shelf near storm wave base
FA-2	F-2, F-3, F-5, F-13	Interbedded bioturbated mudstone (*Cruziana* ichnofacies) and upward-coarsening hummocky and swaley cross-stratified sand (*Skolithos* ichnofacies). Some sand beds obliterated by bioturbation (BI 5-6).	a. Distal Lower Shoreface	Mixed-energy shelf, above storm wave base. Deposition by suspension settling and storm-wave redistribution of sand and silt originally delivered to the coast by deltaic systems.
	F-4, F-5	Amalgamated sand beds with hummocky and swaley cross-laminated very-fine sandstone, with highly bioturbated beds (*Skolithos* ichnofacies)	b. Proximal Lower Shoreface	Storm wave deposition and redistribution of sand between fair-weather and storm wave base.
FA-3	F-4, F-5, F-9, F-13	Low-angle and trough cross-stratified, and plane-laminated fine-grained sandstone. Rare bioturbation (*Skolithos* ichnofacies)	Upper Shoreface/ Foreshore	Subaqueous bar migration above fair-weather wave base, with some swash zone deposits.
FA-4	F-3, F-6a, F-7, F-8, F9, F-10, F-13	Wavy and lenticular bedding with occasional soft sediment deformation coarsens upward into ripple cross-laminated and massive sand. Bioturbation intensity and diversity low	Delta Front	Progradation of distributary mouth bars into muddy prodelta. Rapid deposition associated with massive sand, soft sediment deformation, low BI.
FA-5	F-1, F-2, F-3, F6a, F6b, F-7, F-11, F-12	Carbonaceous mudstone with brackish water bivalve assemblage (*Corbula*), volcanic ash deposits, and plant fossils. Closely associated with the top FA-3 and FA-4. Thin ripple cross-laminated sandstone beds <10 ft.-thick, heavily oxidized.	a. Delta Plain	Suspension settling in protected interdistributary bays or lagoons, with some tidal influence (F-7), organic matter accumulation in marshes or swamps.
	F-3; F-6a, F-7, F-8 (rare), F-13	Wavy bedding coarsens up into flaser bedding and ripple cross-laminated sandstone. Beds are 5-10 ft.-thick. Mud-drapes are common in some sandstone beds, and are often sideritized, especially in Umiat No. 11. Rare mudstone rip-up clasts.	b. Crevasse Sands	Crevasse channel and splay deposits that form during flood or avulsion into interdistributary bays or the delta plain. Some tidal influence indicated by mud drapes.

Table 2.3 Permeability Anisotropy.

Well	Depth (ft.)	Facies Association	Anisotropy (K_v/K_h)	Reservoir Unit[1]
Umiat No. 10	420-490	FA-4: Delta Front/ FA-3 Shoreface	0.09	Ninuluk
Umiat No. 10	1066-1085	FA-4: Delta Front	0.05	Upper Grandstand
Umiat No. 9	873-907	FA-3: Upper Shoreface	0.73	Lower Grandstand B
Umiat No. 9	960-1003	FA-3: Upper Shoreface	0.59	Lower Grandstand A

Table 2.4 Umiat Reservoir Unit Thicknesses (ft.) by Well

	No. 1	No. 2	No. 3	No. 4	No. 5	No. 6	No. 7	No. 8	No. 9	No. 10	No. 11	Mean/ Median
Ninuluk B	35	--	--	--	--	15	20	95	50	10	60	41/35
	10					10	45			35	45	35/40
						30						
Killik	345	305	--	265*	300	325	340	310	330	320	295	319/320
Upper Grandstand	50	70	45	50	45	60	40	40	55	80	35	52/50
Shale Barrier (Tuktu)	290	330	280	305	325	--	290	335	310	--	325	310/310
Lower Grandstand B	45	90	--	85	95	--	100	40*	85	--	140	91/90
Lower Grandstand A	150[2]	155	--	--	160	--	--	--	120	--	130	143/150

Table 2.5 Sand:Mud Ratios of Mud-Dominated Reservoir Units

	No. 1	No. 2	No. 3	No. 4	No. 5	No. 6	No. 7	No. 8	No. 9	No. 10	No. 11
Killik	0.19	0.85	--	0.71	0.88	0.33	0.33	0.17	0.14	0.28	0.40
Shale Barrier	0.76	0.10	0.10	0.21	0.10	--	0.09	0.05	0.29	--	0.10

Chapter 3: $^{40}Ar/^{39}Ar$ ages and geochemical characterization of Cretaceous tephras in the Nanushuk, Seabee, Tuluvak, and Schrader Bluff formations, North Slope, Alaska[1]

3.1 Abstract

New $^{40}Ar/^{39}Ar$ ages of mineral separates from Cretaceous volcanic air-fall deposits in the Nanushuk, Seabee, and Tuluvak formations indicate that an intense period of tephra deposition on Alaska's North Slope began by the late Albian and was persistent throughout the Cenomanian. New results include the first documented radioisotopic ages from bentonites (weathered tephras) in the Nanushuk Formation. Delta plain sediments in the upper Nanushuk Formation date to 102.6 ± 1.5 Ma (late Albian), while a tephra near the base of the overlying Seabee Formation was deposited at 98.2 ± 0.8 Ma, in the early Cenomanian. These ages bracket the Seabee Formation transgression in the area around Umiat, Alaska, placing it near the Albian-Cenomanian boundary (100.5 Ma). Several hundred feet up-section, the non-marine Tuluvak Formation contains bentonites with $^{40}Ar/^{39}Ar$ ages of 96.7 ± 0.7 to 94.2 ± 0.9 Ma, several million years older than previously published K-Ar ages and biostratigraphic constraints suggest.

The major and trace element geochemistry of a sub-sample of six bentonites from exploration wells at Umiat show a range in composition from andesitic to rhyolitic, with a continental arc source. The bentonites become more felsic from the late Albian (102 Ma) to late Cenomanian (94 Ma). A likely source for the bentonites is the Okhotsk-Chukotka Volcanic Belt (OCVB) of eastern Siberia, a continental arc which became active in the Albian and experienced episodes of effusivity throughout the Late Cretaceous. Anomalously old $^{40}Ar/^{39}Ar$ ages coincide with peaks of magmatic activity in the OCVB, suggesting that the anomalous agers may be due to contributions of xenolithic material from older magmatic events. An alternative explanation for the anomalous ages is mixing of bentonites with detrital sediment derived from exhumation and erosion of metamorphic rocks in the ancestral Brooks Range.

---

[1] Shimer, G.T., Benowitz, J., Layer, P.W., Sliwinski, M., McCarthy, P., and Hanks, C.L., in prep., for Cretaceous Research

3.2 Introduction

Though biostratigraphy provides broad age control for Late Cretaceous marine and terrestrial clastic sedimentary rocks of the Colville foreland basin on Alaska's North Slope, the age ranges cover millions of years and do not provide precise dates for high-resolution correlation of sedimentary deposits. Cretaceous bentonites are a component of clastic sedimentary rocks of the Colville foreland basin (Mull et al., 2003; Fig. 3.1), and provide an opportunity for more precise radiometric dating. Bentonites are ubiquitous in many outcrops in the Brooks Range foothills, but are particularly prominent at locations such as Umiat Mountain (Anderson and Reynolds, 1966; Lanphere and Tailleur, 1983; Houseknecht and Schenk, 2005), and Shale Wall bluff (Detterman et al., 1963; Fig. 3.1). Bentonites are also preserved in cores from the numerous legacy wells in the National Petroleum Reserve Alaska (NPRA) and other federal drilling sites on the North Slope (i.e. Gubik No. 1 and No. 2 wells; Fig. 3.1). Despite their ubiquity, there is little published information on the radiometric ages and geochemistry of these bentonites. The purpose of this study is to date bentonites using the $^{40}Ar/^{39}Ar$ method, classify the bentonites using bulk X-ray fluorescence spectroscopy (XRF), and use the results as chronostratigraphic and chemostratgraphic tools to improve understanding of Cretaceous basin evolution in Arctic Alaska.

This $^{40}Ar/^{39}Ar$ study focuses on thirteen bentonites from the Nanushuk, Seabee, Tuluvak, and Schrader Bluff formations (Fig. 3.2). Samples come from one outcrop location and five exploratory wells in the Brooks Range foothills of the central North Slope (Fig. 3.1). We discuss the wide range of ages in the context of known biostratigraphy (Tappan, 1960; Mull et al., 2003; Spicer and Herman, 2010) and regional volcanic events (Moore et al., 1994; Tikhomirov et al., 2012). The results include the first well-documented radioisotopic ages from the Nanushuk Formation, which indicate that delta-plain topsets were accumulating in the Umiat region by the late Albian. We also discuss anomalously old ages and possible sources of detrital or xenolithic minerals in the dated bentonites.

In conjunction with $^{40}Ar/^{39}Ar$ age interpretations, we classify six bentonites from the Umiat wells using major and trace element geochemistry. Based on total-alkali-silica (TAS) and trace element diagrams, the bentonites are interpreted to be derived from continental volcanic arc sources and range in composition from andesitic to rhyolitic. Furthermore, the bentonites cluster by radiometric and stratigraphic age, and become more felsic through time. The initial results of this study suggest that the likely source for these Cretaceous bentonites is the Okhotsk-Chukotka Volcanic Belt (OCVB) in eastern Siberia.

3.3 Geologic Background

The North Slope of Alaska includes both the northern Brooks Range foothills and the Arctic coastal plain (Schindler, 1988). The bedrock geology of the North Slope consists of pre-Mississippian Franklinian basement and several overlying megasequences defined by major tectonic events: the passive margin Ellesmerian sequence (Mississippian-Triassic); the syn-rift Beaufortian sequence (Jurassic-Early Cretaceous) associated with the opening of the Arctic ocean; and the Brookian sequence (Cretaceous-Cenozoic) of sediments derived from the uplift and denudation of the Brooks Range and deposited in the Colville foreland basin (Hubbard et al., 1987; Moore et al., 1994; Bird, 2001; Houseknecht et al., 2011). The Umiat, Square Lake and Gubik sites are all located in the northern foothills of the Brooks Range, parallel to the long axis of the Colville foreland basin (Fig. 3.1). The Colville foreland basin formed in response to Jurassic-Tertiary collisional events that led to the formation of the ancestral Brooks Range and Herald Arch (Bird and Molenaar, 1992; Moore et al., 1994; Cole et al., 1997).

Cretaceous Age boundaries for the formations in this study were originally determined using megafossil biostratigraphy: most of the Nanushuk Formation falls within the middle Albian or later, as distinguished by the presence of the ammonite *Gastroplites* (middle Albian) and the bivalve *Inoceramus anglicus* Woods (late Albian), which are similar to species found in Alberta and British Columbia (Imlay, 1961). The

Cenomanian is most clearly identified by the presence of *Inoceramus dunveganensis*, another bivalve known from localities in western Canada (Jones and Gryc, 1960). Supplemental microfossil data, especially foraminifera zones, were also crucial for age differentiation within the Nanushuk Formation and identification of the Albian-Cenomanian boundary (Tappan, 1960; LePain et al., 2009). Age boundary years are revised here based on the 2013 geologic time scale (Cohen et al., 2013).

We investigate bentonites in the Albian-Cenomanian (113-93.9 Ma) Nanushuk Formation, Cenomanian-Coniacian (100.5-86.3 Ma) Seabee Formation, Cenomanian-Coniacian Tuluvak Formation, and Santonian-Maastrictian (86.3-66.0 Ma) Schrader Bluff Formation (Fig. 3.2). The Nanushuk Formation is part of a larger Torok-Nanushuk depositional sequence, and separated from the Seabee-Tuluvak sequence by a major flooding surface (Decker, 2007). The Torok and Seabee formations are distal shelf to slope and basin mudstones, whereas the Nanushuk and Tuluvak are fluvial, deltaic, and shallow marine deposits (Mull et al., 2003). The Schrader Bluff Formation is also shallow marine in origin and interfingers with the deltaic Prince Creek Formation (Flores et al., 2007). All of these formations are time transgressive and generally young to the east, with the most recent published ages for each formation found to the east of the study area (Mull et al., 2003). Though clinoform foreset dips support west to east migration of depositional sequences, there is also a south to north component as determined from paleocurrent data, particularly in the central-eastern Brooks Range foothills (Molenaar, 1985; LePain et al., 2009).

Burial and diagenesis can influence both $^{40}Ar/^{39}Ar$ ages and geochemical compositions. The maximum burial depth for the Nanushuk Formation near Square Lake No. 1 was approximately 2000 m (6560 ft.: Smosna, 1989), and the Nanushuk in general is though to have undergone low-temperature, low-pressure diagenesis with a maximum temperature of 60º C (Smosna, 1988; O'Sullivan, 1999). Given the shallow burial, Ar-bearing minerals are not likely to have experienced significant argon-loss.

3.4 Materials and Methods

The wells used in this study were part of the 1944-1953 Naval Petroleum Reserve No. 4 drilling program (Schindler, 1988). Drilling reports from the Umiat (Collins, 1958), Square Lake (Collins, 1959), and Gubik (Robinson, 1958) sites contain lithologic descriptions, well logs, petrography, biostratigraphy, and engineering data (porosity, permeability, oil, gas, and water analyses, and drilling operations). These records were used to locate bentonite layers for sampling. Samples were recovered from NPRA cores stored at the Geologic Materials Center in Eagle River, Alaska. A single outcrop sample was taken from a bluff along the Colville River southwest of Umiat, Alaska (Fig. 3.1), located at the top of a 180 ft.-thick stratigraphic section, ~30 ft. above the top of the Nanushuk Formation near the base of the Seabee Formation. The outcrop sample was an unconsolidated grey bentonite containing abundant biotite grains. Core samples were lithified. Bentonites in the Seabee, Tuluvak, and Schrader Bluff formations were yellowish with no visible mineral phases, whereas the Nanushuk Formation samples are whitish, biotite-rich bentonites.

3.4.1 $^{40}Ar/39Ar$ Geochronology

All samples were sieved and washed to produce mineral separates. Separates were magnetically sorted and datable mineral phases (biotite, sanidine, plagioclase, and volcanic glass) were hand-picked under a binocular microscope. Samples and standards of monitor mineral MMbh-1 (Sampson and Alexander, 1987) with an age of 513.9 Ma (Lanphere and Dalrymple, 2000) were irradiated in the research reactor at McMaster University, Hamilton, Canada, for 20 megawatt-hours.

In the UAF geochronology lab, each irradiated sample was loaded into a 2 mm diameter hole in a copper tray, which was then placed into an ultra-high vacuum extraction line. Monitors were fused and samples were heated using a 6-watt argon-ion laser following established techniques (York et al., 1981; Layer et al., 1987; Layer, 2000). Argon purification was achieved using a liquid nitrogen cold trap and SAES Zr-Al getter at

400ºC. Samples were analyzed in a VG-3600 mass spectrometer. Measured argon isotope values were corrected for system blanks and mass discrimination, as well as calcium, potassium, and chlorine interference reactions (McDougall and Harrison, 1999). System blanks were $2x10^{-16}$ mol ^{40}Ar and $2x10^{-18}$ mol ^{40}Ar (10 to 50 times smaller than fraction volumes). Mass discrimination in the system is monitored by running calibrated air shoots and zero-age glass sample measurements on a weekly to monthly basis.

Multiple analyses or "runs" were conducted on sufficiently large samples to reduce error. Multiple runs were not possible in most cases due to a limited amount of datable material. We only report second runs for SQ1-257T and GU2-1387T because previous runs were unsuccessful at producing an $^{40}Ar/^{39}Ar$ age. We report both runs of UM2-311, and use the two runs to create a weighted average age.

3.4.2 Geochemistry

Six samples were selected for X-ray fluorescence (XRF) analysis to determine major and selected trace element compositions. All of the samples are from the Umiat wells. The samples include two bentonites from the Nanushuk (UM11-2258N; UM2-311N), Seabee (UM11-1962S; UM11-1682S), and Tuluvak (UM11-391T; UM11-345T) formations. Due to the small volume of material in the cores, we were limited to the <150 μm residues remaining after the crushing and sieving process for $^{40}Ar/^{39}Ar$ dating. Five residues from Umiat No. 11 (prefix UM11) and one from Umiat No. 2 (prefix UM2) were analyzed. There was sufficient original material from Umiat No. 2 to create a "whole rock" sample for comparative purposes.

All samples were processed to create 39.7 mm pressed powder disks. 12.0-15.0 g of bentonite were mixed with 1.2-1.5 g of PXR-200 powder (binding agent). Powder weight was set at 10% of sample weight. To uniformly crush and homogenize the samples, each mixture was placed in a carbon-steel ball mill for 7 minutes, with 10 mL of Vertrel™ as a lubricant. 11.0 g of dried sample was weighed into a steel press and samples were compressed under 10 tonnes/in^2 pressure for 5 minutes.

For trace element analysis we used the PROtrace 37 routine on a PANalytical Axios XRF. Six standards were run: BE-N (basalt), GSP-1 (granodiorite), JA-2 (andesite), JG-2 (granite), JP-1 (peridotite) and JR-1 (rhyolite). To assess standards, relative percent difference was calculated for barium, cerium, chromium, cobalt, copper, lanthanum, lead, nickel, niobium, scandium, strontium, rubidium, vanadium, yttrium, zinc, zirconium, and titanium oxide using experimental values and preferred values from the GeoReM database (http://georem.mpch-mainz.gwdg.de/).

3.5 Results

3.5.1 $^{40}Ar/^{39}Ar$ Geochronology

All $^{40}Ar/^{39}Ar$ results were calculated using the constants of Steiger and Jaeger (1977) and are reported to ± 1σ. (Table 3.1). Isochron ages were incalculable for most samples due to homogenous radiogenic content of released and documented argon loss. Integrated ages and step-heating age spectra are reported, which are useful for interpreting plateau ages and recognizing argon-loss, recoil, or excess argon. A plateau age was calculated for all but one of the samples (GU1-2845S), and the plateau age reported for CI-006S does not technically meet the criteria for a true plateau because the selected steps only include 45.3% of the total ^{39}Ar release. Plateau ages can be determined if three or more consecutive gas fractions are within two standard deviations of each other (Table 3.2). Most analyses have spectra with relatively flat plateaus and errors of ± 1.5 Ma or less. A single sample from the Schrader Bluff Formation (BU1-736SC) had a plateau error of ± 4.4 Ma. Plateau ages approximate an age based on argon release for a series of selected steps, and are an interpreted approximation of the sample age. An $^{40}Ar/^{39}Ar$ plateau age does not necessarily equal a true geologic age.

The $^{40}Ar/^{39}Ar$ plateau ages range from 133.1-89.3 Ma (Table 3.2). The maximum biostratigraphic age range of the sediments is 112-85.3 Ma. Plateaus were not calculated for samples CI-006S and GU1-2845S. The age from CI-006S is not a true plateau age

because the amount of gas released from the more retentive steps did not meet the criteria. Bentonites from the Nanushuk Formation have ages of 110.4±0.9 Ma (UM11-2258N), 102.6 ± 1.5 Ma (UM2-311N#1) and 102.2±1.1 (UM2-311N#2). All of these ages are Albian (113-100.5 Ma). Bentonites from the Seabee Formation have ages of 106.0±0.9 Ma (GU1-2840S), 98.2±0.8 Ma (CI-006S), 131.1±1.3 Ma (UM11-1962S), and 104.1±1.1 Ma (UM11-1682S). These are Hauterivian (131.1 Ma), Albian (106.0 and 104.1 Ma) and Cenomanian (98.2 Ma).

Bentonites from the Tuluvak Formation have ages of 133.1±2.2 Ma (GU1-1165T), 96.2±2.0 Ma (GU2-1397T), 96.6±1.4 Ma (SQ1-257T), 94.4±0.9 Ma (UM11-345T), and 129.1±1.8 Ma (UM11-391T). The ages are Valanginian (133.1 Ma), Barremian (129.1 Ma), and Cenomanian (96.2, 96.6, and 94.4 Ma). A single bentonite from the Schrader Bluff Formation has an age 89.3±4.4 Ma (GU1-736), which falls within the Turonian (89.8-93.9 Ma). The error is sufficiently large that it may have a Coniacian (89.8-86.3 Ma) or early Cenomanian (100.5-93.9 Ma) age. Sample GU1-2845S (from the Seabee Formation) returned a geologically unrealistic $^{40}Ar/^{39}Ar$ integrated age of 398.7±43.8 Ma.

3.5.2 Geochemistry

Most major and trace elements were present in detectable concentrations (Table 3.3). Only two major elements (MnO, S) and four trace elements (Ge, Sb, Ta, W) were below detection limits for any of the samples. Of these, only Ta is used in the classification diagrams, because only one sample (UM11-345) was below detection limits. For other elements used in characterization diagrams, SiO_2 compositions range from 58.35-72.02%, whereas K_2O (0.18-1.36 %) and Na_2O (2.23-3.30%) are present in much lower concentrations. TiO_2 (1567-7788 ppm), Zr (189-309 ppm), Nb (5.41-12.47 ppm), Ta (1.59-1.79 ppm), Th (20.13-35.39 ppm), Y (15.87-38.56 ppm), and Yb (2.80-5.31 ppm) also show a range of values between samples (Table 3.3).

We assessed the relative error for elements or oxides used in characterization diagrams by comparing standards to recommended values in the GeoReM database (Table 3.4).

Percent error can be very high for some elements, particularly where published values are at or below detection limits (~1 ppm for most elements). Errors range from 0.0% (compiled recommended values same as measured) up to 399% for elements with very low concentrations. Errors were not large enough to exclude the crucial major and trace elements from use in diagrams.

3.6 Discussion

3.6.1 Albian-Cenomanian Bentonites: Nanushuk, Seabee, and Tuluvak Formations

There are five $^{40}Ar/^{39}Ar$ plateau ages in this study that approach a "true" geological age based on the plateau characteristic and biostratigraphically determined formation boundaries (Tappan, 1960; Jones and Gryc, 1960; Imlay, 1961) and age limits (Mull et al., 2003; Cohen et al., 2013) of the Nanushuk (Albian-Cenomanian: 113-93.9 Ma), Seabee (Cenomanian-Coniacian: 100.5-85.8 Ma), and Tuluvak (Cenomanian-Coniacian: 100.5-85.8 Ma) formations. Four samples have plateau ages (UM11-345T; SQ1-257T; GU2-1397T; UM2-311N) and a fifth (CI-006S) has sufficiently low error and flat release to be considered accurate.

One of the advantages of the $^{40}Ar/^{39}Ar$ step-heating method over traditional K-Ar dating is the use of age spectra and plateau ages to identify argon-loss or excess argon and exclude affected steps from the age calculation (McDougall and Harrison, 1999). Several of the age spectra show argon-loss, including UM2-311N, GU2-1397T, and CI-006S (Fig. 3.3 and 3.4). Argon-loss is characterized by the age stepping-up pattern of the spectra. These spectra show lower than average ages in less retentive, low-temperature steps, which is probably due to loss of argon around crystal edges through diffusion (McDougall and Harrison, 1999). Biotite is prone to argon-loss through diffusion along cleavage planes (Harrison et al., 1985), and argon-loss was only detected in biotite samples (UM2-311N #1, UM2-311N #2, CI-006S, GU2-1397T). Despite argon-loss,

spectra UM2-311N and GU2-1397T exceed the plateau age criteria of three or more consecutive gas fractions that represent >50% of total gas release and have mean standard weighted deviations <2.5 (Table 3.2).

The ages discussed here include the first well-documented radiometric age from the Nanushuk Formation, from sample UM2-311N in Umiat No. 2 (Fig. 3.3). As discussed in section 3.4, there were two runs of UM2-311N. The plateau ages from both runs of UM2-311N are within error. UM2-311N #1 produced a plateau age of 102.6 ± 1.5 Ma; UM2-311N #2 produced an age of 102.2 ± 1.1 Ma. A weighted average of these two runs is 102.4 ± 1.0 Ma, placing the delta plain deposits of the upper Nanushuk Formation in the late Albian. The lower Nanushuk Formation in the Umiat area is thought to be mid-Albian in age based on plant fossils (Spicer and Herman, 2010) and ammonites (Imlay, 1961). A late Albian $^{40}Ar/^{39}Ar$ age from the upper Nanushuk is consistent with this biostratigraphic age.

CI-006S is the only sample from the Seabee Formation with a $^{40}Ar/^{39}Ar$ age that we consider geologically reasonable. CI-006, from the base of the Seabee Formation immediately above the Nanushuk Formation, has an age of 98.2 ± 0.8 Ma, placing it in the early Cenomanian. Published K-Ar dates from the upper Seabee Formation in Umiat No. 1, approximately 13 miles northwest of the outcrop site, have weighted mean averages from 92.2 ± 1.2 Ma to 93.7 ± 2.0 Ma, placing them in the Turonian (Lanphere and Tailleur, 1983). K-Ar ages do not take argon-loss into account as $^{40}Ar/^{39}Ar$ age spectra do (McDougall and Harrison, 1999). K-Ar ages are more equivalent to integrated ages. The integrated age for CI-006S is 96.7 ± 0.7 Ma (Table 3.1), which is still older than the K-Ar ages at Umiat, but the K-Ar samples are approximately 400 ft. up-section from CI-006S and are expected to be younger.

A major transgression occurs between the upper Nanushuk and lower Seabee formations (Houseknecht and Schenk, 2005; Shimer et al., in press). The new ages from the upper Nanushuk and lower Seabee formations bracket the timing of this transgression between 102.4 ± 1.0 Ma (Albian) and 98.2 ± 0.8 Ma (Cenomanian). This age is near the Albian-

Cenomanian boundary (100.5 Ma), and older than the major transgression associated with the late Cenomanian-early Turonian anoxic event (Prokoph et al., 2001). Consequently, it may be related to late Albian transgressions recognized worldwide (Hancock and Kauffman, 1978).

The non-marine Tuluvak Formation is genetically related to the Seabee Formation, and together they comprise clinoforms that prograded from west to east along the Colville foreland basin axis (Decker, 2007). There are three Tuluvak Formation ages in this study from three different sites, and all have ages significantly older (Cenomanian) than the Turonian age commonly cited for the Tuluvak Formation (Lanphere and Tailleur, 1983; Mull et al., 2003). The samples, from west to east, are SQ1-257T (96.6 ± 1.4), UM11-345T (94.3± 0.9 Ma), and GU-1397T (96.2 ± 2.0 Ma). The ages do not young to the east, and the youngest (UM11-345T) is stratigraphically lowest (Fig. 3.5). These results may suggest irregular, northward prograding non-marine topset deposits in the Tuluvak Formation. But is important to note that the bentonites in these wells are not assumed to be correlative due to complexities of tephra preservation in a delta plain environment. The variation in dates could also be due to inaccuracy in the dates.

An additional consideration is the different mineral phases dated in this study. Each of the Tuluvak Formation sample are from a different mineral phase. UM11-345T is a suspected sanidine or high-K plagioclase age, based on the Ca/K ratio, whereas GU1-1397T is a biotite age, and SQ1-257T is an age from volcanic glass (Fig. 3.4). Plagioclase has lower argon retentivity than biotite (McDougall and Harrison, 1999), which makes the young age from UM11-345T the most likely outlier. Although volcanic glass like that found in SQ1-257T is also prone to argon-loss during devitrification (McDougall and Harrison, 1999), SQ1-257T has a flat release spectrum with no evidence for argon-loss (Fig. 3.4). Unaltered glass shards have also been dated using K-Ar and $^{40}Ar/^{39}Ar$ at the Ocean Point locality in the overlying Prince Creek Formation, and these too show little argon-loss (Conrad et al., 1990; Flaig, 2010). Even with the 94.3 ± 0.9 Ma age from UM11-345T, all three Tuluvak Formation ages are in the Cenomanian (100.5-

93.9 Ma). Further investigation of Tuluvak Formation geochronology is clearly needed to better assess its age variability across the North Slope.

2.6.2 Anomalous $^{40}Ar/^{39}Ar$ Ages

We obtained six anomalous $^{40}Ar/^{39}Ar$ ages that meet the criteria for good plateau ages, yet are not geologically realistic considering the known biostratigraphic boundaries (Tappan, 1960), chronologic age constraints (Mull et al., 2003; Cohen et al., 2013), published $^{40}Ar/^{39}Ar$ and K-Ar ages (Lanphere and Tailleur, 1983; Conrad et al., 1990) and other ages obtained in this study. These anomalous ages are Albian (113-100.5 Ma; Fig. 3.6), Barremian (125-129.4 Ma; Fig. 3.7), Hauterivian (129.4-132.9 Ma; Fig. 3.7), and Valanginian (132.9-139.8 Ma; Fig. 3.7). We interpret these anomalous ages as the result of incorporation of detrital material from magmatic or metamorphic sources in the sedimentary deposits in which the tephras were preserved.

There are three Albian $^{40}Ar/^{39}Ar$ ages that we interpret as anomalous ages (GU1-2840S, 106.0 ± 0.9 Ma; UM11-1682S, 104.1 ± 1.1 Ma; and UM11-2258N, 110.4 ± 0.9 Ma). Both GU1-2840S and UM11-1682S are from the Seabee Formation. Temporarily ignoring the anomalous ages, they "young" to the east based on the well locations (Fig. 3.8) and support seismic interpretations of clinoform progradation (Houseknecht and Schenk, 2005; Decker, 2007). However, the base of the Seabee Formation is Cenomanian (100.5-93.9 Ma) in the Umiat area (see section 3.5), and these ages are as much as 10 Ma too old based on the date obtained from CI-006S and known stratigraphic constraints (Tappan, 1960; Mull et al., 2003) and Age boundaries (Cohen et al., 2013).

UM11-2258N is the second bentonite dated from the Nanushuk Formation. Unlike the two runs of UM2-311N (weighted average 102.4 ± 1.0 Ma), which is stratigraphically lower in the Nanushuk Formation (Fig. 3.9), UM11-2258N returns an $^{40}Ar/^{39}Ar$ age of 110.4 ± 1.0 Ma). Like UM2-311, UM11-2258 experienced minor argon loss, but this is accounted for in the $^{40}Ar/^{39}Ar$ plateau (Fig. 3.3 and Fig. 3.6; Table 3.2). Both samples are from non-marine to marginal marine delta plain sediments near the top of the

Nanushuk Formation. Though still within the Albian (113-100.5 Ma), based on the stratigraphic position and the age difference between UM2-311N and UM11-2258N, the latter $^{40}Ar/^{39}Ar$ age is as much as 8 Ma too old. The Umiat No. 11 well is heavily faulted, though known faults are not located at these depths (Colllins, 1958). Furthermore, the Nanushuk Formation stratigraphic sections for Umiat No. 2 and Umiat No. 11 (Fig. 3.9) are very similar, which suggests that there is not significant faulting through the interval.

The anomalously old $^{40}Ar/^{39}Ar$ ages may represent bentonite deposits contaminated with detrital or xenolithic biotite from magmatic sources, or altered detrital biotite-chlorite from metamorphic sources. In this paper, mixed igneous sources implies either the contribution of magma with a different initial argon composition or the inclusion of xenoliths with an older $^{40}Ar/^{39}Ar$ age. This is possible in magmatic systems, where previously cooled xenoliths can be incorporated into magma without outgassing preexisting radiogenic argon or re-equilibrating with atmospheric argon before eruption (Gillespie et al., 1982). A potential source region with appropriately aged eruptive events is the Okhotsk-Chukotka Volcanic Belt (OCVB) in eastern Siberia (Fig. 3.10). The OCVB has five main episodes of volcanic activity, with the oldest episode occurring at 106-98 Ma (Tikhomirov et al., 2012). Both the anomalous and geologically reasonable $^{40}Ar/^{39}Ar$ ages from this study cluster around peaks of activity in the OCVB (Fig. 3.11).

An alternative explanation is the contribution of metamorphic biotite and mica from sediment sources for the Nanushuk and Seabee formations in the ancestral Brooks Range. Blueschist facies rocks from the southern Brooks Range (Fig. 3.10) were exhumed from the Late Jurassic to middle Albian. White micas from these deposits have $^{40}Ar/^{39}Ar$ ages as old as 120 Ma (Till, 1992), and metamorphic events at 110-105 Ma (Till and Patrick, 1991) and 105-103 Ma (Vogl et al., 2002) have also been recognized. Additional studies report $^{40}Ar/^{39}Ar$ ages from white mica in metamorphic rocks that indicate remobilization around 108 Ma (Till and Snee, 1995). Since Aptian-Albian chloritoid and muscovite from blueschist facies rocks are found in the Nanushuk Formation (Till, 1992), these detrital sediments may be the source of relict mica ages found in mixed-age bentonites.

The contamination is not thought to completely overprint the volcanic $^{40}Ar/^{39}Ar$ ages, as the anomalous Seabee Formation ages are younger than the anomalous Nanushuk Formation age, and the Seabee Formation ages young to the east.

Three of the samples have even older Early Cretaceous ages. These include UM11-391T (129.1 ± 1.8 Ma; Barremian), UM11-1962S (131.2 ± 1.3 Ma: Hauterivian) and GU1-1165T (133.1 ± 2.2 Ma: Valanginian). All three ages are from biotite separates. The spectra (Fig. 3.7) do not display "saddle" shapes or step up, which are possible indications of excess argon in retentive high temperature sites (Harrison, 1990). Biotites with excess argon are also known to produce flat release patterns if the excess argon is uniformly distributed throughout the mica (McDougall and Harrison, 1999). We interpret this as a more likely explanation, with excess argon in the step-heated collection of biotite separates coming from xenoliths produced during early magmatic activity in the source area. There is a minor peak in volcanic activity during this Barremian-Hauterivian in the OCVB (Akinin and Miller, 2011; Fig. 3.11).

3.6.3 Unknown Phases

GU1-736SC has a $^{40}Ar/^{39}Ar$ plateau that meets the imposed criteria (Table 3.2; Fig. 3.12). The $^{40}Ar/^{39}Ar$ age for GU1-736SC (89.3 ± 4.4 Ma) places it at the Turonian-Coniacian boundary, but GU1-736SC is our only sample from the Schrader Bluff Formation, which is thought to be Santonian-Maastrichtian (83.6-66 Ma) in age (Mull et al., 2003). We do not interpret the $^{40}Ar/^{39}Ar$ age to be accurate, and do not propose an older age for the Schrader Bluff Formation, because the mineral separate was inferred to be plagioclase but it has a Ca/K ratio greater than 500 (Fig. 3.12). This means the sample is not a pure plagioclase separate, and without additional mineralogical information it is not possible to place the age in a geologic context. The large error is also a concern.

GU1-2845S is unique among all the analyses, in that no $^{40}Ar/^{39}Ar$ plateau age or even semi-precise calculated age was possible. The age spectrum is very irregular and clearly does not form a plateau (Fig. 3.12). In this case the cause is clear: a Ca/K ratio greater

than 1000 shows a lack of potassium in the sample and could point to an abundance of calcium. The inferred plagioclase separates from this sample were likely calcite, and the age of 398.7 ± 3.6 Ma is geologically meaningless. We include this spectra to contrast with the anomalous ages that we interpret as geologically significant.

3.6.4 Geochemistry

The goal of this geochemical study was attempt to classify the bentonites using traditional igneous geochemistry diagrams, and to determine whether there was significant variation in bentonite composition through time. We acknowledge the many variables that influence bentonite geochemistry, including original magmatic variation, wind and water sorting of the volcanic ash by density, particle size, and shape, and chemical alteration through surface weathering and burial diagenesis. We use immobile trace element geochemistry to minimize diagenetic factors and focus on the Umiat wells to track changes from the Albian Nanushuk Formation (UM11-2258N; UM2-311N) through the Cenomanian Seabee (UM11-1962S; UM11-1682S) and Tuluvak Formations (UM11-391T; UM11-345T). The bentonites in the Umiat wells are bracketed by $^{40}Ar/^{39}Ar$ ages from UM2-311N (102.4 ± 1.0 Ma) and UM11-345 (94.4 ± 0.9 Ma), though the 94.4 Ma age may be too old. These dates allow us to characterize changes in bentonite composition from the late Albian (113-100.5 Ma) through nearly the entire Cenomanian (100.5-93.9 Ma).

One of the restricting factors in this study was also sample size. Most of the available bentonite was used in the $^{40}Ar/^{39}Ar$ dating process for many of the samples. We used the <150 μm size fraction (residue) from each of the $^{40}Ar/^{39}Ar$ samples in this study to produce XRF disks. There was concern that the size fraction would influence results through the removal of heavy minerals. There was sufficient "whole rock" sample from UM2-311N to compare bulk composition of the two sample size fractions. A cross-plot of trace element geochemistry from the whole rock and <150 μm residue shows a strong correlation (Fig. 3.13A). We interpret this result as evidence for little geochemical

fractionation through size grading, and infer that the XRF results from all of the pressed disks are representative of the true bulk geochemistry of the bentonites.

The Cretaceous tephras in the Brookian deposits of the Colville foreland basin are often referred to as bentonites (Collins, 1958; Robinson, 1958; Collins, 1959; Mull et al., 2003) although the only existing X-ray diffraction study of the Umiat bentonites found evidence for both montmorillonite and beidelite, which are both smectites (Anderson and Reynolds, 1966). Smectites (such as montmorillonite) are known to undergo Si loss (relative to Al), in a transition to illite through burial and diagenesis (Land et al., 1997). It is therefore important to compare major element geochemistry to trace element concentrations to properly characterize a bentonite or a mineral phase within a bentonite. Various studies of bentonites emphasize different immobile elements, such as Nb, Zr, Cr, Ni, V, La, Ce, Nd, and Y (Christidis, 2001), as well as Ti and Th (Kiipli et al., 2008). These are generally high field strength elements or large ion lithophiles (Fanti, 2009). Where there are sufficient exposures and large enough sample sizes to establish statistical significance, it is even possible to statistically group and correlate Cretaceous bentonites using immobile trace element geochemistry (Thomas et al., 1990). Unfortunately our the sample size is too small to conduct cluster or discriminant analysis (Foreman et al., 2008).

We plotted the major element data on a traditional total-alkali-silica (TAS) diagram to compare with trace element characterizations to assess element mobility (Fig. 3.14). The TAS diagram shows that samples from the Nanushuk (UM2-311), Seabee (UM11-1962; UM11-1682) and Tuluvak (UM11-391) formations plot as distinct groups in the andesite, and dacite categories (Fig. 3.14A). UM11-2258 plots closest to the dacitic Seabee Formation bentonite. Temporarily ignoring UM11-2258, there is a trend of increasingly felsic (silica-rich) volcanic ash deposits from the Albian (UM2-311: 102.4 ± 1.0 Ma) to the end of the Cenomanian (UM11-354T: 94.4 ± 0.9 Ma).

We use immobile element concentrations and ratios to characterize magmatic source material (Winchester and Floyd, 1977; Pearce et al., 1984; Pearce, 1996; Hastie et al.,

2007) and infer tectonic setting (Pearce, 1983; Pearce and Peate, 1995). The trace element studies are designed with various proxies for assessing mafic to felsic composition (Zr/TiO_2) and alkalinity (Nb/Y). Increasingly high Zr/TiO_2 ratios show a transition from mafic (basaltic) to felsic (rhyolitic) magmas, whereas increasing Nb/Y shows an increase in alkalinity (Pearce, 1996). Trace element plots from the Umiat bentonites show a pattern of increasingly felsic compositions through the Albian-Cenomanian (Fig. 3.14B). The results are consistent with the TAS diagram (Fig. 3.14A), except that each sample plots as slightly more felsic than shown in the TAS diagram, with Tuluvak Formation samples plotting nearly in the rhyolite field. Si is often lost through burial and diagenesis (Land et al., 1997). The probable loss of Si in these bentonites emphasizes the utility of immobile element diagrams where Zr serves as a proxy for original Si content.

It is probably not a coincidence that the mineral-poor Seabee and Tuluvak bentonites are silica-rich. The lack of heavy minerals may be due to a multitude of sorting factors, from a difference in eruption strength and distance from eruption site, to a change in prevailing wind patterns over time. Both the Tuluvak and Nanushuk formation rocks in this study are fluvial or delta plain deposits (Mull et al., 2003; Houseknecht and Schenk, 2005; Shimer et al., in press), so we expect local sorting or weathering characteristics to be similar.

Since the increase in SiO_2 content appears to be systematic over time, the bentonite geochemistry may be an indicator of magmatic system evolution throughout the Albian-Cenomanian. The outlier in this case is UM11-2258N, which may be contaminated by a significant fraction of detrital minerals from clastic sources. The detrital minerals are also potentially responsible for an older than expected $^{40}Ar/^{39}Ar$ age. Bivariate plots of the major and trace element geochemistry of the UM2-311N and UM11-2258N show a strong correlation (Fig. 3.13B and C), but there are major differences in some of the elemental concentrations. The major differences are in Cr, Nb, Y, Zr, TiO_2, and SiO_2 content (Table 3.3). The relatively high SiO_2 and Zr content for UM11-2258N compared

to UM2-311N is possible evidence for increased content of detrital quartz and heavy minerals. The geochemical correlation between the two samples (Fig. 3.13) may be an indication that the same bentonite can be found in both wells. This would require the approximately 90 ft. stratigraphic difference between UM2-311N and UM11-2258N (Fig. 3.9) to be caused by natural variation in the delta plain and differential compaction of sandstone, mudstone, and coal during burial. If the two samples are correlative, we interpret the UM2-311N geochemistry as the more accurate bentonite geochemistry due to other evidence for detrital contamination in UM11-2258 (discussed below).

Using the Rb vs Y+Nb classification system for granites (Pearce et al., 1984), all of the Umiat bentonites plot as volcanic arc magmas (Fig. 3.15A). Volcanic arcs are likely to produce explosive eruptions with volcanic ash. In the Th/Yb vs Ta/Yb plot (Fig. 3.15B), all of the samples plot specifically as continental arcs. These results help to narrow the potential source areas for the Umiat bentonites. The Early Cretaceous plutons of the Yukon-Koyukuk basin, to the south side of the Brooks Range (Fig. 3.10), are tholeiitic to shoshonitic, and are thought to be sourced from a volcanic island arc (Box and Patton, 1989; Miller, 1989). In contrast, the OCVB was part of an active continental margin with a range of basaltic-andesitic-dacitic-rhyolitic compositions during the Albian-Cenomanian (Tikhomirov et al., 2006; Belyi, 2008). Furthermore, the timing of the Umiat bentonites compares well to periods of volcanic activity in the OCVB (Fig. 3.11), particularly with events in the northern OCVB, including the Western Okhotsk and Anadyr segments (Fig. 3.10; Tikhomirov et al., 2006; Akinin and Miller, 2011). Consequently, the OCVB appears to be the most likely source for bentonite deposits in the Albian-Cenomanian Brookian sediments of Alaska's North Slope.

3.7 Conclusions

$^{40}Ar/^{39}Ar$ plateau ages from bentonites at four sites in the Nanushuk, Seabee, and Tuluvak formations of northern Alaska's Colville foreland basin range from late Albian (102.4 ± 1.0 Ma) to late Cenomanian (94.4 ± 0.9 Ma). This assemblage of ages includes

the first radiometric dates from the Nanushuk Formation. The upper Nanushuk Formation age of 102.4 ± 1.0 Ma and a 98.2 ± 0.8 Ma age from the base of the overlying Seabee Formation bracket the Seabee transgression at the beginning of the Cenomanian (99.6 Ma). All together, the $^{40}Ar/^{39}Ar$ ages are older than expected for the Seabee and Tuluvak formations and call into question the effectiveness of single-run analyses from core.

The combination of $^{40}Ar/^{39}Ar$ ages and geochemical data indicate that the likely source for Albian-Cenomanian bentonites on the North Slope is the Okhotsk-Chukotka Volcanic Belt (OCVB) in eastern Siberia. Albian to Cenomanian dates compare well with known periods of effusive volcanic activity in the OCVB. Though no direct correlation is possible with the existing data set, the continental arc origin of the Brookian bentonites points toward a similar system to the OCVB. The Brookian bentonites in this study are dacitic to rhyolitic, and are sourced from continental arcs like the OCVB. The Umiat bentonites in particular, become increasingly felsic over time, perhaps indicating a change in magmatic composition in the source area. These results are promising, and suggest a more intensive study of Cretaceous bentonite samples from cores should be useful for studying Albian-Maastrichtian volcanic activity in the Cretaceous Arctic.

3.8 Acknowledgements

Dr. Jeff Benowitz and Dr. Paul Layer of the UAF Geochronology Lab analyzed the $^{40}Ar/^{39}Ar$ samples and helped with interpretation. Funding for the $^{40}Ar/^{39}Ar$ analyses came from the U.S. Department of Energy contract DE-FC26-08NT005641. Additional funding for $^{40}Ar/^{39}Ar$ dating came from the Geological Society of America (GSA) and the UAF Geology BP Scholarship Program. Special thanks to Dr. Maciej Sliwinski for assistance on the Axios XRF and with data processing and interpretation, and to Dr. Ken Severin of the Advanced Instrumentation Laboratory at UAF for instrumental time.

3.9 References

Akinin, V.V., and Miller, E.L., 2011, Evolution of calc-alkaline magmas of the Okhotsk-Chukotka Volcanic Belt: Petrology, v. 19, p. 237-277.

Anderson, D.M., and Reynolds, R.C., 1966, Umiat Bentonite: An Unusual Montmorillonite from Umiat Alaska: American Mineralogist, v. 51, 1443-1455.

Belyi, V.F., 2008, Problems of geological and isotopic age of the Okhotsk-Chukotka Volcanogenic Belt (OCVB) : Stratigraphy and Geological Correlation, v. 16, p. 639-649.

Bird, K.J., 2001, Alaska: a twenty-first century petroleum province, *in* M.W. Downney, J.C. Threet, and W.A. Morgan, eds., Petroleum Provinces of the Twenty-First Century: American Association of Petroleum Geologists Memoir 74, p. 137-165.

Bird, K.J., and Molenaar, C.M., 1992, The North Slope foreland basin, Alaska, *in* R.W. Macqueen and D.A. Leckie, eds., Foreland Fold and Thrust Belts: AAPG Memoir 55, p. 363-393.

Box, S.F., and Patton, W.W., 1989, Igneous history of the Koyukuk Terrane, Western Alaska: Constraints on the origin, evolution, and ultimate collision of an accreted island arc terrane: Journal of Geophysical Research, v. 94, p. 15843-15867.

Christidis, G.E., 2001, Geochemical correlation of bentonites from Milos Island, Aegean, Greece: Clay Minerals, v. 35, p. 295-306.

Cole, F., Bird., K.J., Toro, J., Roure, F., O'Sullivan, P.B., Pawlewicz, M., and Howell, D.G., 1997, An integrated model for the tectonic development of the frontal Brooks Range and Colville Basin 250 km west of the Trans-Alaska Crustal Transect: Journal of Geophysical Research, v. 102, p. 20,685-20,708.

Collins, F.R., 1958, Test Wells, Umiat Area, Alaska: U.S. Geological Survey Professional Paper 305-B, p. 71-206.

Collins, F.R., 1959, Test Wells, Square Lake and Wolf Creek Areas, Alaska: U.S. Geological Survey Professional Paper 305-H, p. 423-484.

Conrad, J.E., McKee, E.H., and Turrin, B.D., 1990, Age of tephra beds at the Ocean Point dinosaur locality, North Slope, Alaska, based on K-Ar and $^{40}Ar/^{39}Ar$ analyses: Evolution of Sedimentary Basins-North Slope Basin, U.S. Geological Survey Bulletin 1990, 14 p.

Cohen, K.M., Finney, S., and Gibbard, P.L., 2013, International Chronostratigraphic Chart: International Commission on Stratigraphy. http://www.stratigraphy.org/ICSchart/ChronostratChart2013-01.pdf.

Decker, P.L., 2007, Brookian sequence stratigraphic correlations, Umiat field to Milne Point field, west-central North Slope, Alaska: Alaska Division of Geological and Geophysical Surveys Preliminary Interpretive Report 2007-2, 21 p.

Detterman, R.L., Bickel, R.S., and Gryc, G., 1963, Geology of the Chandler River Region, Alaska: U.S. Geological Survey Professional Paper 303-E, p. 223-324.

Fanti, F., 2009, Bentonite chemical features as proxy of late Cretaceous provenance changes: A case study from the Western Interior Basin of Canada: Sedimentary Geology, v. 217, p. 112-127.

Flaig, P.P., 2010, Depositional environments of the Late Cretaceous (Maastrichtian) dinosaur-bearing Prince Creek Formation: Colville River region, North Slope, Alaska. Ph.D. Dissertation, University of Alaska, 311 p.

Flores, R.M., Myers, M.D., Houseknecht, D.W., Stricker, G.D., Brizzolara, D.W., Ryherd, T.J., and Takahashi, K.I., 2007, Stratigraphy and facies of Cretaceous Schrader Bluff and Prince Creek formations in Colville River bluffs, North Slope, Alaska: U.S. Geological Survey Professional Paper 1748, 52 p.

Foreman, B.Z., Rogers, R.R., Deino, A.L., Wirth, K.R., and Thole, J.T., 2008, Geochemical characterization of bentonite beds in the Two Medicine Formation

(Campanian, Montana) including a new $^{40}Ar/^{39}Ar$ age: Cretaceous Research, v. 29, p. 373-385.

Gillespie, A.R., Huneke, J.C., and Wasserburg, G.J., 1982, An assessment of ^{40}Ar-^{39}Ar dating of incompletely degassed xenoliths: Journal of Geophysical Research, v.87, p. 9247-9257.

Hancock, J.M., and Kauffman, E.G., 1978, The great transgressions of the Late Cretaceous: Journal of the Geological Society, v. 136, p. 175-186.

Harrison, T.M., 1990, Some observations on the interpretation of feldspar $^{40}Ar/^{39}Ar$ results: Chemical Geology (Isotope Geoscience Section), v. 80, p. 219-229.

Harrison, T.M., Duncan, I., and McDougall, I., 1985, Diffusion of ^{40}Ar in biotite: Temperature, pressure, and compositional effects: Geochimica et Cosmochimica Acta, v. 49, p. 2461-2468.

Hastie, A.R., Kerr, A.C., Pearce, J.A., and Mitchell, S.F., 2007, Classification of altered volcanic island arc rocks using immobile trace elements: Development of the Th-Co discrimination diagram: Journal of Petrology, v. 48, p. 2341-2357.

Houseknecht, D.W., and Schenk, C.J., 2005, Sedimentology and sequence stratigraphy of the Cretaceous Nanushuk, Seabee, and Tuluvak formations exposed on Umiat Mountain, North-Central Alaska: U.S. Geological Survey Professional Paper 1709-B, 18 p.

Houseknecht, D.W., Bird, K.J., and Schenk, C.J., 2009, Seismic analysis of clinoform depositional sequences and shelf-margin trajectories in Lower Cretaceous (Albian) strata, Alaska North Slope: Basin Research, v., 21, p., 644-654.

Houseknecht, D.W., Burns, M.W., and Bird, K.J., 2011, Thermal maturation history of Arctic Alaska and the southern Canada basin: Analyzing the Thermal History of Sedimentary Basins.

Hubbard, R.J., Edrich, S.P., and Rattey, P., 1987, Geologic evolution and hydrocarbon habitat of the 'Arctic Alaska microplate': Marine and Petroleum Geology, v. 4, p. 2-34.

Imlay, R.W., 1961, Characteristic Lower Cretaceous Megafossils from Northern Alaska: U.S. Geological Survey Professional Paper 335, 74 p., 20 plates.

Jones, D.L, and Gryc, G., 1960, Upper Cretaceous Pelycypods of the Genus *Inoceramus* from Northern Alaska: U.S. Geological Survey Professional Paper 334-E, p. 149-163.

Kiipli, T., Jeppsson, L., Kallaste, T., and Söderlund, U., 2008, Correlation of Silurian bentonites from Gotland and the eastern Baltic using sanidine phenocryst composition, and biostratigraphical consequences: Journal of the Geological Society, London, v. 15, p., 211-220.

Land, L.S., Mack, L.E., Milliken, K.L., and Lynch, F.L., 1997, Burial diagenesis of argillaceous sediment, south Texas Gulf of Mexico sedimentary basin: a reexamination: Geological Society of America Bulletin, v., 109, p. 1-15.

Lanphere, M.A., and Dalrymple, G.B., 2000, First-principles calibration of ^{38}Ar tracers: Implications for the ages of $^{40}Ar/^{39}Ar$ fluence monitors: U.S. Geological Survey Professional Paper 1621, 10 p.

Lanphere, M.A. and Tailleur, I.L., 1983, K-Ar ages of bentonites in the Seabee Formation, Northern Alaska: A Late Cretaceous (Turonian) time-scale point: Cretaceous Research, v. 4, 361-370.

Layer, P.W., 2000, Argon-40/Argon-39 age of the El'gygytgyn impact event, Chukotka, Russia: Meteoritics and Planetary Science, v. 35, p. 591-599.

Layer, P.W., Hall, C.M., and York, D., 1987, The derivation of $^{40}Ar/^{39}Ar$ age spectra of single grains of hornblende and biotite by laser step heating: Geophysical Research Letters, v. 14, p. 757-760.

LePain, D.L., McCarthy, P.J., and Kirkham, R., 2009, Sedimentology, stacking patterns, and depositional systems in the middle Albian-Cenomanian Nanushuk Formation in outcrop, Central North Slope, Alaska: Alaska Division of Geological and Geophysical Surveys Report on Investigations 2009-1, 86 p.

McDougall I., and Harrison, T.M., 1999, Geochronology and the Thermochronology by the $^{40}Ar/^{39}Ar$ Method: Oxford University Press, New York. 269 p.

Miller, T.P., 1989, Contrasting plutonic rock suites of the Yukon-Koyukuk basin and the Ruby Geanticline, Alaska: Journal of Geophysical Research, v. 94, p. 15969-15987.

Molenaar, C. M., 1985, Subsurface correlations and depositional history of the Nanushuk Group and related strata, North Slope, Alaska, *in* A. C. Huffman, ed., Geology of the Nanushuk Group and Related Rocks, North Slope, Alaska: U.S. Geological Survey Bulletin 1614, p. 37-60.

Moore, G.W., Drummond, K.J., Teraoka, Y., McCoy, F.W., Swint-Iki, T.R., and Gartner, A.L., 2000, Geologic Map of the Circum-Pacific Region, Arctic Sheet: U.S. Geological Society Map CP-48.

Moore, T.E., Wallace, W.K., Bird, K.J., Karl, S.M., Mull, C.G., and Dillon, J.T., 1994, Geology of Northern Alaska, *in* The Geology of North America, v. G-1, The Geology of Alaska: Geological Society of America, p. 49-140.

Mull, C.G., Houseknecht, D.W., and Bird, K.J., 2003, Revised Cretaceous and Tertiary stratigraphic nomenclature in the Colville Basin, northern Alaska: U.S. Geological Survey Professional Paper 173, 51 p.

Mull, C.G., Houseknecht, D.W., Pessel., G.H., and Garrity, C.P., 2004, Geologic Map of the Umiat Quadrangle, Alaska: U.S. Geological Survey Scientific Investigations Map 2817-A, scale 1:250,000.

O'Sullivan, P.B., 1999, Thermochronology, denudation, and variations in paleosurface temperature: a case study form the North Slope foreland basin, Alaska: Basin Research, v. 11, p. 191-204.

Pearce, J.A., 1983, Role of the sub-continental lithosphere in magma genesis at active continental margins, *in* C.J. Hawkesworth and M.J. Norry, eds., Continental Basalt Mantle Xenoliths: Nantwich, Shiva Publications, p. 230-249.

Pearce, J.A., 1996, A users guide to basalt discrimination diagrams, *in* D.A., Wyman, (ed.), Trace Element Geochemistry of Volcanic Rocks: Applications for Massive Sulfide Exploration: Geological Association of Canada, Short Course Notes, v. 12, p. 79-113.

Pearce, J.A., and Peate, D.W., 1995, Tectonic implications of the composition of volcanic arc magmas: Annual Review of Earth and Planetary Sciences, v. 23, p. 251-286.

Pearce, J.A., Harris, N.B.W., and Tindle, A.G., 1984, Trace element discrimination diagrams for the tectonic interpretation of granitic rocks: Journal of Petrology, v. 25, 956-983.

Prokoph, A., Villenueve, M., Agterberg, F.P., and Rachold, V., 2001, Geochronology and calibration of global Milankovitch cyclicity at the Cenomanian-Turonian boundary: Geology, v. 29, p. 523-526.

Robinson, F.M., 1958, Test Wells, Gubik Area, Alaska: U.S. Geological Survey Professional Paper 305-C, p. 207-264.

Sampson, S.D., and Alexander, E.C., 1987, Calibration of the interlaboratory $^{40}Ar/^{39}Ar$ dating standard, MMhb1: Chemical Geology, v. 66, p. 27-34.

Schindler, J.F., 1988, History of exploration in the National Petroleum Reserve in Alaska, with emphasis on the period from 1975-1982, *in* G. Gryc, ed., Geology and Exploration of the National Petroleum Reserve in Alaska, 1974-1982: U.S. Geological Survey Professional Paper 1399, p. 13-76.

Shimer, G.T., McCarthy, P.J, and Hanks, C.L., 2013, Sedimentology, stratigraphy, and reservoir properties of an unconventional reservoir in the Cretaceous Nanushuk Formation at Umiat Field, North Slope, Alaska: AAPG Bulletin, in press.

Smosna, R., 1988, Low-temperature, low-pressure diagenesis of Cretaceous sandstones, Alaskan North Slope: Journal of Sedimentary Petrology, v. 58, p. 644-655.

Smosna, R., 1989, Compaction law for Cretaceous Sandstones of Alaska's North Slope: Journal of Sedimentary Petrology, v. 59, p. 572-584.

Spicer, R.A., and Herman, A.B., 2010, The Late Cretaceous environment of the Arctic: A quantitative reassessment based on plant fossils: Palaeogeography, Palaeoclimatology, Palaeoecology, v. 295, p. 423-442.

Steiger, R.H., and Jaeger, E., 1977, Subcommission on geochronology: Convention on the use of decay constants in geo and cosmochronology: Earth and Planetary Science Letters, v. 36, p. 359-362.

Tappan, H.N., 1960, Cretaceous biostratigraphy of northern Alaska: AAPG Bulletin, v. 44, p. 273-297.

Thomas, R.G., Eberth, D.A., Deino, A.L., and Robinson, D., 1990, Composition, radioisotopic ages, and potential significance of an altered volcanic ash (bentonite) from the Upper Cretaceous Judith River Formation, Dinosaur Provincial Park, southern Alberta, Canada: Cretaceous Research, v. 11, p. 125-162.

Tikhomirov, P.L., Akinin, V.V., Ispolatov, V.O., Alexander, P., Cherapanova, I.Y. Cherapanova, and Zagoskin, V.V., 2006, The Okhotsk-Chukotka Volcanic Belt: Age of its northern part according to new Ar-Ar and U-Pb geochronological data: Stratigraphy and geological Correlation, 2006, v. 15, p. 524-537.

Tikhomirov, P.L., Kalinina, E.A., Moriguti, T., Makishima, A., Kobayashi, K., Cherpanova, I.Yu., and Nakamura, E., 2012, The Cretaceous Okhotsk-Chukotka

Volcanic Belt (NE Russia): Geology, geochronology, magma output ranges, and implications on the genesis of silicic LIPs: Journal of Volcanology and Geothermal Research, v., 221-222, p. 14-32.

Till, A.B., 1992, Detrital blueschist-facies metamorphic mineral assemblages in Early Cretaceous sediments of the foreland basin of the Brooks Range, Alaska, and implications for orogenic evolution: Tectonics, v. 11, p. 1207-1223.

Till, A.B. and Patrick, B.E., 1991, Ar-Ar evidence for a 110-105 a amphibolite facies overprint on blueschist in the south-central Brooks Range, Alaska: Geological Society of America Abstracts Programs, 23, A436.

Till, A.B., and Snee, L.W., 1995, $^{40}Ar/^{39}Ar$ evidence that formation of blueschists in continental crust was synchronous with foreland fold and thrust belt deformation, western Brooks Range, Alaska: Journal of Metamorphic Geology, v. 13, p. 41-60.

Vogl, J.J., Calvert, A.T., and Gans, P.P., 2002, Mechanisms and timing of exhumation of collision-related metamorphic rocks, southern Brooks Range, Alaska: insights from $^{40}Ar/^{39}Ar$ thermochronology: Tectonics, v. 21, doi 10.1029/2000TC001270.

Winchester, J.A., and Floyd, P.A., 1977, Geochemical discrimination of different magma series and their differentiation products using immobile elements: Chemical Geology, v. 20, p. 325-343.

York, D., Hall, C.M., Yanase, Y., Hanes, J.A., and Kenyon, W.J., 1981, $^{40}Ar/^{39}Ar$ dating of terrestrial minerals with a continuous laser: Geophysical Research Letters, v. 8, p. 1136-1138.

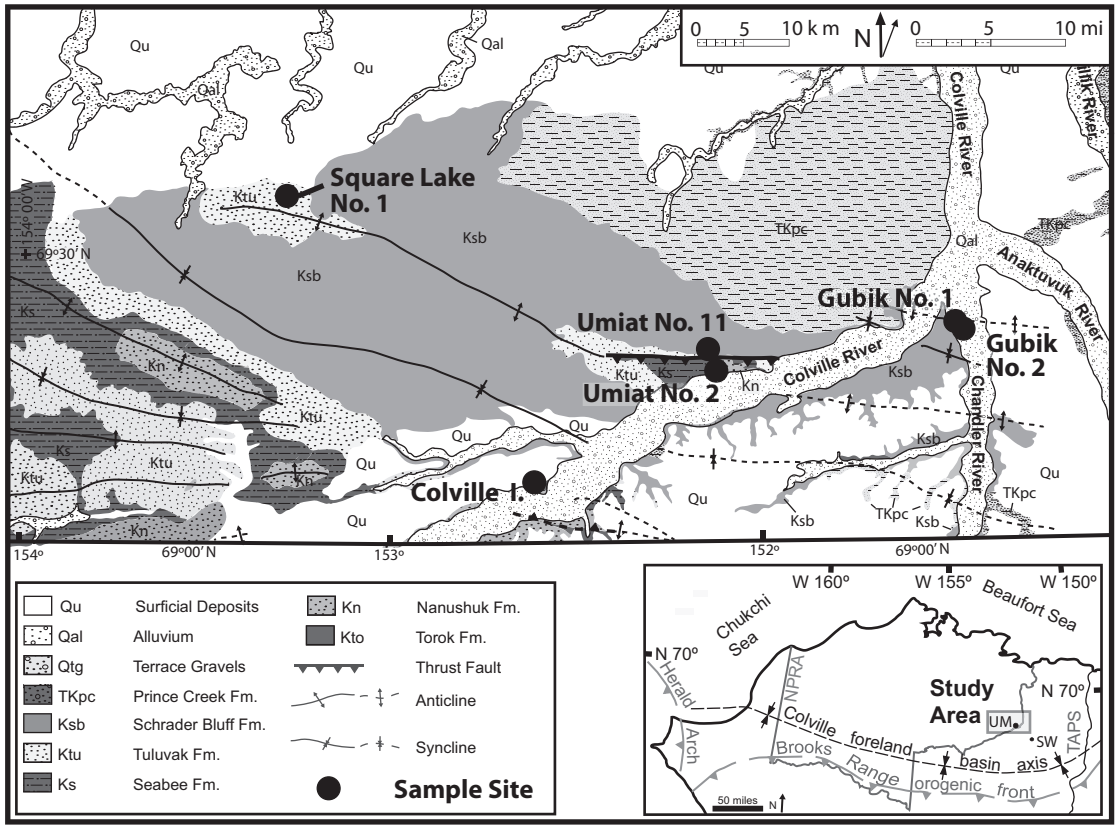

Figure 3.1 Geologic Map of the Study Area
The sites featured in this study are located in the central Brooks Range foothills along the Colville River, near the border of the National Petroleum Reserve – Alaska. The Brooks Range foothills contain fold and thrust structures, including anticline-syncline pairs, that expose the Brookian foreland basin deposits at the surface (Geologic map modified from Mull et al., 2004). The inset map in the lower right corner shows the location of the study area along the Colville River, as well as locations mentioned in the text: Umiat (UM) and Shale Wall Bluff (SW). Inset map modified from Decker (2007).

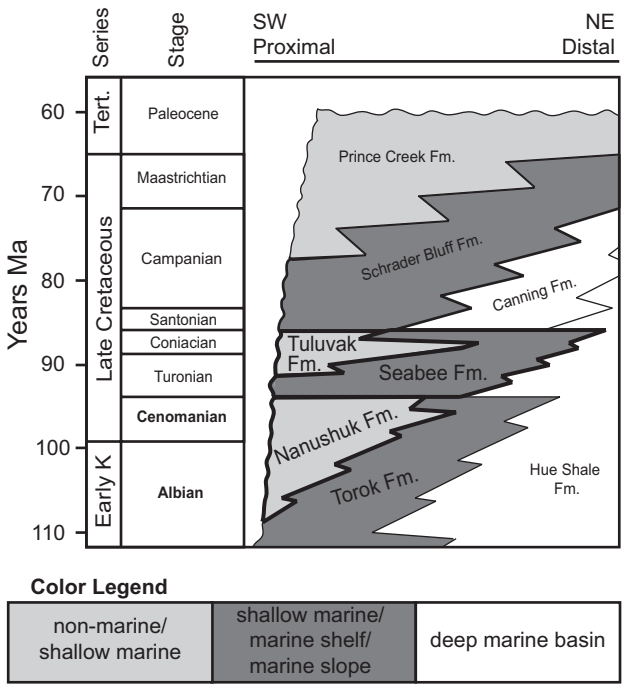

Figure 3.2 Brookian Stratigraphy of the North Slope
Bentonites in this study are taken from the Tuluvak, Seabee, and Nanushuk Formations, which are highlighted in with a bold black line in the stratigraphic section chart (modified from Mull et al., 2003). These formations range from Albian-Coniacian in age. A single sample from the base of the Schrader Bluff Formation is also included. The Schrader Bluff Formation is Santonian to Maastrichtian in age.

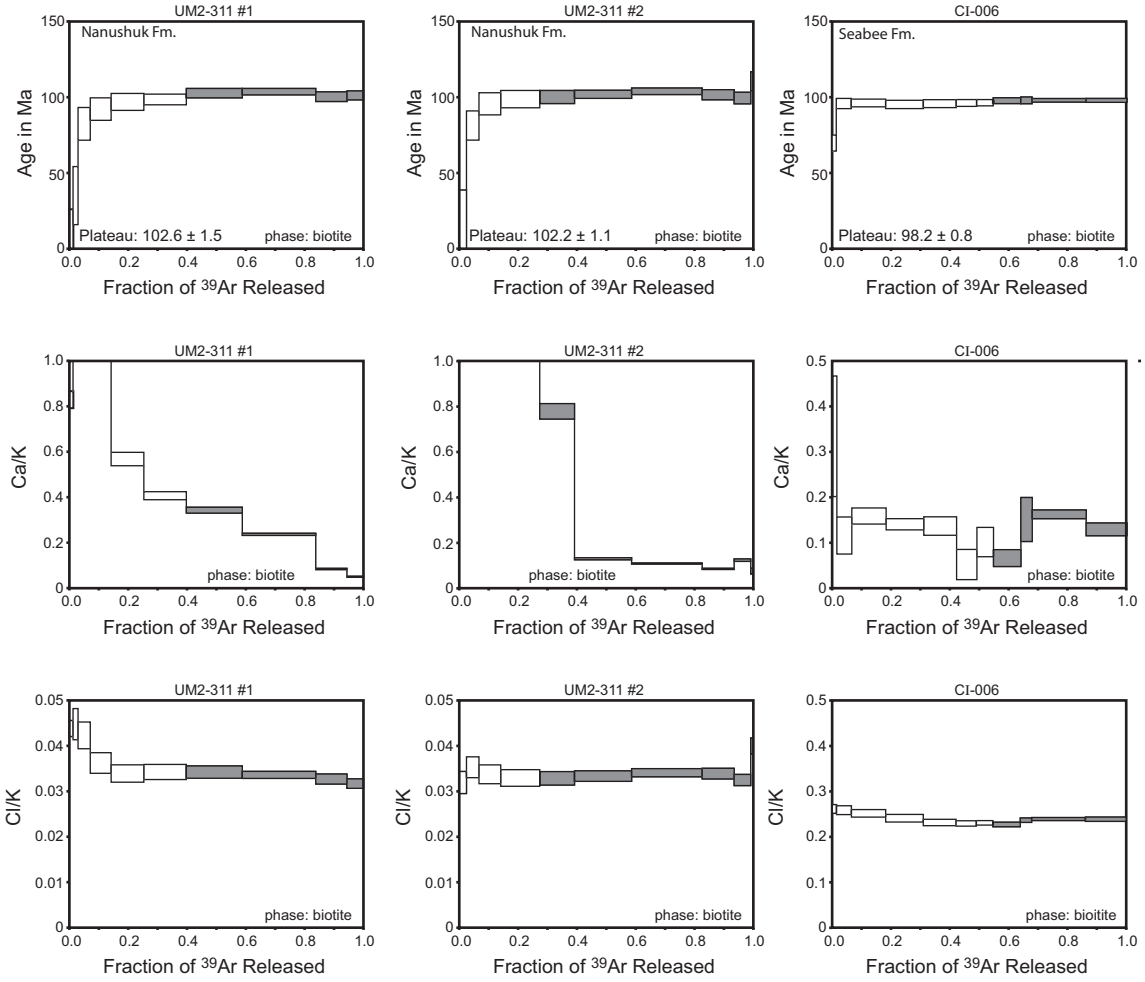

Figure 3.3 $^{40}Ar/^{39}Ar$ Age Spectra, Nanushuk and Seabee Formations
The age spectra from UM2 have flat release spectra that meet the criteria for a plateau age. Grey boxes indicate steps selected for plateau ages. The step-up release pattern indicates argon-loss. Sample CI-006 technically does not meet the criteria for a plateau age, despite having a flat release spectrum.

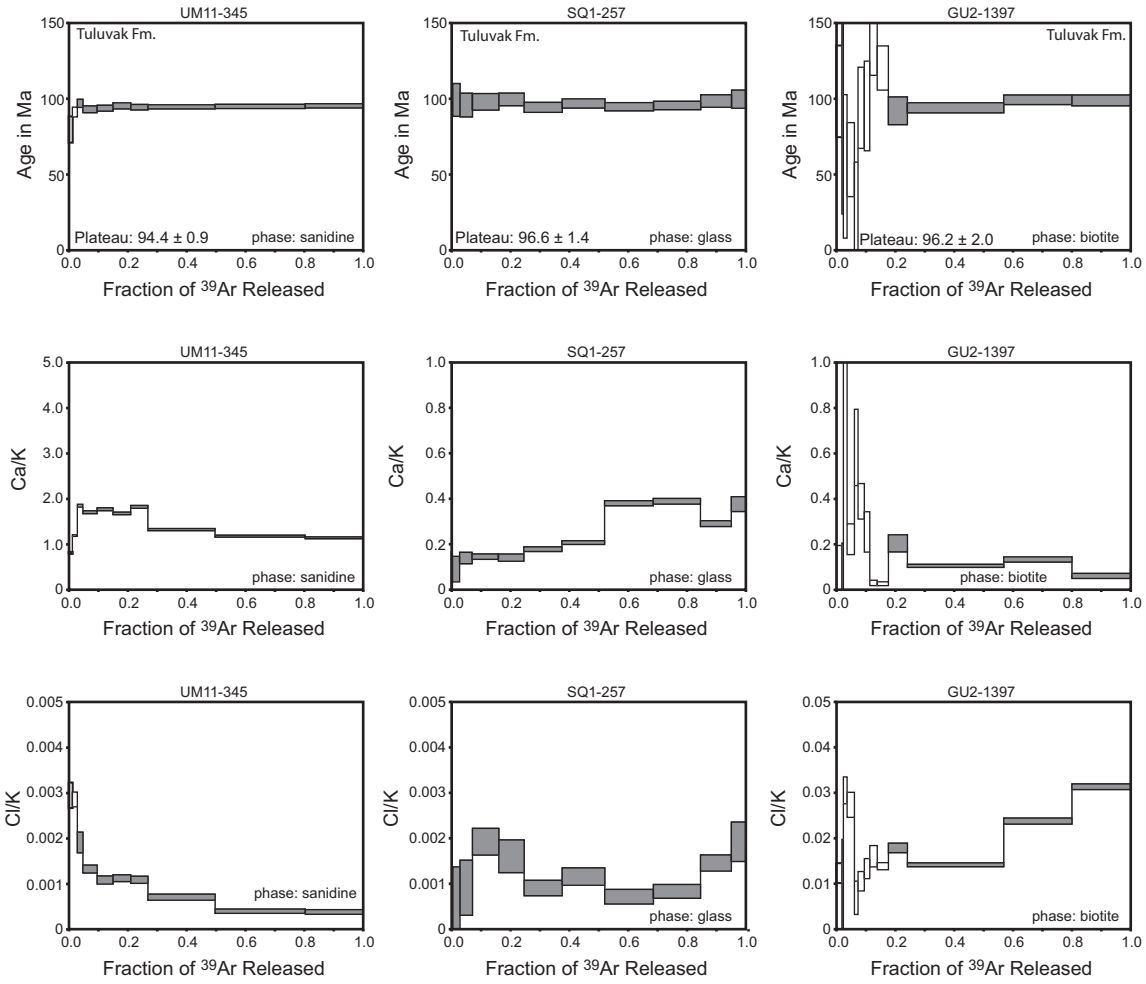

Figure 3.4 $^{40}Ar/^{39}Ar$ Age Spectra, Tuluvak Formation
The age spectra from all three samples presented here have flat release spectra that meet the criteria for plateau ages. Grey boxes indicate steps selected for plateau ages.

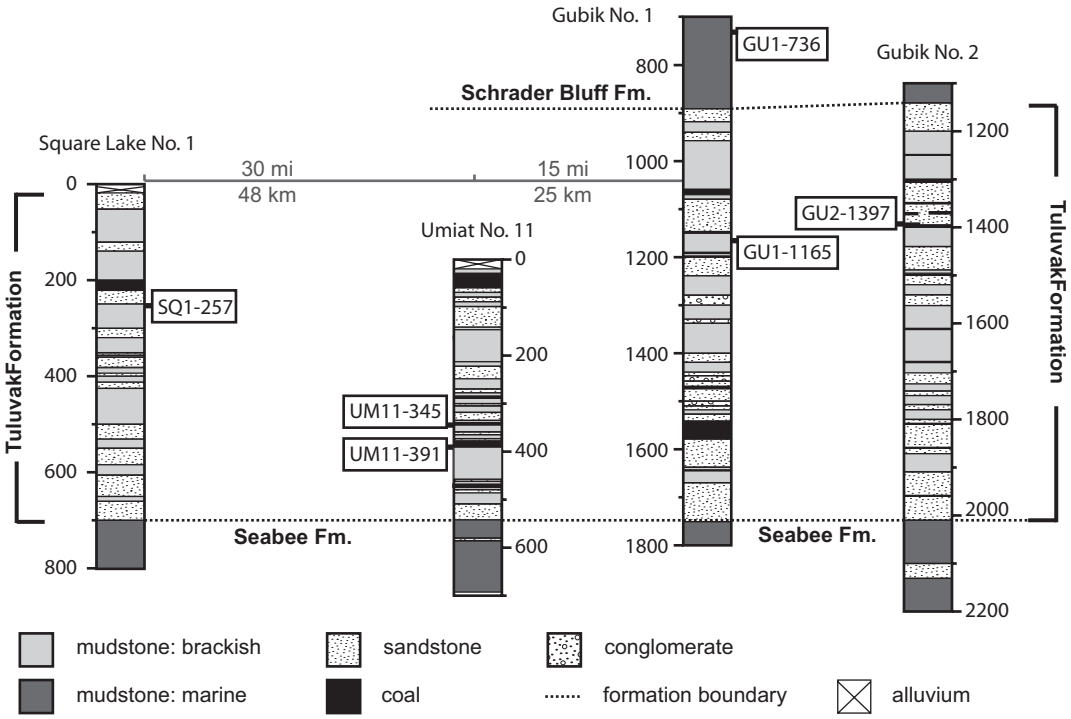

Figure 3.5 Tuluvak Formation Stratigraphy
Stratigraphic sections from four of the wells in this study illustrate the thickness and lithology of the Tuluvak Formation, as well as the depths of tephra samples. Wells are "hung" on the base of the lowest sandstones in the Tuluvak Formation

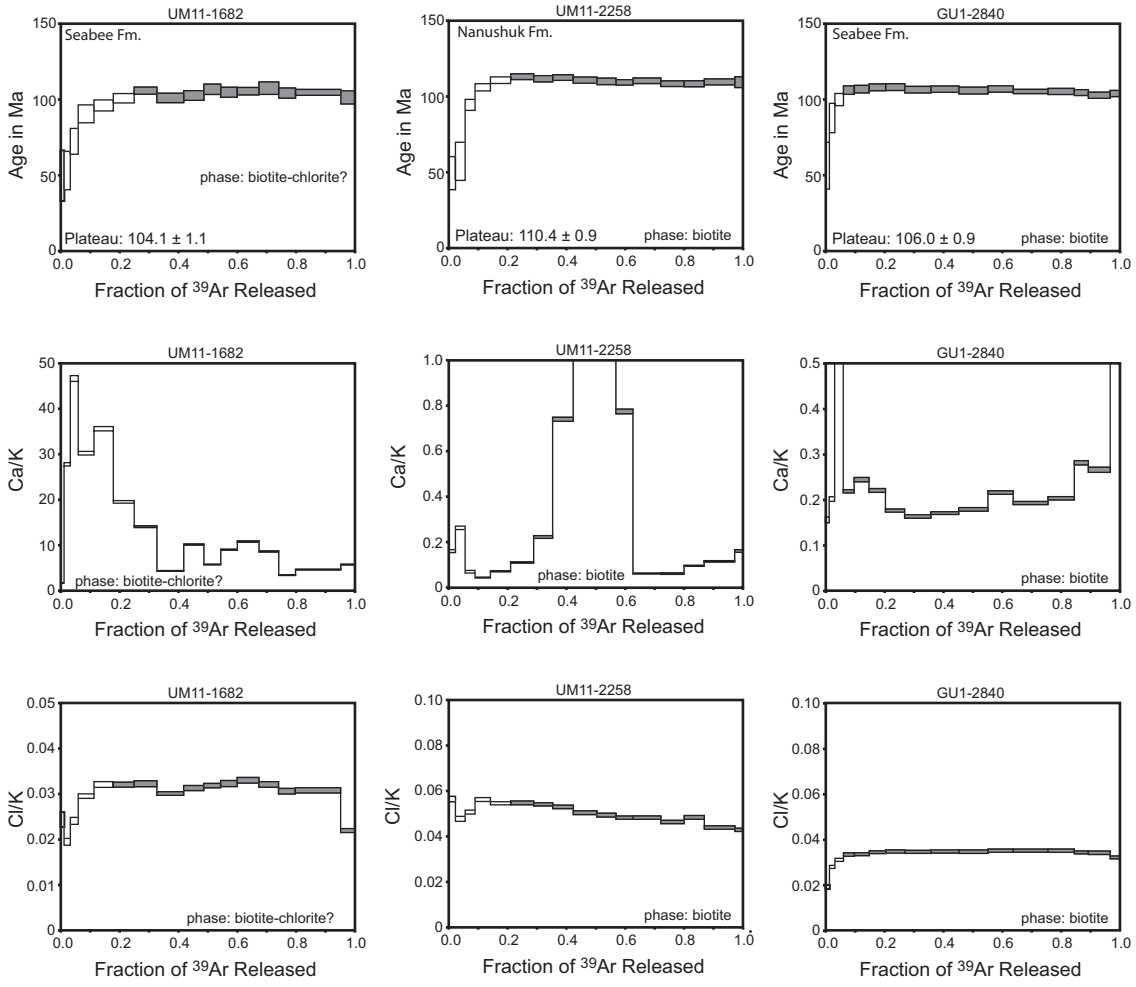

Figure 3.6 Anomalous Albian $^{40}Ar/^{39}Ar$ Age Spectra
The age spectra in this figure have anomalous $^{40}Ar/^{39}Ar$ plateau ages that do not realistically compare to their stratigraphic positions. The Seabee and Tuluvak formations are Cenomanian and younger. UM11-2258 is considered too old based on its relative stratigraphic position in comparison to UM2-311 (Fig. 2.3a)

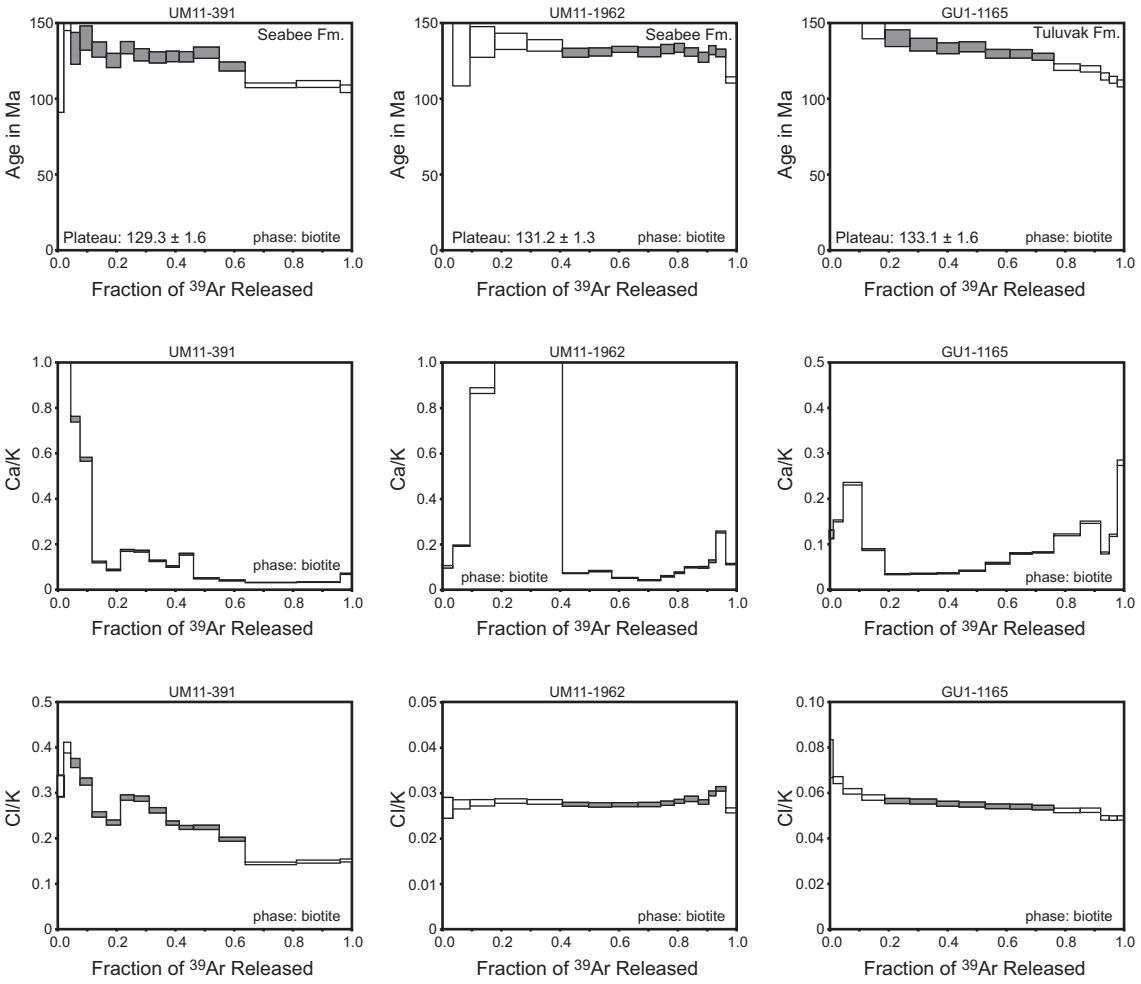

Figure 3.7 Anomalous Valanginian-Barremian $^{40}Ar/^{39}Ar$ Age Spectra
The age spectra in this figure have anomalous $^{40}Ar/^{39}Ar$ plateau ages that do not realistically compare to their stratigraphic positions. The three samples here are from the Seabee and Tuluvak formations, which are Cenomanian and younger. The Valanginian-Barremian dates are unrealistic, and indicate excess argon.

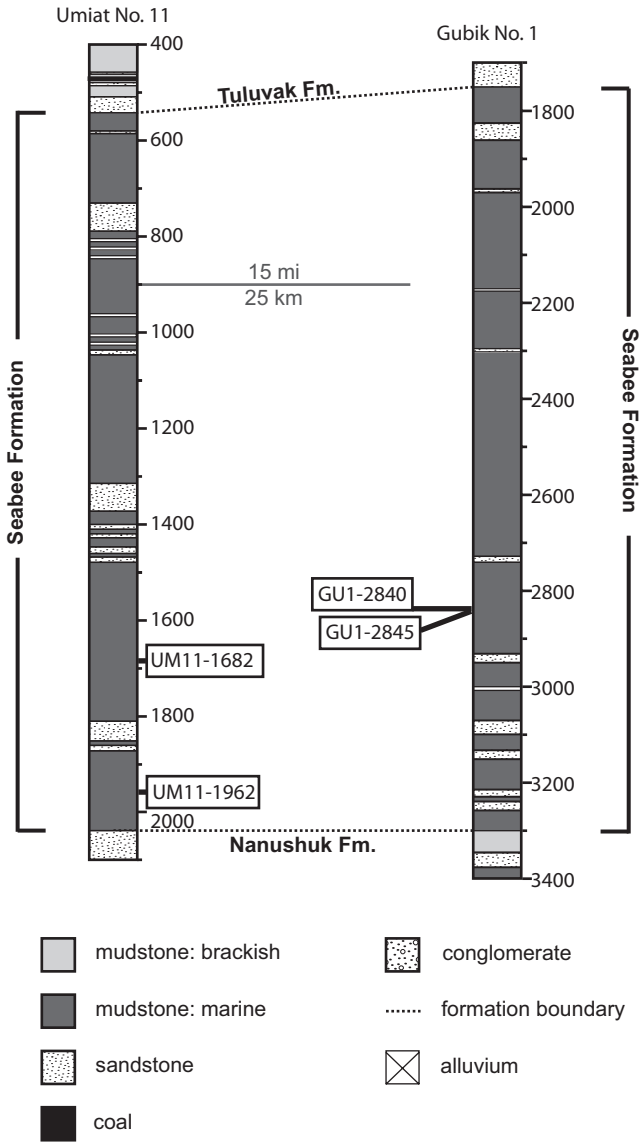

Figure 3.8 Seabee Formation Stratigraphy
Stratigraphic sections from two of the wells in this study illustrate the thickness and lithology of the Seabee Formation, as well as the relative depths of tephra samples..

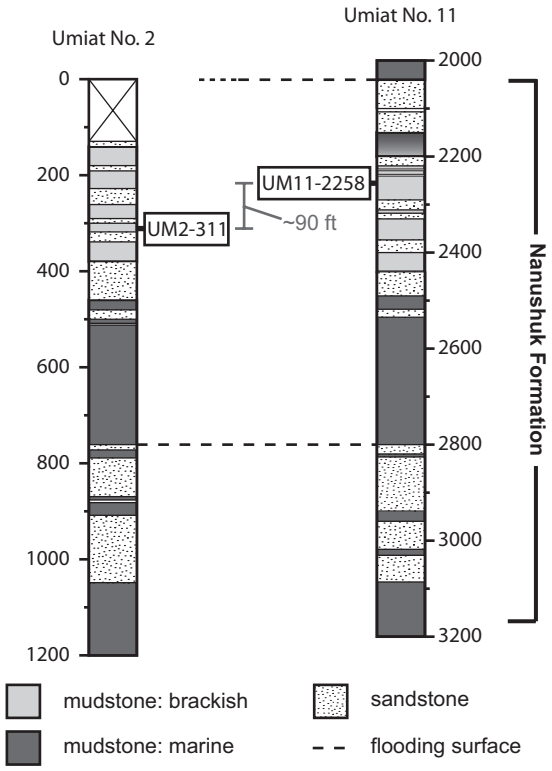

Figure 3.9 Nanushuk Formation Stratigraphy
Stratigraphic sections from two of the wells in this study illustrate the thickness and lithology of the Nanushuk Formation, as well as the relative depths of tephra samples. Wells are "hung" on a flooding surface at the top of the lower Nanushuk Formation sandstones. UM11-2258 is stratigraphically higher than UM2-311.

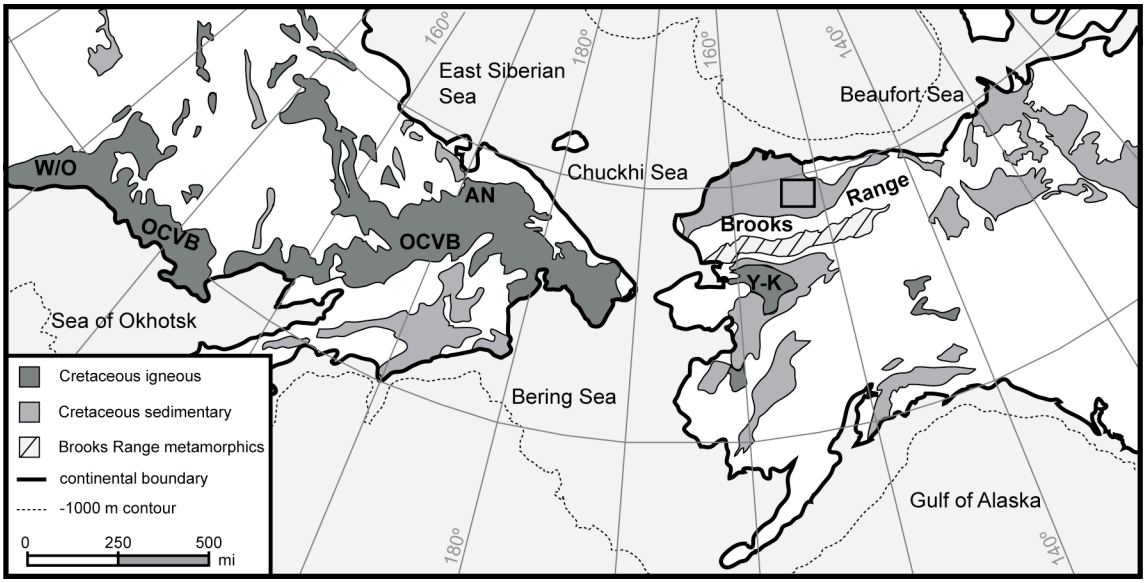

Figure 3.10 Cretaceous Units in Siberia, Alaska, and Canada
The Okhotsk-Chukotka Volcanic Belt (OCVB) is a potential source for Brookian tephra deposits. Both the OCVB and metamorphic rocks in the southern Brooks Range could be sources of detrital sediment or xenoliths responsible for anomalous $^{40}Ar/^{39}Ar$ ages. The regions depicted include the western Okhotsk (W/O) and Anadyr (AN) segments of the OCVB, and the Yukon-Koyukuk terrane (Y-K). Modified from Moore et al. (2000) with additional data from Moore et al. (1994).

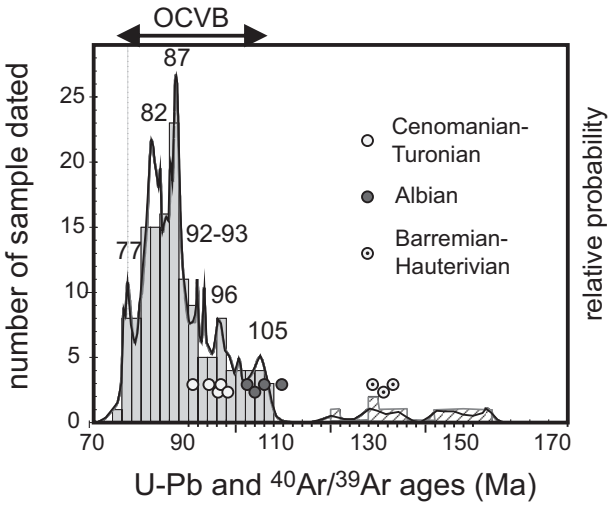

Figure 3.11 $^{40}Ar/^{39}Ar$ Plateau Ages Versus Okhotsk-Chukotka Volcanic Belt Ages
When plotted against a histogram of radiometric ages for the Okhotsk-Chukotka Volcanic Belt (OCVB), the results of this study (dots) fall near peaks in activity. Modified from Akinin and Miller (2011).

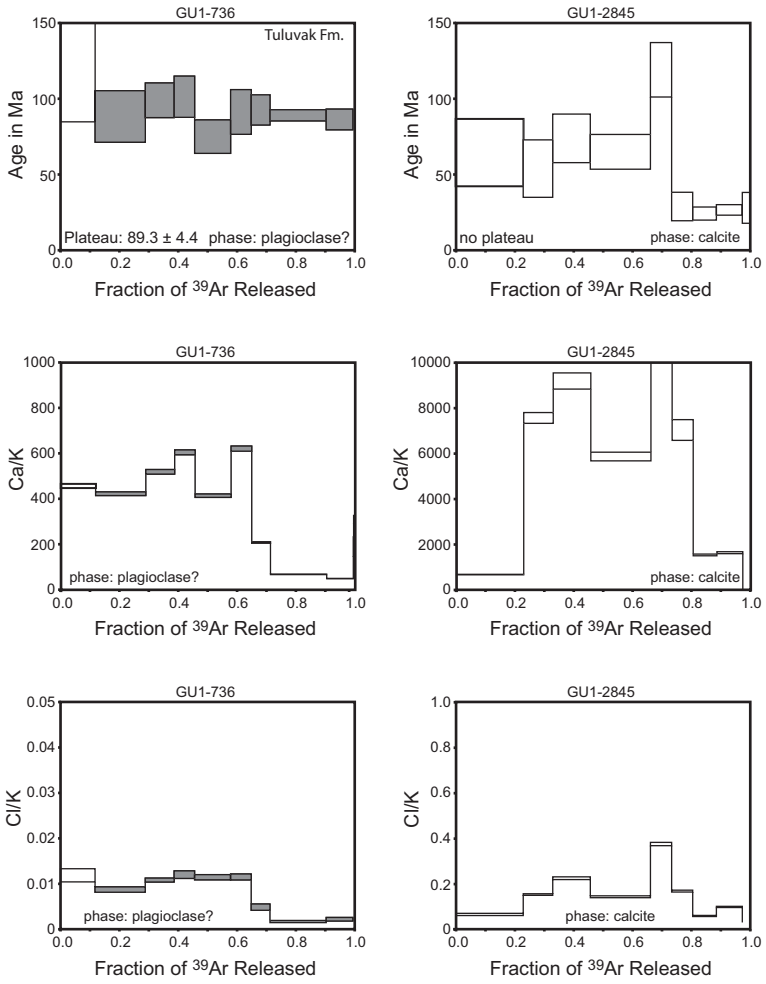

Figure 3.12 $^{40}Ar/^{39}Ar$ Age Spectra of Unknown Phases
The two samples depicted here are from unknown mineral phases, as evidenced by high Ca/K ratios. Sample Gu1-736 is a possible calcic plagioclase, but without further mineralogic data the age is geologically uninterpretable. GU1-2845 is from likely calcite separates.

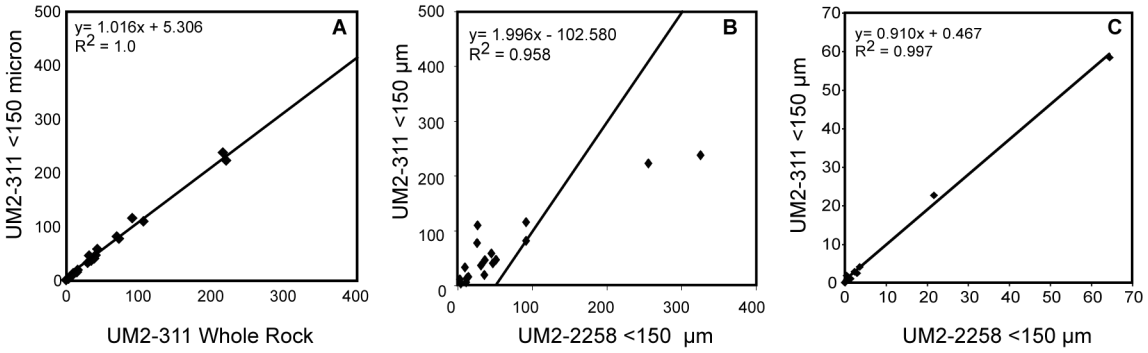

Figure 3.13 Nanushuk Formation Bentonite Geochemistry
Bivariate plots comparing tephra geochemistry from Nanushuk Formation samples. A) The correlation between the < 150 µm and whole rock trace element geochemistry from UM2-311 is strong enough to infer minimal geochemical fractionation based on particle size. B) The UM2-311 and UM11-2258 trace element geochemistry are similar, but not correlative. C) A bivariate plot of major element geochemistry of UM2-311 and UM11-2258 shows a strong correlation. Based on B and C we cannot rule out a correlation between UM2-311 and UM11-2258.

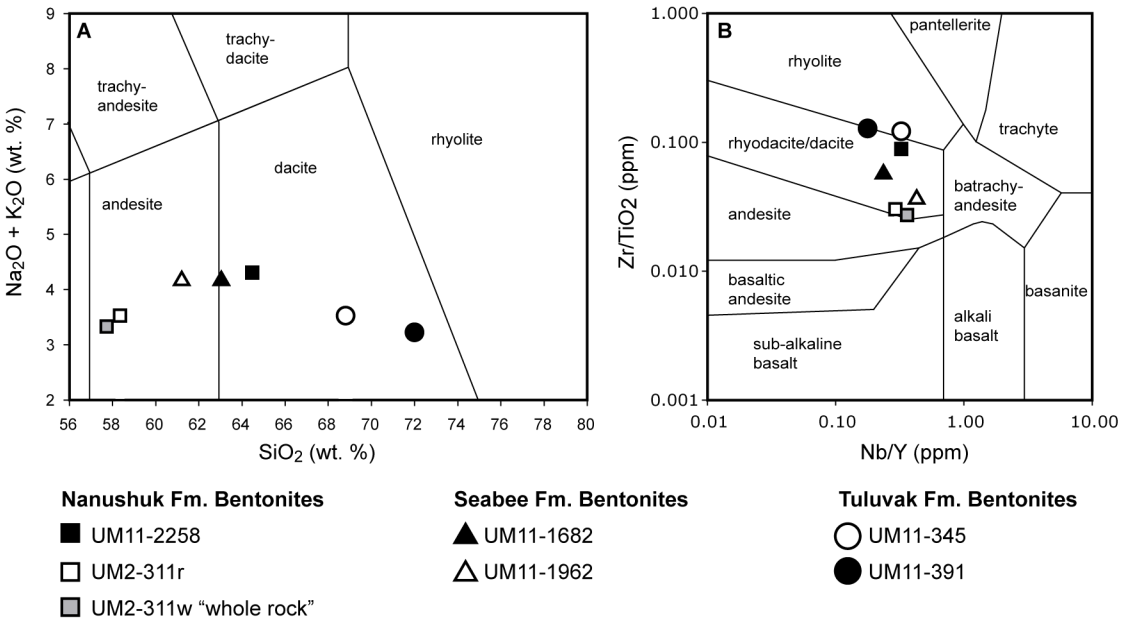

Figure 3.14 Igneous Classification Diagrams
A) Total-Alkali-Silica (TAS) diagram of the Umiat bentonites. The Umiat bentonites become increasingly felsic with time, with the exception of UM11-2258, which may be contaminated with detrital sediment. B) A similar trend of increasingly felsic composition appears in the trace element classification diagram, where Zr/TiO_2 serves as a proxy for SiO_2 content. Some SiO_2 loss is expected, and the trace element diagram does classify the tephras as more felsic than the TAS diagram.

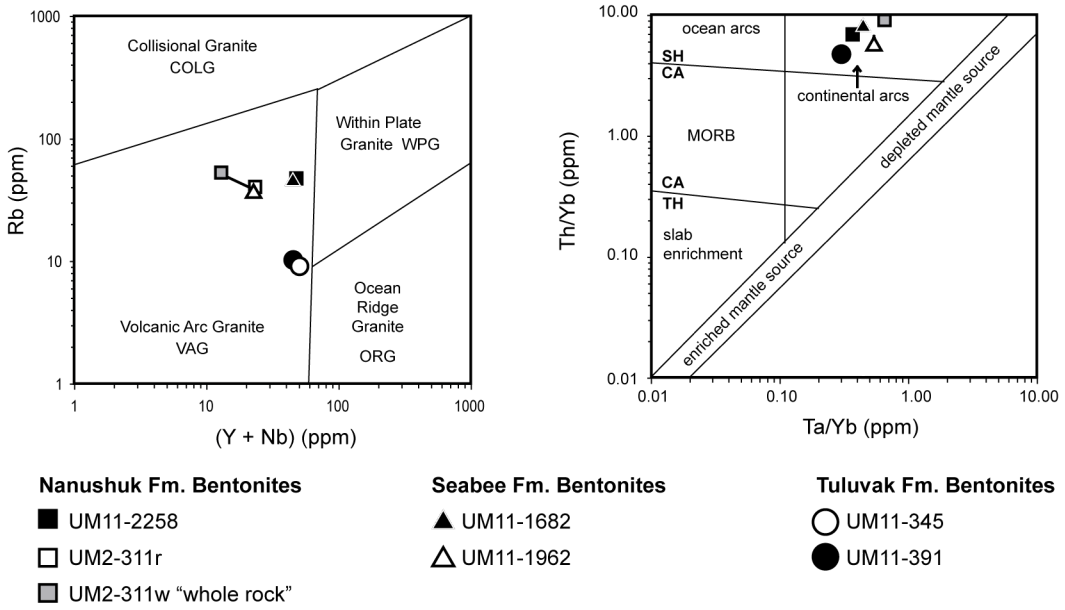

Figure 3.15 Volcanic Arc Classification Diagrams
A) The likely source of the Umiat bentonites was a volcanic arc. B) More specifically, the Umiat tephras are geochemically similar to igneous rocks in continental arc settings.

Table 3.1 $^{40}Ar/^{39}Ar$ Results

Sample	Formation	Phase	Integrated Age	**Plateau Age**	Isochron Age
GU1-736SC	Schrader Bluff	plagioclase?	93.6±6.5	**89.3 ± 4.4**	87.6±3.6
GU1-1165T	Tuluvak	biotite	158.1±5.6	**133.1±2.2**	
GU1-2840S	Seabee	biotite	104.8±0.9	**106.0±0.9**	
GU1-2845S	Seabee	calcite	398.7±43.8	**None**	
GU2-1397T	Tuluvak	biotite	96.2±2.5	**96.2±2.0**	
SQ1-257T	Tuluvak	glass	96.7±1.5	**96.6±1.4**	95.3±2.8
CI-006S	Seabee	biotite	96.7±0.7	**98.2±0.8**	
UM2-311N #1*	Nanushuk	biotite	97.4 ± 1.5	**102.6 ± 1.5**	
UM2-311N #2*	Nanushuk	biotite	98.3±1.6	**102.2±1.1**	
UM11-345T	Tuluvak	sanidine?	94.2±0.9	**94.4±0.9**	94.2±1.1
UM11-391T	Tuluvak	biotite	123.5±2.0	**129.1±1.8**	125.6±2.0
UM11-1682S	Seabee	biotite	100.3±1.1	**104.1±1.1**	
UM11-1962S	Seabee	biotite	137.3±3.5	**131.2±1.3**	131.3±2.4
UM11-2258N	Nanushuk	biotite	106.5±1.0	**110.4±0.9**	

Table 3.2 $^{40}Ar/^{39}Ar$ Plateau Information

Sample	Formation	Plateau Age (Ma)	Fractions	% ^{39}Ar release	MSWD
GU1-736SC	Schrader Bluff	91.3±4.4	93.6±6.5	91.3±4.4	87.6±3.6
GU1-1165T	Tuluvak	133.1±1.6	158.1±5.6	133.1±1.6	
GU1-2840S	Seabee	106.0±0.9	104.8±0.9	106.0±0.9	
GU2-1397T	Tuluvak	96.2±2.0	96.2±2.5	96.2±2.0	
SQ1-257T	Tuluvak	96.6±1.4	10 of 12	99.6	0.25
CI-006S	Seabee	98.2±0.8*	4 of 11	45.3	
UM2-311N #1	Nanushuk	102.6 ± 1.5	4 of 10	60.2	0.33
UM2-311N #2	Nanushuk	102.2 ± 1.4	6 of 10	72.6	0.64
UM11-345T	Tuluvak	94.4±0.9	8 of 10	97.2	0.27
UM11-391T	Tuluvak	129.3±1.6	11 of 16	59.3	1.23
UM11-1682S	Seabee	104.1±1.1	11 of 16	82.0	0.51
UM11-1962S	Seabee	131.2±1.3	10 of 16	55.5	0.36
UM11-2258N	Nanushuk	110.4±0.9	11 of 16	79.0	0.67

Table 3.3 XRF Major and Trace Element Analysis Results

Oxides (wt. %)	UM11-345	UM11-391	UM11-1682	UM11-1962	UM11-2258	UM2-311	UM2-311w
SiO_2	**68.80**	**72.02**	**63.03**	**61.27**	**64.49**	**58.35**	**57.67**
Al_2O_3	19.67	18.71	20.24	21.40	21.73	22.62	23.37
Fe_2O_3	4.96	4.02	4.70	5.48	3.63	4.07	4.23
MgO	2.49	2.54	2.41	2.93	2.37	2.85	2.81
CaO	0.72	0.51	4.18	1.36	0.43	1.88	3.58
MnO	---	---	0.09	0.02	0.01	0.02	0.03
Na_2O	**3.30**	**3.07**	**3.27**	**3.15**	**2.94**	**2.48**	**2.23**
K_2O	**0.21**	**0.18**	**0.92**	**1.03**	**1.36**	**1.03**	**1.09**
TiO_2	0.23	0.16	0.53	0.51	0.37	0.79	0.77
P_2O_5	0.01	0.01	0.08	0.23	0.07	0.17	0.18
Cl	0.01	0.01	0.02	0.03	0.02	0.04	0.03
S	0.04	---	0.26	0.13	0.01	---	0.01
Trace Elements (ppm)	UM11-345	UM11-391	UM11-1682	UM11-1962	UM11-2258	UM2-311	UM2-311w
Ba	737.74	382.91	994.69	790.43	1317.81	1137.21	1092.27
Ce	109.16	116.55	119.18	74.57	92.15	114.96	91.59
Co	3.65	2.05	4.10	5.97	3.34	10.16	9.73
Cr	2.83	3.51	8.88	21.21	2.95	108.79	106.94
Cs	1.29	2.08	11.48	5.43	4.67	1.29	2.77
Cu	4.78	4.39	10.20	8.08	14.56	14.81	15.28
Ga	27.93	27.93	22.85	24.85	28.08	29.57	28.50
Hf	7.28	7.00	5.87	4.44	10.23	6.45	5.85
La	48.78	57.82	68.52	43.85	45.56	57.56	43.54
Mn	21.06	18.07	660.78	159.27	60.14	147.21	218.77
Mo	1.23	0.48	4.13	2.19	2.40	1.06	1.59
Nb	**12.47**	**7.85**	**8.93**	**6.83**	**11.77**	**5.41**	**5.88**
Nd	49.98	51.20	58.09	29.93	36.61	45.32	32.04
Ni	12.25	2.41	4.64	7.54	10.23	32.13	30.19
Pb	30.89	36.57	24.63	28.77	51.78	46.37	41.24
Rb	9.56	9.54	46.48	37.31	47.52	39.91	39.33
Sc	14.49	10.75	14.86	8.10	12.50	12.40	10.65
Sm	9.91	5.96	7.74	2.40	3.73	1.44	3.36
Sn	7.19	10.10	7.04	8.25	9.98	9.53	9.19
Sr	331.84	218.60	361.31	356.59	255.87	22.09	22.15
Ta	**---**	**1.59**	**1.62**	**1.79**	**1.73**	**1.44**	**2.50**
Th	**25.50**	**25.51**	**29.91**	**20.13**	**31.61**	**35.99**	**35.39**
TiO_2	**2343.50**	**1567.15**	**5291.84**	**5097.02**	**3725.19**	**7855.94**	**7788.39**
U	12.02	9.91	11.78	8.53	12.39	13.90	10.51
V	10.67	4.31	28.80	49.63	26.22	76.80	73.13
Y	38.56	44.18	37.33	15.87	36.08	18.51	16.30
Yb	2.83	5.31	3.68	3.30	4.65	2.80	3.86
Zn	77.54	42.74	105.41	88.00	91.96	80.96	70.30

Table 3.4 XRF Trace Element Standards

Sample	TiO_2	Nb	Rb	Ta	Th	Y	Yb	Zr
JA-2 measured:	7130	9	72	<DL	5	18	1.0	118
• compiled:	6700	9.8	68	0.61	4.7	18	1.6	119
• % difference:		-8.0%	5.9%	---	6.4%	0.0%	-37.5%	-0.8%
BE-N measured:	30143	106	55	8.0	11	30	1.0	303
• compiled:	26100	100	47	5.5	11	30	1.8	265
• % difference		-6.0%	17.0%	45.5%	0.0%	0.0%	-44.4%	14.3%
GSP-1 measured:	5079	20	206	4.0	82	21	3	420
• compiled:	6500	27.9	254	---	106	26	---	530
• % difference:		-28.3%	-18.9%	---	-22.6%	-19.2%	---	-20.8%
JG-2 measured:	449	14	302	<DL	32	85	10	93
• compiled:	440	15	297	1.9	29.7	89	8.3	97
• % difference:		-6.7%	1.7%	---	7.7%	-4.5%	20.5%	-4.1%
JR-1	1019	16	262	3.0	29	45	6	100
• compiled:	1100	15.5	257	1.9	26.5	46	4.6	102
• % difference:		3.2%	1.9%	57.9%	9.4%	-2.2%	30.4%	-2.0%
JP-1 measured:	32	1	1	6	2	<DL	8	5
• compiled:	17	1.2	0.8	0.02	0.2	1	0.02	6
• % difference:	88.0%	69.4%	25.0%	299%	90.0%	---	399.0%	-16.7%

Chapter 4: Trajectory analysis, stacking patterns, and topset facies distribution a high accommodation foreland basin, mid-Cretaceous Nanushuk Formation, North Slope, Alaska[1]

4.1 Abstract

The Albian-Cenomanian Nanushuk Formation comprises marine shelf, shoreface, deltaic, and fluvial facies deposited as clinoform topsets in the Colville foreland basin on Alaska's North Slope. The lower and upper Nanushuk Formation can be distinguished based on dominant distributive mechanisms, which are controlled by basin bathymetry and have a direct effect on shoreline trajectories and stacking patterns. The lower Nanushuk Formation primarily consists of marine, shoreface, and wave-influenced deltaic facies deposited in a marine-distributive systems defined by wave, ocean current, and tidal energy. The upper Nanushuk Formation, in contrast, is comprised of deltaic and non-marine facies, described here as river-distributive because fluvial and deltaic processes are the dominant mechanisms for sediment dispersal. Analysis of subsurface wells in the central Brooks Range foothills show that marine-distributive and river-distributive sediments are stacked in a similar succession in each well, and that the pattern advances from west-to-east with prograding Nanushuk-Torok formation clinoforms. Marine-distributive conditions are attributed to deposition at or near the shelf edge, while river-distributive conditions occurred as systems prograded across a shallow Nanushuk-Torok shelf following local transgressive events. Wave-influenced marine-distributive deposits are to be highly aggradational, which helped preserve and amplify already steep clinoforms in the Colville foreland basin. River-distributive deltaic deposits, in contrast, are highly progradational at their onset, with aggradation occurring away from the coast in more proximal association with the thrust belt, as is common in asymmetric foreland basins. New models of Nanushuk Formation depositional systems during the Albian-Cenomanian emphasize accumulation of sediment in these distributive systems, rather than as localized deltaic deposits.

[1] Shimer, G.T., McCarthy, P.J., and Hanks, C.L., in prep., for Cretaceous Research

4.2 Introduction

The dominant controls on the distribution of sediment within a foreland basin are tectonic setting, eustatic sea level, and climatic variables (Van Wagoner and Bertram, 1995). Therefore, spatial or temporal changes in sedimentary facies or stratigraphic relationships can be used to interpret the complex evolution of a basin (Vail et al., 1991; Catuneanu et al., 2009). These analyses are commonly made through sequence stratigraphic interpretations of sigmoidal clinoforms or clinothems, which are observable using seismic reflection data (Sircombe and Kamp, 1998), and at well-exposed outcrops in sparsely vegetated regions like Spitsbergen (Helland-Hansen, 1992; Pontén and Plink-Björklund, 2009) or the Book Cliffs of the western United States (Swift et al., 1987; Hampson, 2000). Though visible in dip-oriented seismic sections, such as on the North Slope (Houseknecht et al., 2009), high-relief slope clinoforms in any region, which by definition exceed 500-700 m in height, are difficult to observe in outcrop because of limited exposure and muddy composition (Hubbard et al., 2010). Furthermore, in regions like the central Brooks Range foothills of Alaska it is difficult to observe topsets and the shelf-slope break in seismic data due to the shallow depth of the targeted intervals and structural complications caused by folding and thrust faulting. In these regions, traditional sequence stratigraphic interpretations are difficult to apply on a local scale from either outcrop or seismic data (LePain et al., 2009).

An effective alternative for interpreting the progradational history of foreland basin systems is shoreline or shelf trajectory analysis, in which the lateral and vertical migration of depositional environments observed in wells can be interpreted from two-dimensional dip-oriented sections (Helland-Hansen and Hampson, 2009). Shoreline trajectories, which can be inferred from sediment facies and thickness data available in subsurface wells, are determined by rates of relative sea level change, sediment supply, and basin physiography (Helland-Hansen and Martinsen, 1996). Through the identification of sedimentary facies and stacking patterns on the shelf, and the

determination of shoreline trajectories, it is possible to interpret the history of relative accommodation and sediment supply in the basin.

The Albian-Cenomanian Nanushuk Formation, North Slope, Alaska, comprises alluvial, fluvial, deltaic, shallow marine, and marine shelf sedimentary facies associations deposited in topset positions on high-relief clinoforms in the Colville foreland basin (Mull et al., 2003; LePain et al., 2009). Geologists have long recognized two major types of deposits in the Nanushuk Formation; lower marine-dominated facies with evidence of wave-influence, and overlying river-dominated deltaic and non-marine alluvial or fluvial facies (Ahlbrandt et al., 1979; Molenaar, 1985). We suggest that the distribution of facies is linked to basin evolution during the Albian and records the history of Albian-Cenomanian basin fill in the central North Slope. Similar facies distributions are found in other regions (Bhattacharya and Walker, 1991), which may indicate a definitive pattern for sedimentary evolution of foreland basins.

To address questions of changing influence in the Colville foreland basin, we study core and outcrop records from the Nanushuk Formation at several localities in the Brooks Range foothills of the central North Slope (Fig. 4.1). The area is located in a part of the foreland basin that experienced progradation from both the west and the south, and is known to have abundant wave-influenced features such as hummocky and swaley cross stratification (Molenaar, 1985; LePain et al., 2009). Our interpretations focus on the role of wave-influence and sediment dispersal in the modification of the Nanushuk shelf during the mid-late Albian and the relationship between shoreline trajectories and relative sea-level and accommodation. We emphasize the role of bathymetry, ocean energy (waves, tides, and currents), and the balance between sediment supply and accommodation in a model of shelf construction and progradation during the Albian-Cenomanian. We also consider the role of climatic factors and eustatic sea level rise. Finally, we present new models of deltaic systems in the Nanushuk Formation that consider these variables in the context of modern geomorphic analogues.

4.3 Geologic Background

The Albian-Cenomanian Nanushuk Formation is a major component of the clastic sedimentary fill of the Colville foreland basin on the North Slope. The Nanushuk Formation consists of clastic deposits in topset positions in large Torok-Nanushuk clinoforms (Mull, 1985; Molenaar, 1985). Largely eastward prograding Torok-Nanushuk clinoforms dominate the Brookian foreland basin fill and reach up to 2000 m in height (6500 ft.) in the south along the basin axis (Houseknecht et al., 2009). Torok-Nanushuk clinoforms form part of a larger Brookian "megasequence" that filled the Colville foreland basin with detritus from the ancestral Brooks Range and undetermined sources to the west (Hubbard et al., 1987; Decker, 2007; Houseknecht et al., 2009). The Brookian is one of several megasequences that comprise the sedimentary record of the Arctic Alaska microplate or terrane (Hubbard et al., 1987) and North Slope. It overlies Beaufortian deposits (Berriasian-Barremian: 145.5-125 Ma), which formed above a Lower Cretaceous unconformity during rifting of the Canada Basin and formation of the Beaufort Rift and associated Barrow Arch (LePain et al., 2009). The Beaufortian overlies a much older Ellesmerian passive margin sequence and Franklinian basement (Moore et al., 1994).

Foreland basins with high-relief foredeep clinoforms like the Colville foreland basin are particularly unusual, and occur in tectonic settings with significant basin margin relief along elongate troughs, where rapid sediment supply and lack of collapse features result in progradation of smooth sigmoidal clinoforms (Hubbard et al., 2010). High accommodation in the Colville foreland basin of Northern Alaska is thought to be responsible for steep, high-angle clinoforms up to 700 m in height (Houseknecht et al., 2009; Houseknecht and Wartes, 2013). The significant thickness of clinothems in the Colville foreland basin attests to a very high sedimentation rate, particularly during the Albian-Cenomanian, when large Torok-Nanushuk depositional sequences filled much of the basin (Decker, 2007; Houseknecht et al., 2009) and overtopped the northern boundary along the Barrow Arch (LePain et al., 2009).

The Nanushuk Formation, formerly known as the Nanushuk Group, was sub-divided into a number of formations (Detterman, 1956). The Nanushuk Group was downgraded and and the former formations were combined into the new Nanushuk Formation in recognition of the general trend of a marine lower Nanushuk and non-marine to deltaic upper Nanushuk (Mull et al., 2003). The abandoned terms intersect in the study area, and are of some use for interpreting the depositional history of the region (Fig. 4.2). Marine 'formations' of the former Nanushuk Group include the Tuktu, Grandstand (east) and Kukpowruk (west). The name change from Kukpowruk to Grandstand occurs at an arbitrary dividing line around 156º W longitude (Molenaar, 1985). The Kukpowruk and Grandstand contain interbedded marine, deltaic, and non-marine deposits, but he Grandstand itself has distinct marine and deltaic deposits (Chapter 2). Non-marine and deltaic units of the Nanushuk Formation include the upper portion of the Grandstand, as well as the Chandler and Corwin 'formations'. The Corwin represents significant accumulations of deltaic, fluvial, and alluvial sediments in the western North Slope (Ahlbrandt et al., 1979, Molenaar, 1985). A the top of the Nanushuk Formation, particularly in the eastern North Slope, the Ninuluk comprises shoreface, deltaic, and estuarine deposits at the top of the Nanushuk Formation (Houseknecht and Schenk, 2005; LePain et al., 2009).

Most reports place the bottom of the Nanushuk Formation (Grandstand) in the central North Slope at the base of the lowest shoreface sandstone (Molenaar, 1985), but do not take into account the volume of genetically related distal lower shoreface and prodelta sediments deposited on the shelf. A good example of this confusion is the Topagoruk 'formation', now considered part of the Torok Formation (Bird and Andrews, 1979) but indistinguishable from the Tuktu in many wells (Robinson, 1958b; Collins, 1959). We consider these deposits (Tuktu, Kukpowruk) as part of the marine Nanushuk Formation (Fig. 4.2).

The Cretaceous ages for Brookian formations are based on biostratigraphic boundaries (Jones and Gryc, 1960; Imlay, 1961; Tappan, 1960) adjusted by recent updates to the

geologic time scale (Cohen et al., 2013), with more recent radiometric dating of Cenomanian and younger volcanogenic deposits (Lanphere and Tailleur, 1983; Conrad et al., 1990; Chapter 3). Most of the Nanushuk Formation was deposited during the Albian (Mull et al., 2003), and $^{40}Ar/^{39}Ar$ dates from a bentonite in the upper Nanushuk Formation at Umiat have a mean plateau age of 102.4 ± 1.0 Ma, placing it in the late Albian (Chapter 3). However, the easternmost upper Nanushuk (Houseknecht and Schenk, 2005) and non-marine deposits along the ancestral Brooks Range mountain front in the south (LePain et al., 2009) are as young as Cenomanian. The top of the Nanushuk Formation is marked by a transgressive event and deposition of the overlying marine shale of the Seabee Formation (Houseknecht and Schenk, 2005). The base of the Seabee Formation in the Umiat area contains a biotite-rich bentonite that has an $^{40}Ar/^{39}Ar$ age of 98.2 ± 0.8 Ma, just within the Cenomanian (100.5-93.9 Ma; Chapter 3).

The Albian was a tectonically active period in Arctic Alaska, with evidence for extension and exhumation (Till, 1992), compression, subsidence, rapid sedimentation (Cole et al., 1997), and the onset of distant volcanism (Tikhomirov et al., 2012). The Colville foreland basin is thought to have reached its maximum paleobathymetry during the Aptian, largely due to tectonic loading but also in response to sediment loading from active depositional systems (Cole et al., 1997). The subsequent Albian was a period of widespread exhumation in the Brooks Range and rapid sedimentation (Cole et al., 1997; Till and Snee, 1995; Vogl et al., 2002). There is also evidence for thrust propagation to the north (Cole et al., 1997), and thermochronologic studies show denudation in the northern Brooks Range as late as 100 Ma (O'Sullivan et al., 1997). This Aptian-Albian tectonic activity strongly influenced sedimentation patterns in the Colville foreland basin by creating accommodation, shaping basin bathymetry (Houseknecht and Wartes, 2013), and providing distinct sediment sources for the western and eastern parts of the Nanushuk Formation (Fox et al., 1979; Bartsch-Winkler, 1985).

Once considered an important hydrocarbon play, the Nanushuk Formation has been the subject of a series of investigations since the 1940's, when it was the primary target of

the U.S. Navy's Pet-4 drilling program in Naval Petroleum Reserve No. 4, which is now the National Petroleum Reserve Alaska, or NPRA (Schindler, 1988). Wells are identified by a location site name, and then a number that generally corresponds to the order in which they were drilled at that site. The wells used here in this study are Wolf Creek No. 3, Square Lake No. 1, Umiat No. 1, 2, 9, and 11, Seabee No. 1, Grandstand No. 1, and Gubik No. 1 (Fig. 4.1). The Grandstand and Gubik wells are not within the boundary of the NPRA, but fall under the same series of U.S. Geological Survey reports (Robinson 1958a and 1958b) as Wolf Creek, Square Lake (Collins, 1959) and Umiat (Collins, 1958).

4.4 Nanushuk Formation Facies Associations and Stratigraphy

Stratigraphic sections presented here are based on new core interpretation, core photos, published drilling notes and core descriptions (Collins, 1958; Robinson, 1958a and 1958b; Collins, 1959; Fox et al., 1979), and published sections (LePain and Kirkham, 2001; LePain et al., 2009). Facies associations of the Nanushuk Formation in the central North Slope (Table 4.1) include offshore to prodelta mudstones (FA-1), lower shoreface (FA-2) and upper shoreface/foreshore (FA-3) deposits, distributary mouth bars (FA-4), and heterolithic delta plain mudstones, channel sandstones, and coals (FA-5; Shimer et al., in press). Other studies distinguish additional facies associations (e.g. LePain et al., 2009), but we focus on facies associations observed in the subsurface at Umiat field and other relevant well sites (Chapter 2; LePain and Kirkham, 2001).

Wave-influenced sandstones are found near the base of the Nanushuk Formation in all of the well locations in this study (Fig. 4.1). No distinct channel sandstones were identified in the lower Nanushuk Formation at Umiat (Shimer et al., in press). We do not distinguish between wave-dominated shoreface environments (Hampson and Storms, 2003) and wave-influenced deltas (Bhattacharya and Giosan, 2003) in this core-based analysis because we lack the spatial data to conclusively define or rule out deltaic processes. Similar challenges occur in outcrop in the central Brooks Range foothills

(LePain et al., 2009). Wave-influenced features in distal shoreface or wave-influenced deltaic environments include low angle laminations (interpreted to be hummocky cross stratification) and a distinct ichnology dominated by *Paleophycus, Planolites, Phycosiphon,* and *Schaubcylindrichnus freyi* (Shimer et al., in press). Sandstones in these successions generally coarsen upward from laminated very fine sandstone with highly bioturbated intervals to massive or plane laminated fine-sand with a low level of bioturbation (Fig. 4.3 and 4.4). Foreshore, beach, and back barrier facies are largely absent, though some evidence of brackish water fauna can be found at the top of shoreface successions.

Wolf Creek No. 3 (Fig. 4.3) contains wave-influenced successions with hummocky cross stratification from 2500-2600 ft. and 1885-2075 ft. The base of the Wolf Creek succession, from 3800-3900 ft. is also wave-influenced (LePain and Kirkham, 2001). A similar wave-influenced succession occurs at the base of the Nanushuk Formation in Square Lake No. 1, several miles to the north of the Wolf Creek site (Fig. 4.1). To the east, there are lower Nanushuk Formation wave-influenced sandstones at Umiat, Grandstand No. 1, and Gubik No. 1 (Fig. 4.4). At Umiat there are at least three stacked shoreface successions separated by minor flooding surfaces, which are represented by abrupt upward transitions to more distal facies. We define these flooding surfaces as discontinuities in shallow water or non-marine facies topped by offshore marine mudstones. Two of these thick successions are depicted in Umiat No. 9 (Fig. 4.4). The 20 ft.-thick sandstone at the top of the shoreface successions is also wave-generated, but it represents transgressive deposits and the base of a transgressive event in the Nanushuk Formation at Umiat (Shimer et al., in press). Wave-influenced successions are thinner at Grandstand No. 1 and Gubik No. 1 (Fig. 4.4). The Gubik No. 1 wave-influenced facies are unique, in that they are coarser and contain unique trace fossils (*Gyrolithes*) that do not occur in deposits of the Nanushuk Formation at other sites in this study. The upward-coarsening shoreface package at Gubik is thick (~120 ft.), but is truncated by a probable transgressive pebble lag and an upward fining wave-influenced succession.

Wave-influenced packages in the Nanushuk Formation generally thin to the east. A similar trend was not observed from south to north, between the Grandstand No. 1 and Umiat No. 11 wells. The modern distance from Umiat to both the Wolf Creek and Grandstand drilling sites is roughly 48 km, but is also sub-parallel to fold and thrust axes (Fig. 4.1). In contrast, the Gubik site is only 24 km from Umiat. That transect is perpendicular to folds, and there is a significant change in thickness of the Nanushuk Formation between Umiat and Gubik. Without additional subsurface data, it is difficult to predict where exactly any given shelf edge was in relation to the sites, but the use of slope clinoforms observed in seismic reflection data (Molenaar, 1985; Houseknecht et al., 2009) allows for approximate edges to be predicted.

The highest density facies studies are from Umiat Field, where there are twelve wells within a three-mile radius (Collins, 1958; Shimer et al., in press). Two sections from Umiat wells 9 and 11 are almost continuously cored through deltaic and non-marine deposits in the upper Nanushuk Formation (Fig. 4.5). These intervals consist of distributary channel mouth bars (FA-4), distributary channel fill, overbank deposits and coals (FA-5a) and crevasse sands (FA-5b). The approximate base of these deltaic and non-marine deposits is an extensive delta mouth bar complex found in all of the Umiat wells, and known as the Upper Grandstand (Shimer et al., in press). The deltaic and non-marine portion of the upper Nanushuk Formation comprises the Upper Grandstand and Chandler units (Fig. 4.2). The Upper Grandstand was originally separated from the Chandler based on the presence or absence of foraminifera and bivalves that associate each unit with marine and non-marine environments, respectively (Collins, 1958). The difference between the units is less clear in palynological studies (May and Shane, 1985).

The stratigraphic sections depicted here (Figs. 4.3-4.5) are only for new observations and interpretations made in this paper, but Wolf Creek No. 3 and Square Lake No. 1 have significant thicknesses of non-marine or marginal marine delta plain strata based on core descriptions and biostratigraphy (Collins, 1958), and on previous well interpretations (Molenaar, 1985). There are two deltaic and non-marine sections in Wolf Creek No. 3

that are 630 ft. and 590 ft.-thick. In Square Lake No. 1, a similar succession is 520 ft.-thick and, at Umiat, it is 390 ft.-thick (Fig. 4.6). The most easterly well, Gubik No. 1, lacks a significant accumulation of deltaic and non-marine facies above the wave-influenced lower Nanushuk Formation. The non-marine record at Grandstand No. 1 is truncated by an unconformity overlain by Cenozoic sediments (Robinson, 1958b).

The Ninuluk is well represented at Umiat Field, where it consists of two 40-50 ft.-thick sandstones in the subsurface (Shimer et al., in press) and in outcrop, and is overlain by marine shales and bentonites (Houseknecht and Schenk, 2005). The overlying mudstones are part of the Seabee Formation (Collins, 1958; Houseknecht and Schenk, 2005). Similar sandstones also occur in Square Lake No. 1 and Wolf Creek No. 3. The Ninuluk is generally considered to be transgressive in origin (Houseknecht and Schenk, 2005; LePain et al., 2009). The transgressive deposits include a 40 ft.-thick deltaic sandstone and an overlying 50-60 ft.-thick upper shoreface succession observed in Umiat No. 11 (Fig. 4.5).

4.5 Discussion

4.5.1 Distributive Environments and Depositional Patterns

Stratigraphic sections based on core interpretations and published data from five federal legacy well sites in the central Brooks Range foothills support the division of the Nanushuk Formation into a largely shallow marine lower Nanushuk, and predominantly river-dominated deltaic and non-marine upper Nanushuk, as recognized previously (Molenaar, 1985; Mull et al., 2003; LePain et al., 2009). An idealized, well-based west-east cross section adapted from Molenaar (1985) illustrates the vertical and lateral extent of dominantly marine sandstone and shale and non-marine deposits of the Nanushuk Formation, as well as underlying Torok Formation mudstones and the Pebble Shale (Fig. 4.6). The dominantly marine sediments consist of shelf deposits, including offshore mudstones (former Tuktu and Kukpowruk formations) and shoreface or wave-influenced deltaic sands (lower portions of the former Grandstand formation). Dominantly non-

marine sediments consist of delta plain and fluvial deposits (Corwin and Chandler formations). We equate the dominantly marine and non-marine deposits (Figs. 4.3-4.5) with what refer to as marine-distributive and river-distributive systems, respectively. These new broad classification systems are intended to focus interpretation on dominant basin conditions, as opposed to localized depositional environments. We define marine-distributive systems as depositional conditions where waves, tides, or currents are the dominant sediment distributary mechanism and much of the sediment is deposited and reworked away from shore. In river-distributive systems, including river-dominated deltas, autocyclic river processes are responsible for sediment dispersal, and fluvial processes do most sediment reworking. The river-distributive systems broadly encompass all non-marine clastic sedimentary environments, and are not the same as distributive fluvial systems (DFS), which are characterized by radial, unconfined, aggradational river systems (Hartley et al., 2010; Weissman et al., 2010).

In the west-east cross section (Fig. 4.6), the thickness of both marine- and river-distributive systems varies considerably. River-distributive systems, for instance, are much thicker in the west. There are also flooding surfaces where tongues of either very distal Nanushuk shelf deposits or Torok Formation mudstones are deposited above more proximal deposits of the Nanushuk Formation. One of these marine incursions is evident at Umiat Field, where a 300 ft. interval of mudstone separates shoreface sands of the Lower Grandstand from deltaic sandstones of the Upper Grandstand (Fig. 4.7). The Lower Grandstand represents the lowest sandstone in the Nanushuk Formation in the Umiat area and was often used to define the base of the Nanushuk Formation (Molenaar, 1985). The mudstone interval separating the Lower and Upper Grandstand overlies a thin sandstone at the top of upward-coarsening shoreface successions that we interpret as a transgressive sandstone, best observed in Umiat No. 9 at 810-830 ft. (Fig. 4.4). At the top of the marine mudstone are delta mouth bar sands and several hundred feet of delta plain deposits (Fig. 4.7). Transgressive sandstones of the former Ninuluk formation, some of which may be estuarine in origin (Houseknecht and Schenk, 2005), truncate the delta plain deposits at the top of the Nanushuk Formation. These deposits define a

succession of marine-distributive and river-distributive systems separated by a marine transgression onto the shelf.

The succession of deposits and surfaces observed at Umiat is present at Wolf Creek, Square Lake, Grandstand, and Gubik sites to different degrees. As at Umiat, the succession begins with wave-influenced shelf facies deposited in a marine distributive environment, followed by a marine transgression, then progradation of a river-distributive system and accumulation of non-marine deposits (Fig. 4.8). At Wolf Creek No. 3 there is a significant accumulation of shoreface sandstones, capped by a flooding surface at 1900 ft. The marine interval is overlain by deltaic and fluvial facies of river-distributive systems, as observed at Umiat, but the marine mudstone interval is significantly thinner at Wolf Creek No. 3 (Fig. 4.8). This is expected, as north-south oriented shelf margins in the area (Houseknecht et al., 2009) imply a more landward, shallower paleo-bathymetry at Wolf Creek No. 3. In contrast, Gubik No. 1 is located in the east near the most distal Nanushuk shelf margin (Decker, 2007; Houseknecht et al., 2009) and contains wave-influenced sandstones but little non-marine component. The Nanushuk Formation at Gubik No. 1 is considerably thinner than it is at Umiat, 24 km to the west (Figs. 4.6 and 4.8).

In a north-south cross section, the Umiat and Grandstand No. 1 wells have similar Nanushuk Formation stratigraphy (Fig. 4.9). Marine-distributive systems are responsible for wave-influenced sandstones at the base of both stratigraphic sections. Immediately above the marine-distributive deposits, both wells contain facies that indicate deepening of marine conditions, though at Grandstand No. 1 there is more evidence for brackish water (Robinson, 1958b), possibly indicating a higher elevation or more protected position at that site. This may be due to the initiation of folding in the south due compressional events that began in the Albian (Cole et al., 1997) or simply due to a position affected by both west-east and south-north progradation. A well to the north of Umiat would help differentiate the relative input of western and southern sediment sources, but given the similarities between the Umiat and Grandstand wells, we interpret

a dominantly west-east progradation of a roughly north-south to northwest-southeast oriented shoreline through the Umiat area.

Given the repeated pattern of marine-distributive systems at the base of the Nanushuk Formation that precede a transgression and subsequent river-distributive system, we suggest that both distributive conditions are tied directly to bathymetry and shelf-building processes. Marine-distributive systems form during progradation of Torok-Nanushuk clinoforms into open-ocean, near-shelf conditions in the deep Colville foreland basin. The redistribution of sediment delivered to the coast is responsible for widespread deposition of wave-influenced sand and the lack of clear deltaic features. This occurs in modern deltas with high sediment loads that debouch into high-energy marine environments (Wright and Nittrouer, 1995). Under these conditions, high bed shear stress created by waves, tides, and ocean currents re-suspends sediment and helps produce smooth shoreline and submarine topography (Wright and Nittrouer, 1995). River-distributive systems then dominate above the newly formed shelf in shallower water conditions. The combination of higher subsidence closer to the thrust front, as is common in foreland basins (Swift et al., 1987), and nearly continuous accumulation of non-marine deposits away from the shelf margin, explains the great thickness of non-marine Nanushuk Formation deposits in the west.

There are bentonites in the non-marine upper Nanushuk (former Corwin Formation) in the west. Bentonites also occur at the top of the much thinner non-marine Nanushuk Formation (former Chandler Formation) in the east. Bentonites in the Nanushuk Formation at Umiat Field have an $^{40}Ar/^{39}Ar$ plateau age of 102.4 ± 1.0 Ma. If the bentonites from the Nanushuk Formation at Umiat are coincident with the bentonites in the west, it supports the assumption of coeval proximal aggradation of non-marine deposits away landward of the shoreline throughout the Albian-Cenomanian.

The depositional cycles recognized here are both time transgressive and laterally extensive, from early to mid Albian in the west, to late Albian and possibly Cenomanian in the east. The Nanushuk Formation was periodically subjected to marine-distributive

conditions throughout the Albian, depending on the positions of depositional centers relative to the shelf margin. The time-transgressive nature of this pattern is one reason why we discount the silling effect of the Beaufort Rift shoulder or Barrow Arch as a cause for the cessation of wave-influenced deposits in the Nanushuk Formation (Molenaar, 1985; LePain et al., 2009). Furthermore, the Barrow Arch is draped by the Pebble Shale, a marine mudstone deposited mostly below wave base during the Barremian-Hauterivian (136-125 Ma), well before the initial Nanushuk Formation topsets were deposited in the Albian (Mull et al., 2003). Subsurface well records and seismic lines show that bottomsets in the Torok Formation initially onlap the Barrow Arch, until foresets eventually downlap upon it (Molenaar, 1985). This indicates that the Barrow Arch was submerged at depths equal to the height of Torok forests during the Albian, a depth far greater than the 50 m generally assumed necessary for the development of hummocky cross stratification (Dumas and Arnott, 2006)

4.5.2 Stacking Patterns and Systems Tracts

The distance between wells on the North Slope makes it challenging to interpret stacking patterns and systems tracts in the Nanushuk Formation. We base our interpretations on trends observed in wells, including unit thicknesses, facies changes, upward-coarsening or upward-fining successions, and the presence or absence of stacked successions separated by flooding surfaces. These observations give us sufficient data to interpret whether a portion of a well is aggradational, progradational, or retrogradational.

Nanushuk Formation deposition appears to occur in discrete cycles of aggradation, transgression (retrogradation), progradation and transgression based on convex-up (progradation) and concave-up (aggradational) trajectories interpreted from the Wolf Creek, Umiat, and Gubik wells (Fig. 4.8). This deviates slightly from a previously described pattern of repetitive motifs observed in seismic data, where transgression is followed by aggradation and then progradation (McMillen, 1991; Houseknecht and Schenk, 2001; Houseknecht et al., 2009). The cycle we identify here is dominated by

progradation following transgression, with aggradation mostly occurring in less proximal locations.

Aggradation is common in the Nanushuk Formation because the high rate of subsidence was balanced by a high rate of sedimentation (Houseknecht and Schenk, 2001; LePain et al., 2009). We recognize aggradation both in marine-distributive systems and in delta plain and fluvial river-distributive systems away from the coast (Figs. 4.5 and 4.7). Aggradation in marine-distributive environments is also slightly progradational. The aggradational profiles of the marine-distributive systems resemble concave-up accretionary transgressive trajectories, which are aggradational but have an overall retrogradational trajectory, and form in response to rising sea level (Helland-Hansen and Hampson, 2009). We can interpret a trajectory from the shoreface sandstones, particularly at Wolf Creek and Umiat, because the wells contain a series of stacked, upward-coarsening shoreface deposits that become thicker up section (Fig. 4.8). We cannot interpret trajectories from the aggradational delta plain because it is too heterolithic.

Both Wolf Creek No. 3 and the Umiat wells have relatively thin (10-20 ft.-thick) sandstones that we interpret as retrogradational (transgressive) because of upward-fining profiles and the presence of distal lower shoreface sandstones over upper shoreface (Umiat No. 9) or foreshore (Wolf Creek No. 3) deposits. These thin sandstones represent transgressions within the Nanushuk Formation that underlie marine mudstones. We interpret these surfaces as separate events that occurred during the shelf building process because they are separated by nearly 1000 ft. in a cross section "hung" on retrogradational packages at the top of the Nanushuk (Fig. 4.8). These prominent retrogradational packages occur at the top of the Nanushuk Formation in the Ninuluk sands (Figs. 4.6 and 4.7). The observations and interpretations of retrogradational packages, which thicken to the west, agree with previous work (Houseknecht and Schenk, 2005).

River-distributive systems appear to be highly progradational at Umiat, where distributary mouth bar sandstones with no evidence of wave influence top the marine mudstone interval that we interpret as either tongue of the former Tuktu Formation of the former Nanushuk Group or marine shelf deposits of the Torok Formation (Fig. 4.5, Umiat No. 9). The distributary mouth bar sands can be traced between the Umiat wells across the site (Fig. 4.7), indicating a single major progradation of the delta front system through the area. Following the advancement of the delta front, up to 200 ft. of delta plain sediment accumulated. The convex-up trajectory of the river-distributive system is similar to the ascending regressive trajectory described in Helland-Hansen and Hampson (2009).

By the time the Upper Grandstand delta front identified at Umiat reached Gubik No. 1, it showed abundant evidence of wave-influence (Fig. 4.8). We interpret this as evidence of the delta approaching the shelf margin, based on the progradational character of the upward-coarsening shoreface and the lack of proximal facies beneath it. Based on the appearance of thin sandstones in the marine mudstone interval between the Lower and Upper Grandstand at Umiat, the maximum delta front clinoform height of the prograding river-distributive system was approximately 200 ft. The lateral continuity of the sandstones, which pinch-out towards the east (Fig. 4.7), implies a relatively low dip. In contrast, Torok-Nanushuk clinoform foresets are as steep as 6.7º in the Umiat area (Molenaar, 1985), and range from 600-2000 m (~1970-6560 ft.) in height. This significant change in bathymetry would coincide with drastically different marine energy, which we invoke as the mechanism effecting the change to marine-distributive systems.

The pattern of aggradational to slightly progradational marine-distributive deposits in the lower Nanushuk Formation and highly progradational river-distributive deposits in the upper Nanushuk Formation, with retrogradational intervals in between, relates directly to accommodation and sediment supply during the Albian. LePain et al. (2009), describe an accommodation dominated mid-late Albian Nanushuk Formation that evolved into a system characterized by pulses of positive accommodation (accommodation >

sedimentation) and negative accommodation (accommodation < sedimentation). Though the creation of accommodation in the Nanushuk Formation is directly tied to tectonic and sediment loading (Houseknecht and Schenk, 2001), we propose that on short timescales associated with specific depositional environments, the accommodation that controls topset geometry is related to near-shore bathymetry, as opposed to overall basin depth. A shallow continental shelf, in this case above the lower Nanushuk Formation, would have an accommodation/sedimentation (A/S) ratio that was very small, because the sediment supply would exceed the available space on the shelf. In this case, rapid progradation would overpower the distributive power of the marine environment until the prograding system reached the shelf edge. We also suggest that accommodation-controlled shelf aggradation by both marine- and river-distributive systems would maintain or enhance steep clinoform profiles, which were originally inherited from early in the basin history (Houseknecht and Wartes, 2013).

Transgressive events separating marine- and river-distributive systems may be best explained by changes in accommodation and sediment supply (A/S ratio) as well. Relative sea-level rise (increased accommodation) can create imbalances in the A/S ratio and cause auto-retreat in a progradational system (Muto and Steel, 1997). This would account for flooding surfaces that punctuate the Nanushuk Formation. Reduction in sedimentation rate is also important, as a reduced sediment supply can lead to the formation of discontinuities, particularly in high-energy wave environments (Storms and Hampson, 2005).

Previous authors have defined systems tracts in the Nanushuk Formation. Houseknecht and Schenk (2001), assign aggradational topsets in the lower Nanushuk Formation to an early highstand and progradational topsets to late highstand. We do not identify any fluvial incisions, shelf margins, or basin floor fans in this study and thus have no evidence for lowstand systems tracts (Shimer et al., in press). It is therefore possible that all of the observed facies and stacking patterns discussed were produced during relative sea level highstands that persisted throughout the Albian-Cenomanian in Arctic Alaska.

High relative sea level conditions would be likely given the high subsidence rate in the basin while the Nanushuk Formation was deposited (Houseknecht and Schenk, 2001; LePain et al., 2009) and considering gradually increasing eustatic sea levels (Fig. 4.10: Müller et al., 2008). Furthermore, the accretionary transgressive and ascending regressive trajectories discussed above both indicate a response to rising relative sea level (Helland-Hansen and Hampson, 2009). Marine-distributive systems would thus represent the early highstand, with consistent sea level rise, while river-distributive systems would represent late highstand, with accommodation reduced by sediment aggradation on the shelf as opposed to lowered relative sea-level. Though we find highstand conditions probable, we caution that characterization of the marine-distributive lower Nanushuk as early highstand and the river-distributive upper Nanushuk as late highstand must consider "early" and "late" to be relative terms, in reference to shelf margins as they prograded west-east across the Colville basin axis. In other words, late highstand would have occurred in the west at the same time as early highstand in the east.

4.5.3 Climatic Variables

The Albian was a time of rising sea level (Hancock and Kauffman, 1978; Müller et al., 2008). Megafossil evidence indicates a relatively temperate ocean (Imlay, 1961), and paleobotanical evidence suggests year-round Arctic Ocean temperatures above 0ºC (Herman and Spicer, 1996). The warming trend that began during the Albian lasted well into the Late Cretaceous, ending in the Campanian-Maastrichtian (Huber et al., 2002). But global sea level peaked at the Albian-Cenomanian boundary (Fig. 4.10; Müller et al., 2008), which likely contributed to the transgression at the top of the Nanushuk Formation.

Following eustatic sea level rise, Arctic warming probably peaked during the Turonian, possibly due to increased from carbon-dioxide emission from mid-ocean ridges and large igneous provinces (Moriya, 2011). Terrestrial mean annual temperature estimates during the Cenomanian-Turonian range from 7.7-14.3ºC (Spicer and Herman, 2010), while the Late Cretaceous Arctic Ocean may have reached surface temperatures of up to 15ºC

(Jenkyns et al., 2004). The warm Late Cretaceous Arctic Ocean was probably stratified, with possible seasonal ice cover in winter months based on the layering of diatom ooze and terrigenous sediment (Davies et al., 2009). These factors may have affected ocean circulation and distribution of marine sediment, but their apparent consistency over millions of years makes it less likely that they were the primary controls on depositional patterns. In addition, though eustatic sea level must have played an important part in maintaining accommodation in the Colville foreland basin, other climatic effects (storm frequency, seasonality, circulation) are difficult to reconstruct with the currently available data. In some cases the climatic data does provide important context, however. Precipitation estimates from Nanushuk Formation siderite $\delta^{18}O$ range from 485-626 mm/yr, sufficient moisture to allow for the accumulation of peat (Ufnar et al., 2004), which eventually became coal. This would be particularly important factor in the aggradation of overbank or back-swamp deposits in river-distributive systems of the Nanushuk Formation, particularly in the west.

4.5.4 Ancient and Modern Analogues and Nanushuk Formation Models

Albian-Cenomanian storm deposits with evidence of wave-influence are common, with a distribution related to climatic and geographic controls (Barron, 1989). The wavelength of hummocky cross-strata, which corresponds to the diameter of storm wave orbitals, reached a peak during greenhouse (highstand) conditions during the mid-Cretaceous (Ito et al., 2001). It should therefore be possible to find an ancient analogue for the Nanushuk Formation. The Blackhawk Formation of Utah and Colorado (Swift et al, 1987; Pattison, 1995) appears to be a good foreland basin analogue in terms of facies distribution, though the basin conditions are slightly different. Both systems display typical foreland basin geometry, with maximum subsidence along the thrust front. This subsidence leads to the accumulation of thick deposits along the basin axis, proximal to the tectonic loading (Swift et al., 1987). In the Nanushuk, this accounts for the great thickness of non-marine deposits in the west along the basin axis (Fig. 4.6), which accumulated sediment throughout the entire Albian (Molenaar, 1985). Like the Nanushuk, the Blackhawk, and

specifically the Kenilworth member, show wave-influence (Pattison, 1995). The Kenilworth member is complex, with highstand, lowstand, and transgressive shoreface deposits (Pattison, 1995). Thicker distal lower shoreface and inner shelf deposits are associated with normal regressive conditions (Hampson, 2000), and we assume similar conditions for the lower Nanushuk Formation as it filled the basin under marine-dispersive conditions. The shoreface-shelf profile in the Kenilworth steepens during early progradation, as aggradation occurs (Hampson and Storms, 2003). This appears to be analogous to the Nanushuk Formation, as progradation shifts to aggradation and the development of accretionary transgressive trajectories. Unlike the Blackhawk, the Nanushuk Formation has limited evidence for lowstand erosion and most sediment was trapped on the shelf (LePain et al., 2009), possibly due to higher rates of accommodation through a variety of factors, such as compaction of the underlying Torok Formation.

A possible modern analogue for marine-distributive conditions is the Amazon River, which does not have a true "delta" using traditional classifications (Nittrouer et al., 1986). The Amazon River debouches into a high-energy marine environment in the Atlantic Ocean, where wave and tidal currents cause the majority of sediment to be deposited and reworked away from the shore (Kuehl et al., 1986). The Amazon can be classified as a subaqueous delta (Walsh and Nittrouer, 2009). Subaqueous deltas can develop substantial compound clinoforms on the shelf (Swenson et al., 2005), and the Amazon indeed has its highest accumulation rates in water as deep as 30-50 m tens of kilometers offshore (Kuehl et al., 1986). Modern rivers with high sediment supply and subaqueous deltas can produce rapid sediment accumulation of up to 10s of centimeters per year (Wright and Nittrouer, 1995), creating aggradational clinoforms (Nittrouer et al., 1986). We invoke similar conditions for aggradational to slightly progradational shoreface and wave-influenced deltaic deposits in the marine-distributive lower Nanushuk Formation.

The first of two new schematic models for the Nanushuk Formation (Fig. 4.11A) is based on marine-distributive conditions similar to that of the Amazon, but with an axial river. Though the Albian Arctic Ocean (Amerasia Basin) would not have resembled the current

Atlantic Ocean in size or tectonic setting, the large Torok-Nanushuk clinoforms with heights of up to 2000 m (Houseknecht et al., 2009) indicate basin depths similar to the modern passive margin of South America. The model illustrates subaqueous sediment distribution along a narrow shelf in aggradational clinoforms (Fig. 4.11A). Alongshore sediment distribution is to the northwest, with an active delta front in the east and abandoned delta lobes in the west. The large deltaic depocenter would represents a moment in time, not the permanent depositional center. Smaller, cuspate wave-influenced deltas are depicted along the basin margin in the southeast. The shelf margin is oriented roughly north-south in accordance with seismic interpretations (Houseknecht et al., 2009) and patterns observed in the subsurface from west-to-east (Fig. 4.8) and north-to-south (Fig. 4.9). The model assumes a dominant clockwise current for the Amerasia Basin, similar to the Beaufort Gyre, but we acknowledge that the Beaufort Gyre is a modern phenomenon influenced by freshwater input, sea ice, wind, and modern ocean bathymetry (Dijkstra, 2008), and ocean currents in a warmer Cretaceous Arctic Ocean may have been different.

The second model (Fig. 4.11B) illustrates the river-distributive condition, with rapid progradation of deltaic deposits over a shallow shelf following transgression. For a modern analogue, we look to the current active lobe of the Yukon River (Nelson and Creager, 1977), which is building out over the Bering Shelf during highstand conditions. The model is meant to show river-dispersive sedimentation on a broad, shallow shelf that is rapidly progradational, with accumulation of steep delta foresets proximal to the delta front (proximal accumulation delta, *sensu* Walsh and Nittrouer, 2009). The shelf margin is also shifted to the east, to indicate some progradation of the Torok-Nanushuk clinoforms over time.

Nanushuk Formation topsets clearly have value for interpreting large-scale processes formerly active in the Colville foreland basin. The use of modern Arctic analogues presents an opportunity for future research on the Nanushuk Formation and other Brookian foreland basin deposits and the many deltas that feed sediment into the

Amerasian and Canada basins. The scale of these systems, the unique high-latitude environments, and the lack of anthropogenic influence make them more useful than traditional analogues like the Mississippi or Brazos rivers.

4.6 Conclusions

We broadly define two broad depositional systems in the Nanushuk Formation based on sedimentary facies observed in subsurface wells: marine-distributive and river-distributive systems. The lower Nanushuk Formation is dominated by marine-distributive systems, with abundant wave-influenced facies in shoreface environments. In contrast, the upper Nanushuk Formation is dominated by facies indicating mostly deltaic and fluvial processes.

Shoreline trajectories interpreted from facies observed in subsurface wells help to reconstruct the history of Nanushuk Formation topset creation in the Colville foreland basin. Wave-distributive conditions are associated with progradational to aggradational trajectories. Using existing shoreline trajectory models, we interpret wave-distributive conditions to have been controlled by high accommodation, near-shelf margin conditions. The aggradation of wave-distributive systems served to construct and enlarge steep Brookian clinoforms. The high accommodation and substantial shelf heights in marine-distributive systems in the Nanushuk Formation suggest similar processes as modern passive margins.

The upper Nanushuk Formation was deposited following transgression at the top of marine-distributive systems in the lower Nanushuk Formation. Shoreline trajectories in the river-distributive systems of the upper Nanushuk Formation indicate rapid progradation, with little initial aggradation. We interpret this as an indication of low relative accommodation on the shelf. Unlike the lower Nanushuk Formation, where aggradation occurred at or near the shoreline, aggradation in the upper Nanushuk Formation primarily occurred in delta plain or fluvial settings more proximal to sediment

sources. These interpretations imply that the presence of river- and wave-distributive systems in the Nanushuk Formation was determined by local basin bathymetry and relative accommodation, a pattern that should be applicable to other foreland basin systems.

4.7 Acknowledgements

Much of the work for this project was conducted under a U.S. Department of Energy contract DE-FC26-08NT005641. Core research was conducted at the Alaska Geologic Materials Center, with assistance from director Ken Papp and the other staff members. Thanks to David LePain, formerly of the Alaska Division of Geological and Geophysical Surveys for guidance early in the project, and to David Houseknecht and Paul Decker for conversations on the Colville foreland basin. Additional thanks to reviewers who helped shape the final manuscript.

4.8 References

Ahlbrandt, T.S., Huffman Jr., A.C., Fox, J.E., and Pasternack, I., 1979, Depositional framework and reservoir-quality studies of selected Nanushuk group outcrops, North Slope, Alaska, *in,* T.S. Ahlbrandt, ed., Preliminary geologic, petrologic, and paleontologic results of the study of Nanushuk Group rocks, North Slope, Alaska: U.S. Geological Survey Circular 794, p. 14-31.

Barron, E.J., 1989, Severe storms during Earth history: Geological Society of America Bulletin, v. 101, p. 601-612.

Bartsch-Winkler, S., 1985, Petrography of sandstones of the Nanushuk Group from four measured sections, central North Slope, Alaska, *in* A.C. Huffman, Jr., ed., Geology of the Nanushuk Group and Related Rocks, North Slope, Alaska: U.S. Geological Survey Bulletin 1614, p., 75-96.

Bhattacharya, J.P., and Giosan, L., 2003, Wave-influenced deltas: geomorphological implications for facies reconstruction: Sedimentology, v. 50, p. 187-210.

Bhattacharya, J.P., and Walker, R.G., 1991, Facies and facies successions in river- and wave-dominated depositional systems of the Upper Cretaceous Dunvegan Formation, northwestern Alberta: Bulletin of Canadian Petroleum Geology, v. 39, p. 165-191.

Bird, K.J., and Andrews, J., 1979, Subsurface studies of the Nanushuk Group, North Slope, Alaska, *in* T.S. Ahlbrandt, ed., Preliminary Geologic, Petrologic, and Paleontologic Results of the Study of Nanushuk Group Rocks, North Slope, Alaska: U.S. Geological Survey Circular 794, p. 32-41.

Catuneanu, O., Abreu, V., Bhattacharya, J.P., Blum, M.D., Dalrymple, R.W., Eriksson, P.G., Fielding, C.R., Fisher, W.L., Galloway, W.E., Gibling, M.R., Giles, K.A., Holbrook, J.M., Jordan, R., Kendall, C.G.St.C., Macurda, B., Martinson, O.J., Miall, A.D., Neal., J.E., Nummedal, D., Pomar, L., Posamentier, H.W., Pratt, B.R., Sarg, J.F., Shanley, K.W., Steel, R.J., Strasser, A., Tucker, M.E., and Winker, C., 2009, Towards the standardization of sequence stratigraphy: Earth-Science Reviews, v. 92, p. 1-33.

Cohen, K.M., Finney, S., and Gibbard, P.L., 2013, International Chronostratigraphic Chart: International Commission on Stratigraphy. http://www.stratigraphy.org/ICSchart/ChronostratChart2013-01.pdf.

Cole, F., Bird., K.J., Toro, J., Roure, F., O'Sullivan, P.B., Pawlewicz, M., and Howell, D.G., 1997, An integrated model for the tectonic development of the frontal Brooks Range and Colville Basin 250 km west of the Trans-Alaska Crustal Transect: Journal of Geophysical Research, v. 102, p. 20,685-20,708.

Collins, F.R., 1958, Test Wells, Umiat Area Alaska: U.S. Geological Survey Professional Paper 305-B, p. 71-206.

Collins, F.R., 1959, Test Wells, Square Lake and Wolf Creek Areas Alaska: U.S. Geological Survey Professional Paper 305-H, p. 423-484.

Conrad, J.E., McKee, E.H., and Turrin, B.D., 1990, Age of tephra beds at the Ocean Point dinosaur locality, North Slope, Alaska, based on K-Ar and $^{40}Ar/^{39}Ar$ analyses: Evolution of Sedimentary Basins-North Slope Basin, U.S. Geological Survey Bulletin 1990, 14 p.

Davies, A., Kemp, A.E.S., and Pike, J., 2009, Late Cretaceous seasonal ocean variability from the Arctic: Nature, v. 460, p. 254-258.

Decker, P.L., 2007, Brookian sequence stratigraphic correlations, Umiat field to Milne Point field, west-central North Slope, Alaska: Preliminary Interpretive Report, Alaska Division of Geological and Geophysical Surveys 2007-2, 21 p.

Detterman, R.L., 1956, New and redefined nomenclature of the Nanushuk group, *in* G. Gryc, and others, eds., Mesozoic Sequence in Colville River Region, Northern Alaska: American Association of Petroleum Geologists Bulletin, v. 40, p. 233-244.

Dijkstra, H.A., 2008, Arctic Ocean Circulation, *in* Dynamical Oceanography, Springer Berlin Heidelberg, p. 351-374.

Dumas, S., and R. W. C. Arnott, 2006, Origin of hummocky and swaley cross-stratification–the controlling influence of unidirectional current strength and aggradation rate: Geology, v. 34, p. 1073-1076.

Fox, J.E., Lambert, P.W., Pitman, J.K., and Wu, C.H., 1979, A study of reservoir characteristics of the Nanushuk and Colville Groups, Umiat Test Well 11, National Petroleum Reserve in Alaska: U.S. Geological Survey Circular 820, 47 p.

Hampson, G.J., 2000, Discontinuity surfaces, clinoforms, and facies architecture in a wave-dominated, shoreface-shelf parasequence: Journal of Sedimentary Research, V. 70, p. 325-340.

Hampson, G.J., and Storms, J.E.A., 2003, Geomorphological and sequence stratigraphic variability in wave-dominated, shoreface-shelf parasequences: Sedimentology, v. 50, p. 667-701.

Hancock, J.M., and Kauffman, E.G., 1978, The great transgressions of the Late Cretaceous: Journal of the Geological Society, v. 136, p. 175-186.,

Haq, B.U., and Al-Qahtani, A.M., 2005, Phanerozoic cycles of sea-level change on the Arabian Platform: GeoArabia, v. 10, p. 128-160.

Hartley, A.J., Weissmann, G.S., Nichols, G.J., and Warwick, G.L., 2010, Large distributive fluvial systems: Characteristics, distribution, and controls on development: Journal of Sedimentary Research, v. 80, p. 167-183.

Helland-Hansen, W., 1992, Geometry and facies of Teritary clinothems, Spitsbergen: Sedimentology, v. 39, p. 1013-1029.

Helland-Hansen, W., and Hampson, G.J., 2009, Trajectory analysis: concepts and applications: Basin Research, v. 21, p. 454-483.

Helland-Hansen, W., and Martinsen, O.J., 1996, Shoreline trajectories and sequences: Description of variable depositional-dip scenarios: Journal of Sedimentary Research, v. 66, p. 670-688.

Herman, A.B., and Spicer, R.A., 1996, Palaeobotanical evidence for a warm Cretaceous Arctic Ocean: Nature, v. 380, p. 330-333.

Houseknecht, D.W., Bird, K.J., and Schenk, C.J., 2009, Seismic analysis of clinoforms depositional sequences and shelf-margin trajectories in Lower Cretaceous (Albian) strata, Alaska North Slope: Basin Research, v. 21, p. 644-654.

Houseknecht, D.W., and Schenk, C.J., 2001, Depositional sequences and facies in the Torok Formation, National Petroleum Reserve – Alaska (NPRA), *in* D.W., Houseknecht, ed., NPRA Core Workshop Petroleum Plays and Systems in the National Petroleum Reserve – Alaska: SEPM Core Workshop No. 21, Denver Colorado, June 7-8, p., 179-199.

Houseknecht, D.W., and Schenk, C.J., 2005, Sedimentology and sequence stratigraphy of the Cretaceous Nanushuk, Seabee, and Tuluvak formations exposed on Umiat Mountain, North-Central Alaska: U.S. Geological Survey Professional Paper 1709-B, 18 p.

Houseknecht, D.W., and Wartes, M.A., 2013, Clinoform deposition across a boundary between orogenic front and foredeep – an example from the Lower Cretaceous in Arctic Alaska: Terra Nova, v. 25, p. 206-211.

Hubbard, R.J., Edrich, S.P., and Rattey, P., 1987, Geologic evolution and hydrocarbon habitat of the 'Arctic Alaska microplate': Marine and Petroleum Geology, v. 4, p. 2-34.

Hubbard, S.M., Fildani, A., Romans, B.W., Covault, J.A., and McHargue, T.R., 2010, High-relief slope clinoform development: Insights from outcrop, Magallanes basin, Chile: Journal of Sedimentary Research, v. 80, p. 357-375.

Huber, B.T., Norris, R.D., and MacLeod, K.G., 2002, Deep-sea paleotemperature record of extreme warmth during the Cretaceous: Geology, v. 30, p. 123-126.

Imlay, R.W., 1961, Characteristic Lower Cretaceous Megafossils from Northern Alaska: U.S. Geological Survey Professional Paper 335, 74 p., 20 plates.

Ito, M., Ishigaki, A., Nishikawa, T., Saito, T., 2001, Temporal variation in the wavelength of hummocky cross-stratification: Implications for storm intensity through Mesozoic and Cenozoic : Geology, v. 29, p. 87-89.

Jenkyns, H.C., Forseter, A., Schouten, S., and Sinninghe Damsté, J.S., 2004, High temperatures in the Late Cretaceous Arctic Ocean: Nature, v. 432, p. 888-892.

Jones, D.L., and Gryc, G., 1960, Upper Cretaceous Pelycycpods of the genus *Inoceramus* from northern Alaska: U.S. Geological Survey Professional Paper 334-E, 164 p.

Kuehl, S.A., DeMaster, D.J., and Nittrouer, C.A., 1986, Nature of sediment accumulation on the Amazon continental shelf: Continental Shelf Research, v. 6, p. 209-225.

Lanphere, M.A. and Tailleur, I.L., 1983, K-Ar ages of bentonites in the Seabee Formation, Northern Alaska: A Late Cretaceous (Turonian) time-scale point: Cretaceous Research, v. 4, 361-370.

LePain, D.L., McCarthy, P.J., and Kirkham, R., 2009, Sedimentology, stacking patterns, and depositional systems in the middle Albian-Cenomanian Nanushuk Formation in outcrop, central North Slope, Alaska: Alaska Division of Geological and Geophysical Surveys Report on Investigations 2009-1, 86 p.

LePain, D.L., and Kirkham, R., 2001, Potential reservoir facies in the Nanushuk Formation (Albian-Cenomanian), central North Slope, Alaska: examples from outcrop and core, *in* D.W., Houseknecht, ed., NPRA Core Workshop Petroleum Plays and Systems in the National Petroleum Reserve – Alaska: SEPM Core Workshop No. 21, Denver Colorado, June 7-8, p., 19-36.

May, F.E., and Shane, J.D., 1985, An analysis of the Umiat delta using palynologic and other data, North Slope, Alaska, *in* A.C. Huffman, ed., Geology of the Nanushuk Group and Related Rocks, North Slope, Alaska: U.S. Geological Survey Bulletin 1614, p. 97-120.

McMillen, K.J., 1991, Seismic stratigraphy f Lower Cretaceous foreland basin submarine fans in the North Slope, Alaska, *in* P. Weimer and M.H. Link, eds., Seismic Facies and Sedimentary Processes of Submarine Fans and Turbidite Systems: Springer Verlag, New York, p. 289-302.

Molenaar, C.M., 1985, Subsurface correlations and depositional history of the Nanushuk Group and related strata, North Slope, Alaska, *in* A.C. Huffman, Jr., ed., Geology of the Nanushuk Group and Related Rocks, North Slope, Alaska: U.S. Geological Survey Bulletin 1614, p., 37-60.

Moore, T.E., Wallace, W.K., Bird, K.J., Karl, S.M., Mull, C.G., and Dillon, J.T., 1994, Geology of Northern Alaska, *in* The Geology of North America, v. G-1, The Geology of Alaska: Geological Society of America, p. 49-140.

Moriya, K., 2011, Development of the Cretaceous greenhouse climate and the oceanic thermal structure: Paleontological Research, v. 15, p. 77-88.

Mull, C.G., 1985, Cretaceous tectonics, depositional cycles, and the Nanushuk Group, Brooks Range and Arctic Slope, Alaska, *in* , *in* A.C. Huffman, Jr., ed., Geology of the Nanushuk Group and Related Rocks, North Slope, Alaska: U.S. Geological Survey Bulletin 1614, p., 7-36.

Mull, C.G., Houseknecht, D.W., and Bird, K.J., 2003, Revised Cretaceous and Tertiary stratigraphic nomenclature in the Colville Basin, northern Alaska: U.S. Geological Survey Professional Paper 173, 51 p.

Müller, R.D., Sdrolias, M., Gaina, C., Roest, W.R., 2008, Age, spreading rates, and spreading asymmetry of the world's ocean crust: Geochemistry, Geophysics. Geosystems, v. 9, doi: 10.1029/2007GC001743.

Muto, T.J., and Steel., R.J., 1997, Principles of regression and transgression: the nature of the interplay between accommodation and sediment supply: Journal of Sedimentary Research, v. 67, p. 994-1000.

Nelson, H., and Creager, J.S., 1977, Displacement of Yukon-derived sediment from Bering Sea to Chukchi Sea during Holocene time: Geology, v. 5, p. 141-146.

Nittrouer, C.A., Kuehl, S.A., Demaster, D.J., and Kowsmann, R.O., 1986, The deltaic nature of Amazon shelf sedimentation: Geological Society of America Bulletin, v. 97, p. 444-458.

O'Sullivan, P.B., Murphy, J.M., and Blythe, A.E., 1997, Late Mesozoic and Cenozoic thermotectonic evolution of the central Brooks Range and adjacent North Slope foreland basin, Alaska: Including fission track results from the Trans-Alaska Crustal Transect (TACT): Tectonics, v. 102, p. 20,821-20,845.

Pattison, S.A.J., 1995, Sequence stratigraphic significance of sharp-based lowstand shoreface deposits, Kenilworth Member, Book Cliffs, Utah: AAPG Bulletin, v. 79, p. 444-462.

Pontén, A., and Plink-Björklund, P., 2009, Process regime changes across a regressive to transgressive turnaround in a shelf-slope basin, Eocene Central Basin of Spitsbergen: Journal of Sedimentary Research, v. 79, p. 2-23.

Robinson, F.M., 1958a, Test wells, Gubik area Alaska, U.S. Geological Survey Professional Paper 305-C, p. 207-264.

Robinson, F.M., 1958b, Test well Grandstand area Alaska, U.S. Geological Survey Professional Paper 305-E, p. 317-339.

Schindler, J.F., 1988, History of exploration in the National Petroleum Reserve in Alaska, with emphasis on the period from 1975-1982, *in* G. Gryc, ed., Geology and Exploration of the National Petroleum Reserve in Alaska, 1974-1982: U.S. Geological Survey Professional Paper 1399, p. 13-76.

Shimer, G.T., McCarthy, P.J, and Hanks, C.L., 2013, Sedimentology, stratigraphy, and reservoir properties of an unconventional reservoir in the Cretaceous Nanushuk Formation at Umiat Field, North Slope, Alaska: AAPG Bulletin, in press.

Sircombe, K.N., and Kamp, P.J.J., 1998, The South Westand Basin: seismic stratigraphy, basin geometry and evolution of a foreland basin within the Southern Alps collision zone, New Zealand: Tectonophysics, 300, p. 359-387.

Spicer, R.A., and Herman, A.B., 2010, The Late Cretaceous environment of the Arctic: A quantitative reassessment based on plant fossils: Palaeogeography, Palaeoclimatology, Palaeoecology, v. 295, p. 423-442.

Storms, J.E.A., and Hampson, G.J., 2005, Mechanisms for forming discontinuity surfaces within shoreface-shelf parasequences: sea level, sediment supply, or wave regime: Journal of Sedimentary Research, v. 75, p. 67-81.

Swenson, J.B., Paola, C., Pratson, L., Voller, V.R., and Murray, A.B., 2005, Fluvial and marine controls on combined suabaerial and subaqueous delta progradation: Morphodynamic modeling of compound-clinoform development: Journal of Geophysical Research, v. 110 (F02013) p. 1-16.

Swift, J.P., Hudelson, P.M., Brenner, R.L., and Thompson, P., 1987, Shelf construction in a foreland basin: storm beds, shelf sandbodies, and shelf-slope depositional sequences in the Upper Cretaceous Mesaverde Group, Book Cliffs, Utah: Sedimentology, v. 34, p. 423-457.

Tappan, H.N., 1960, Cretaceous biostratigraphy of northern Alaska: AAPG Bulletin, v. 44, p. 273-297.

Tikhomirov, P.L., Kalinina, E.A., Moriguti, T., Makishima, A., Kobayashi, K., Cherpanova, I.Yu., and Nakamura, E., 2012, The Cretaceous Okhotsk-Chukotka Volcanic Belt (NE Russia): Geology, geochronology, magma output ranges, and implications on the genesis of silicic LIPs: Journal of Volcanology and Geothermal Research, v., 221-222, p. 14-32.

Till, A.B., 1992, Detrital blueschist-facies metamorphic mineral assemblages in Early Cretaceous sediments of the foreland basin of the Brooks Range, Alaska, and implications for orogenic evolution: Tectonics, v. 11, p. 1207-1223.

Till, A.B., and Snee, L.W., 1995, $^{40}Ar/^{39}Ar$ evidence that formation of blueschists in continental crust was synchronous with foreland fold and thrust belt deformation, western Brooks Range, Alaska: Journal of Metamorphic Geology, v. 13, p. 41-60.

Ufnar, D.F., Ludvigson, G.A., González, L.A., Brenner, R.L., and Witzke, B.J., 2004, High latitude meteoric $\partial^{18}O$ compositions: Paleosol siderite in the Middle Cretaceous Nanushuk Formation, North Slope, Alaska: Geological Society of America Bulletin, v. 116, p. 463-473.

Vail, P.R., Audemard, F., Bowman, S.A., Eisner, P.N., and Pere-Cruz, C., 1991, The stratigraphic signatures of tectonics, eustasy and sedimentology-an overview, *in*, G. Einsele and A. Seilacher, eds., Cyclic and Event Stratification, Springer-Verlag, Berlin, p. 617-659.

Van Wagoner, J.C., and Bertram, G.T., 1995, Introduction, *in* J.C Van Wagoner and G.T. Bertram, Sequence Stratigraphy of Foreland Basin Deposits, American Association of Petroleum Geologists Memoir 64 Sequence Stratigraphy of Foreland Basin Deposits, American Association of Petroleum Geologists Memoir 64, p. ix-xxi.

Vogl, J.J., Calvert, A.T., and Gans, P.P., 2002, Mechanisms and timing of exhumation of collision-related metamorphic rocks, southern Brooks Range, Alaska: insights from $^{40}Ar/^{39}Ar$ thermochronology: Tectonics, v. 21, doi 10.1029/2000TC001270.

Walsh, J.P., and Nittrouer, C.A., 2009, Understanding fine-grained river-sediment dispersal on continental margins: Marine Geology, v. 263, p. 34-45.

Weissmann, G.S., Hartley, A.J., Nichols, G.J., Scuderi, L.A., Olson, M., Buehler, H., and Banteah, R., 2010, Fluvial form in modern continental sedimentary basins: Distributive fluvial systems: Geology, v. 38, p. 39-42.

Wright, L.D., and Nittrouer, C.A., 1995, Dispersal of river sediments in coastal seas: Six contrasting cases: Estuaries, v. 18, p. 494-508.

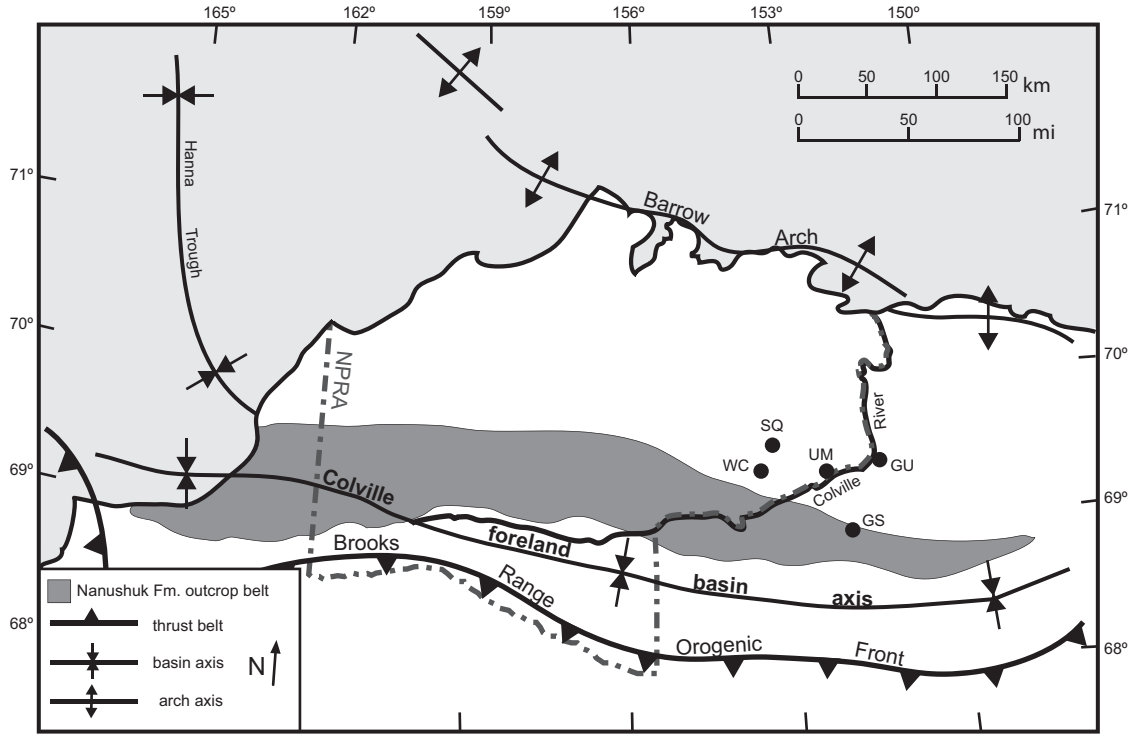

Figure 4.1 Map of Northern Alaska
Map illustrating the major structural features of Northern Alaska, as well as the outcrop belt of the Nanushuk Formation, which lies in the northern foothills of the Brooks Range. The wells used in this study are located on the eastern boundary of the National Petroleum Reserve – Alaska (NPRA), along the Colville River. The Wolf Creek (WC), Square Lake (SQ) and Umiat (UM) sites are within the NPRA, while the Grandstand (GS) and Gubik (GU) sites are outside of the boundary. Modified from Molenaar (1985), with structural information from Moore et al. (1994).

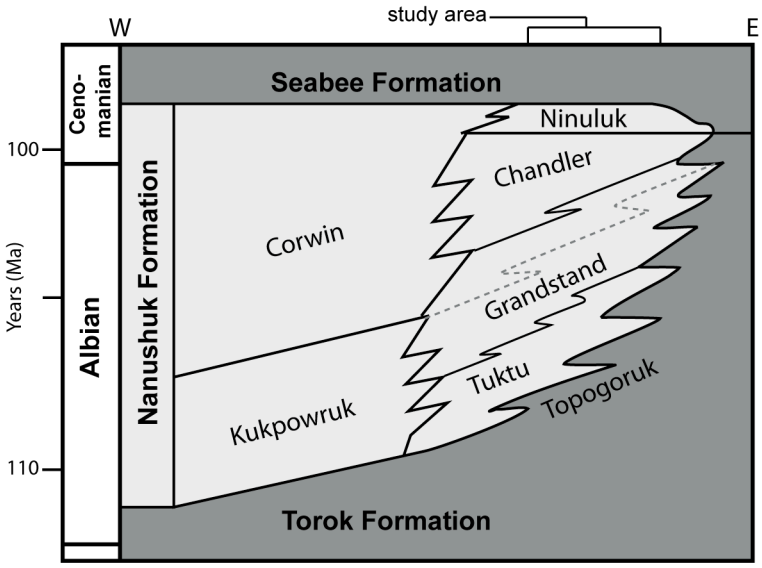

Figure 4.2 Nanushuk Formation Stratigraphy
The Albian-Cenomanian Nanushuk Formation consists of topset deposits associated with the underlying Torok Formation, and is separated from the overlying Seabee Formation by a transgressive event and maximum flooding surface. The figure shows the stratigraphic relationships of the formations of the former Nanushuk Group. The "formations", now informal unit names, relate to depositional setting and are used in this study. Ages and structure of the diagram modified from Mull et al. (2003), with additional age control from Chapter 3.

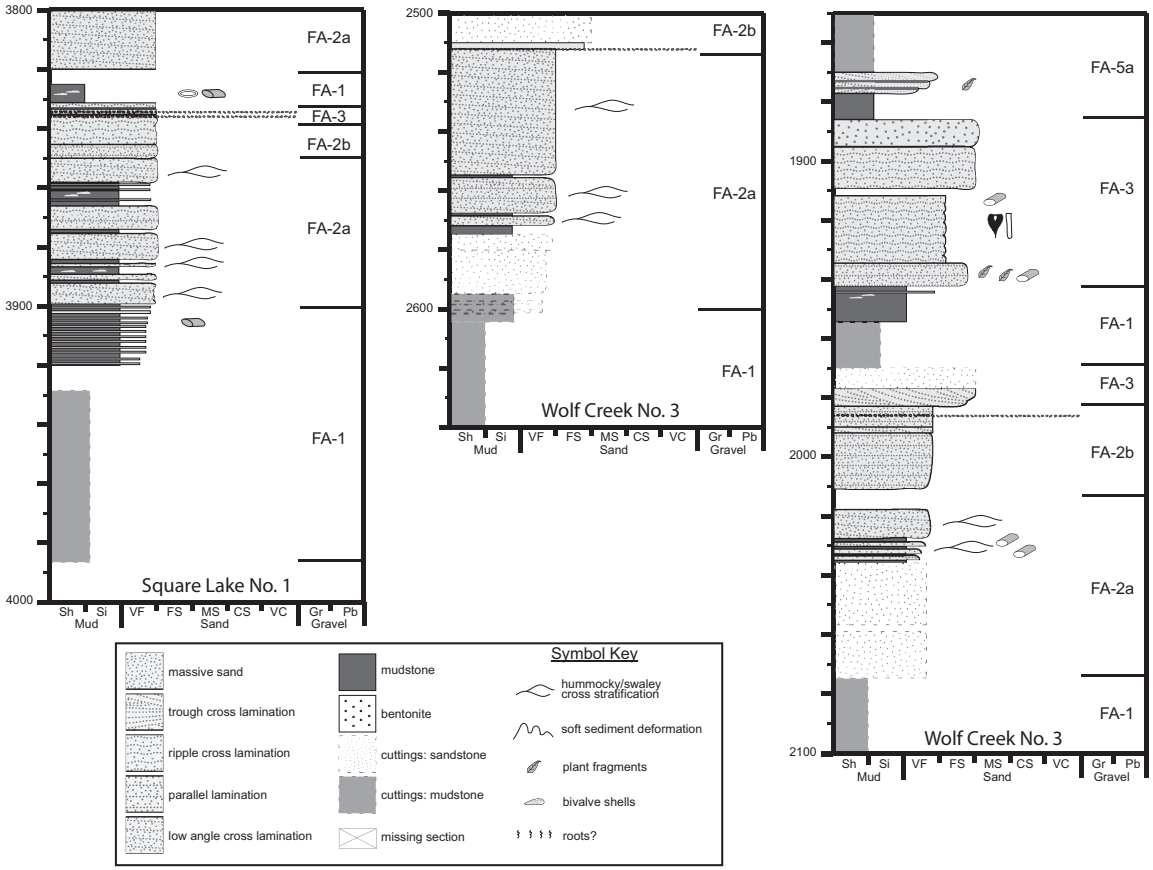

Figure 4.3 Wave Influenced Facies Associations (Western Wells)
Western wells: The presence of hummocky cross stratification in upward-coarsening sandstone successions indicates wave influence and distal shoreface or wave-influenced deltaic settings. Stratigraphic sections modified from LePain and Kirkham (2001). All stratigraphic columns are from the lower Nanushuk, hundreds of feet below river-dominated facies. For well locations, see Figure 4.1. For trace fossil symbol key, see Figure 4.4, and for facies associations codes, see Figure 4.5.

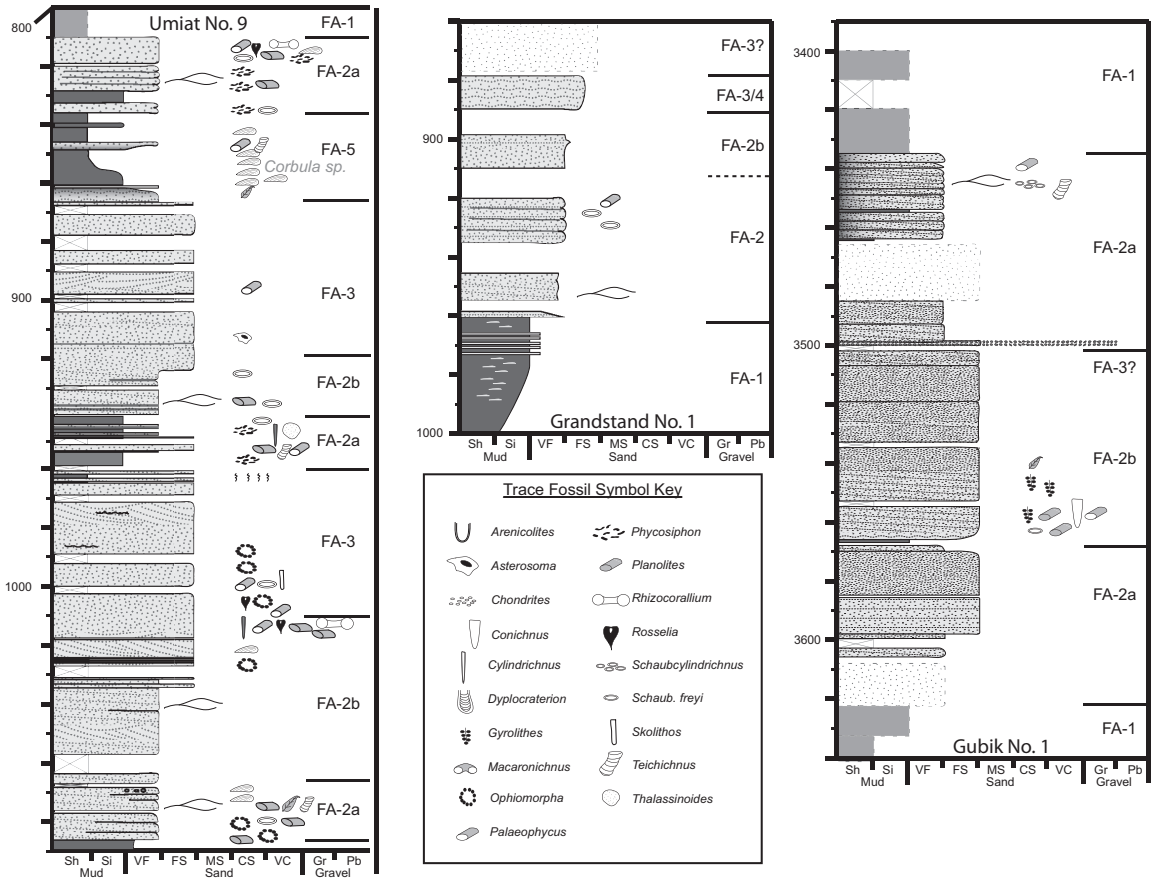

Figure 4.4 Wave-Influenced Facies (Eastern Wells)
Eastern wells: Stratigraphic sections from the Umiat, Grandstand, and Gubik sites show evidence of hummocky cross-stratification and wave-influenced trace fossil assemblages. For sedimentary structure symbol key, see Figure 4.3. For facies association codes, see Figure 4.5.

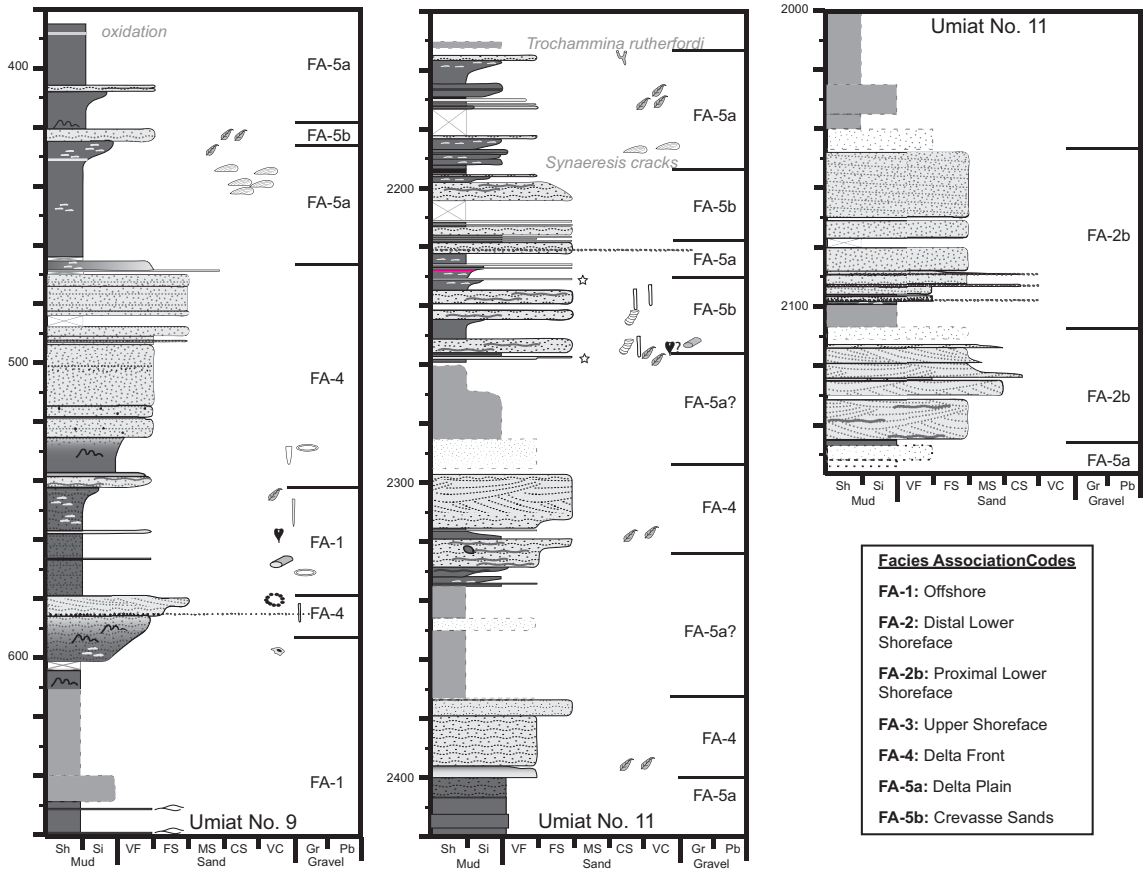

Figure 4.5 River-Dominated Facies
Delta mouth bar deposits (FA-4: Umiat No. 9) are common near the base of deltaic and non-marine deposits in the Nanushuk Formation. Overlying delta plain (FA-5a) and crevasse channels and splays (FA-5b) are also present, often with brackish water bivalves and abundant plant fossils. The transgressive Ninuluk sands (Umiat No. 11-right) have both delta front and shoreface affinities. For sedimentary structure key, see Figure 3.3a, and for trace fossil symbols, see Figure 3.4.

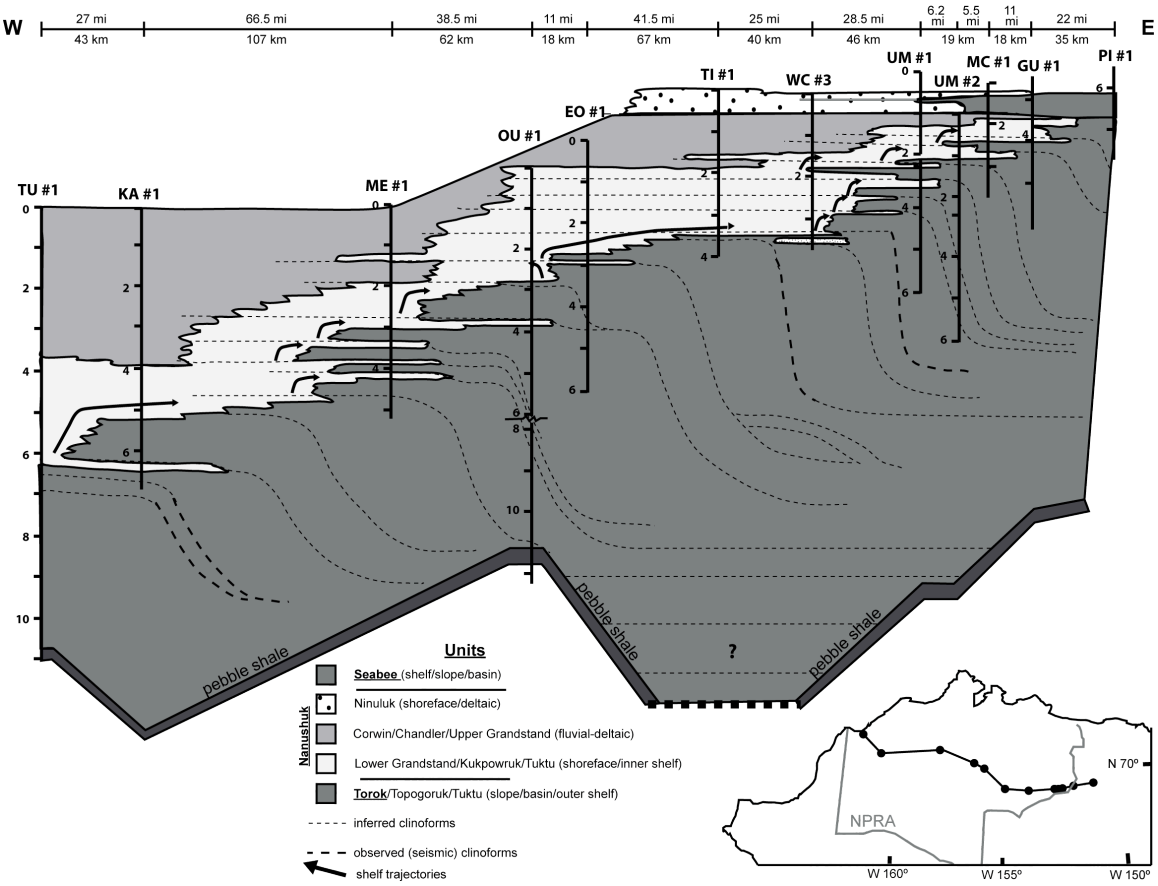

Figure 4.6 West-to-East Cross Section of the Nanushuk Formation
In this figure, modified from Molenaar (1985), shoreline trajectories show aggradational to rapidly progradational cycles in the Nanushuk Formation. The cycles are most clear in proximal shelf deposits of the lower Nanushuk Formation. The figure also shows the significant accumulation of upper Nanushuk Formation non-marine deposits to the west. Dashed clinoforms are taken from seismic data. Shelf margins are inferred, and are extended past the illustrated topset deposits to reflect uncertainty in marking of the base of the Nanushuk Formation. Codes: TU-Tunalik; KA-Kaolak; ME-Meade; OU-Oumalik; EO-East Oumalik; TI-Titaluk; WC-Wolf Creek, UM-Umiat; MC-McCulloch Colville; GU-Gubik; PI-British Petroleum Itkillik. The line of the cross section is shown on the inset map, a larger version of which appears in Figure 4.1.

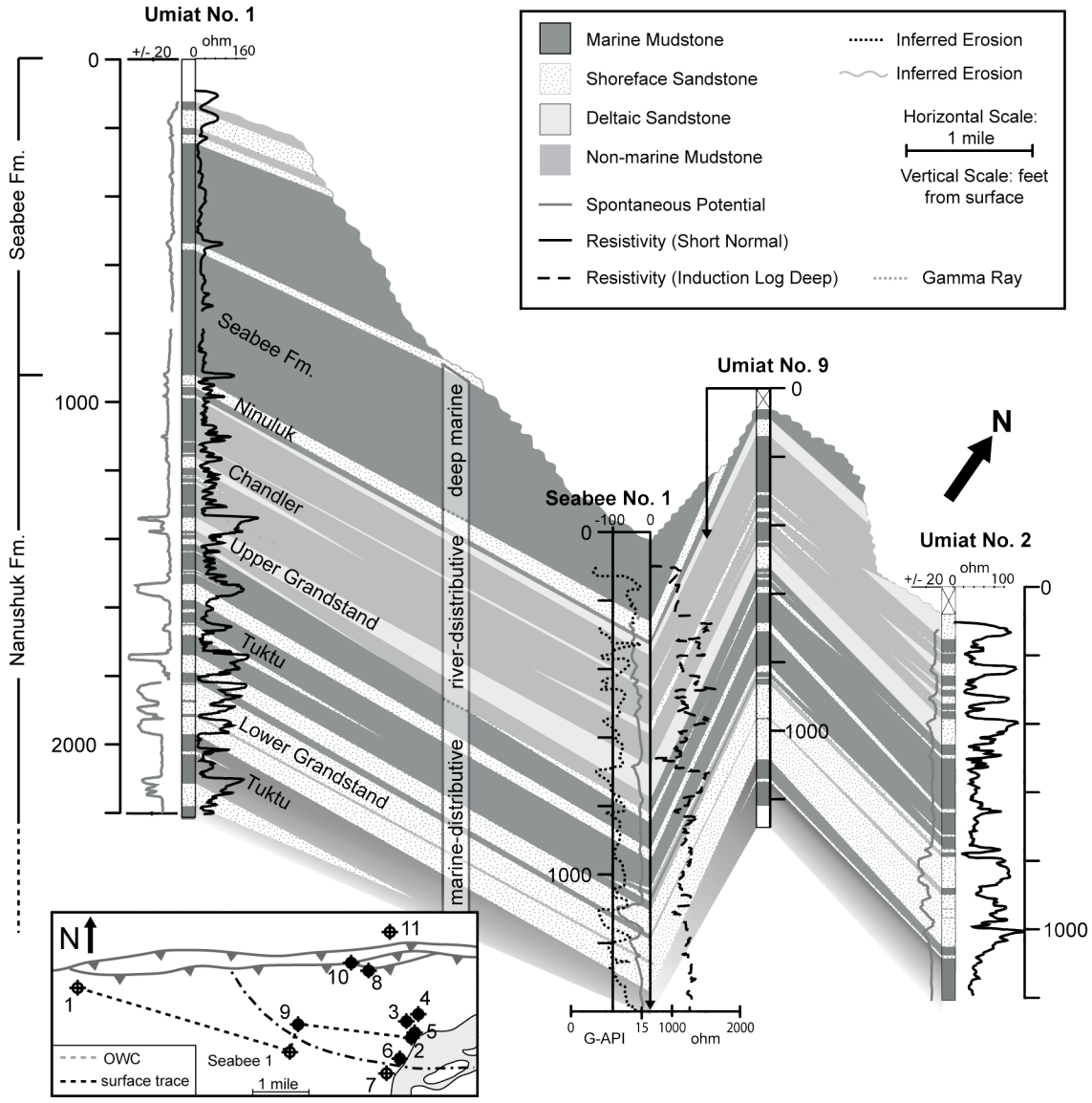

Figure 4.7 Umiat Field Fence Diagram
The Nanushuk Formation at Umiat can be clearly divided into a marine dominated lower Nanushuk and river-dominated (deltaic) upper Nanushuk. The change in depositional style occurs above a flooding surface and accumulation of shelf mudstones, shown as a tongue of the Tuktu unit, which appears as marine mudstone and sandstone between the Upper and Lower Grandstand. The grey bar in the center-left defines the boundaries of marine and deltaic units. Inset shows line of cross-section. Figure modified from Chapter 2 (Shimer et al., in press).

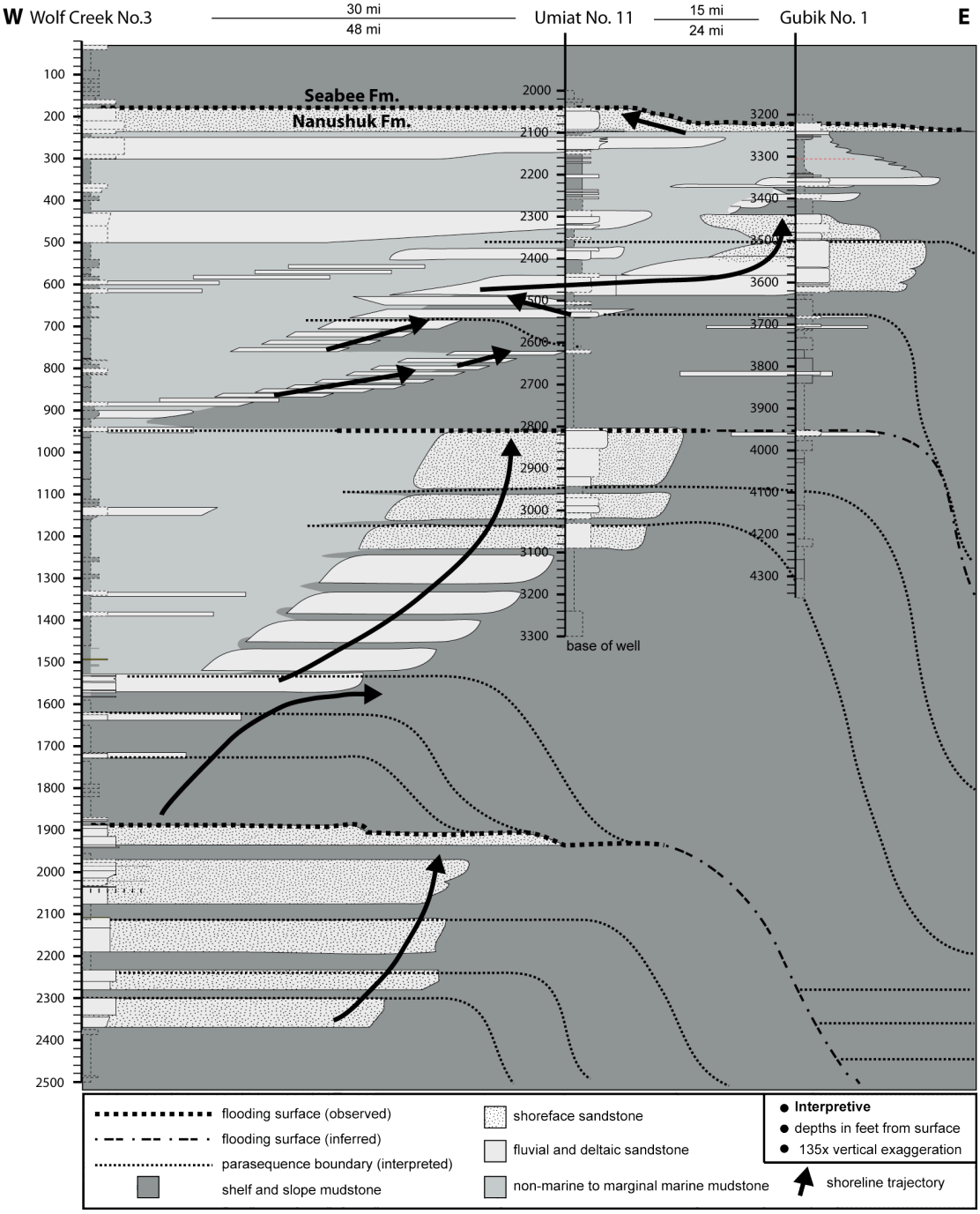

Figure 4.8 Interpretive W-E Cross Section from Wolf Creek No. 3 to Gubik No. 1
Facies and shoreline trajectory interpretations of wells in the central Brooks Range foothills. Wave-influenced facies in the lower Nanushuk Formation are associated with aggradational packages of sandstone with concave-up trajectories, while river-dominated facies of the upper Nanushuk Formation are associated with rapidly progradational, convex-up trajectories. A set of aggradational-regressive/aggradational-transgressive/and progradational-regressive trajectories make up a depositional cycle.

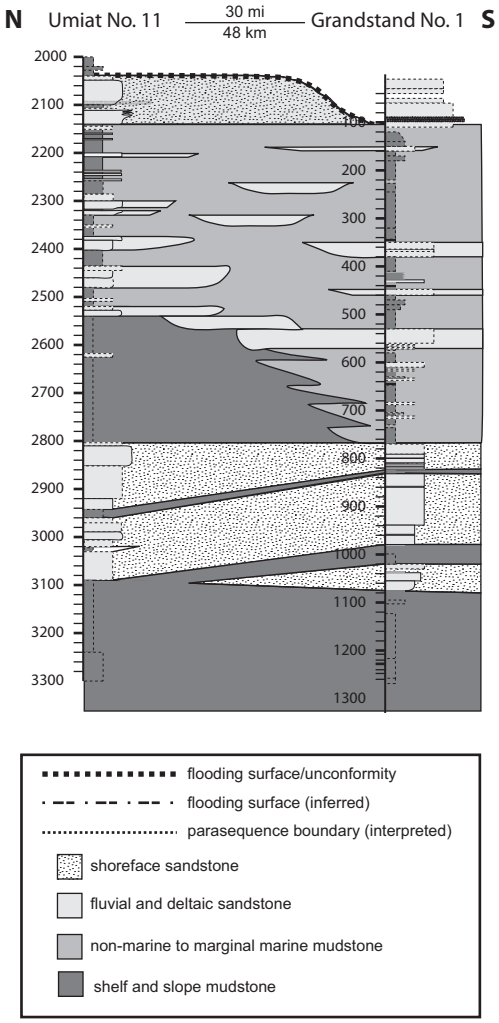

Figure 4.9 Interpretive N-S Cross Section from Umiat No. 11 to Grandstand No. 1
The Umiat wells and Grandstand No. 1 have similar stratigraphy. Umiat No. 11 was selected from Umiat Field to illustrate a complete, well-cored section through the Nanushuk Formation. In contrast to the Umiat wells, Grandstand No. 1 is more non-marine in character, with less evidence of a transgression above the lower Nanushuk Formation wave-influenced facies. This is probably due to the influence of sediment sources from the south.

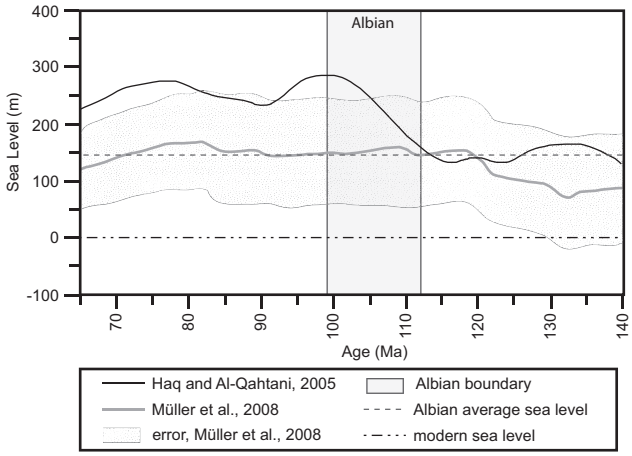

Figure 4.10 Cretaceous Sea Level
The Albian was a time of high and rising sea-level, relative to the Early Cretaceous and to modern times. The magnitude and timing of eustatic sea-level rise is subject to debate. The black curve is based on sequence stratigraphy on the Arabian plate (Haq and Al-Qahtani, 2005), and shows a rapid increase in sea level during the Albian. When corrected for ocean spreading (grey curve, with error), the eustatic sea-level curves are less dramatic, and sea-level rise begins in the Aptian, prior to the Albian. Modified from Müller et al. (2008). These discrepancies make it difficult to determine how eustatic sea-level fluctuations affected the Nanushuk Formation, but both curves show that sea level was at least 100 m higher than modern.

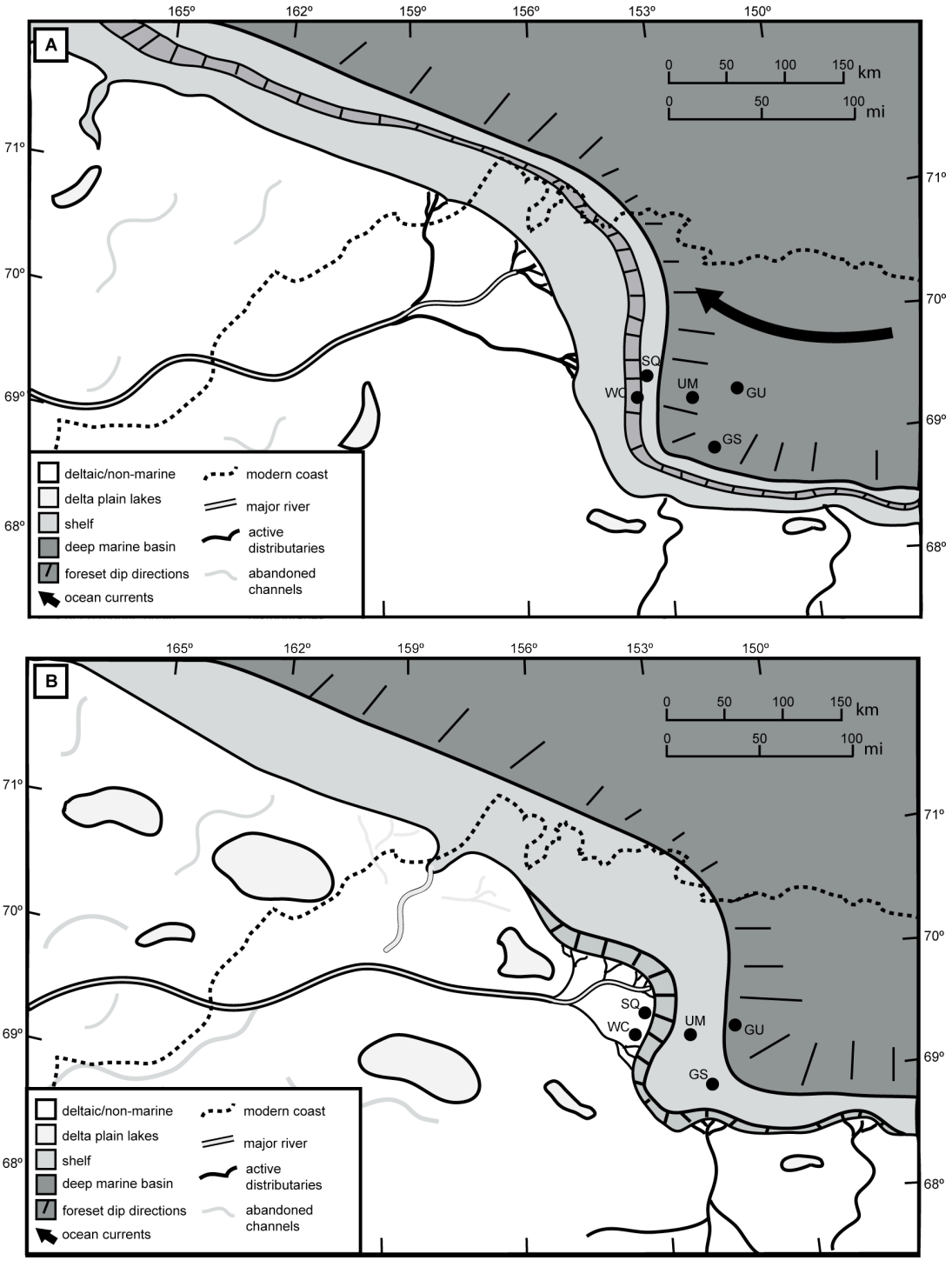

Figure 4.11 Nanushuk Formation Depositional Models
A) Albian: In a distributive environment, sediment is dispersed in broad subaqueous clinoforms on the shelf. Aggradation of these clinoforms helps build the shelf. B) Albian-Cenomanian: Once a shelf is constructed, and following possible autocyclic transgression, river-dominated deltas with steep, proximally-accumulating clinoforms prograded rapidly across the shelf.

Table 4.1 Facies Associations in the Nanushuk Formation, Central North Slope

Facies Association	Diagnostic Features	Interpretation	Depositional Systems
FA-1	Laminated shale or bioturbated mudstone (*Cruziana* ichnofacies)	Offshore/Prodelta	Suspension settling in the prodelta or the marine shelf near storm wave base
FA-2	Interbedded bioturbated mudstone (*Cruziana* ichnofacies) and upward-coarsening hummocky and swaley cross-stratified sand (*Skolithos* ichnofacies). Some sand beds obliterated by bioturbation (BI 5-6).	a. Distal Lower Shoreface	Mixed-energy shelf, above storm wave base. Deposition by suspension settling and storm-wave redistribution of sand and silt originally delivered to the coast by deltaic systems.
	Amalgamated sand beds with hummocky and swaley cross-laminated very-fine sandstone, with highly bioturbated beds (*Skolithos* ichnofacies)	b. Proximal Lower Shoreface	Storm wave deposition and redistribution of sand between fair-weather and storm wave base.
FA-3	Low-angle and trough cross-stratified, and plane-laminated fine-grained sandstone. Rare bioturbation (*Skolithos* ichnofacies)	Upper Shoreface/ Foreshore	Subaqueous bar migration above fair-weather wave base, with some swash zone deposits.
FA-4	Wavy and lenticular bedding with occasional soft sediment deformation coarsens up into ripple cross-laminated and massive sand. Bioturbation intensity and diversity low	a. Delta Front	Progradation of distributary mouth bars into muddy prodelta. Rapid deposition associated with massive sand, soft sediment deformation, low BI.
FA-5	Carbonaceous mudstone with brackish water bivalve assemblage (*Corbula*), volcanic ash deposits, and plant fossils. Closely associated with the top FA-3 and FA-4. Thin ripple cross-laminated sandstone beds <10 ft.-thick, heavily oxidized.	a. Delta Plain	Suspension settling in protected interdistributary bays or lagoons, with some tidal influence (F-7), organic matter accumulation in marshes or swamps.
	Wavy bedding coarsens up into flaser bedding and ripple cross-laminated sandstone. Beds are 5-10 ft thick. Mud-drapes are common in some sandstone beds, and are often sideritized, especially in Umiat #11. Rare mudstone rip-up clasts.	b. Crevasse Sands	Crevasse channel and splay deposits that form during flood or avulsion into interdistributary bays or the delta plain. Some tidal influence indicated by mud drapes.
	Poorly sorted sand and gravel. Sand beds fine upwards and are often massive or trough cross-laminated.	c. Distributary Channels	Incision and lateral accretion in delta distributary channels.

Chapter 5: Conclusions

This dissertation comprises three distinct but related projects focused on the Nanushuk Formation in the central Brooks Range foothills of the North Slope, Alaska. The initial motivation was to thoroughly investigate the Nanushuk Formation at Umiat Field, on the southeastern boundary of the National Petroleum Reserve – Alaska, and use what I learned in that study to identify additional research questions. The following discussion summarizes the results and conclusions of each study.

5.1 Umiat Field

There are major engineering challenges at Umiat, a shallow, frozen reservoir, so the identification and description of facies, permeability characteristics, and geometries of reservoir intervals in the Nanushuk Formation is important for the design of accurate reservoir models. Though there had been previous work at Umiat Field (Collins, 1958; Fox et al., 1979; Molenaar, 1982), the subsurface had not been described using modern techniques.

I re-examined the existing cores from the Umiat wells and defined three major Nanushuk Formation reservoir intervals at Umiat Field; Lower Grandstand A and B, and the Upper Grandstand. The Lower Grandstand intervals consist of shoreface or wave-influenced deltaic deposits, while the Upper Grandstand has characteristic features of a river-dominated delta with extensive distributary mouth bars. The three intervals are laterally continuous in the subsurface across the entire field, though the Upper Grandstand is more internally heterolithic.

Horizontal permeability (K_h) increases towards the top of each of the three reservoir units, with high-permeability zones limited to well-sorted fine- to medium-grained shoreface and delta front sandstones at the top of upward-coarsening successions. The Lower and Upper Grandstand differ in vertical permeability, however, because the delta front sandstones of the Upper Grandstand have more carbonaceous or micaceaous

laminae that create flow barriers. The resulting permeability anisotropy is predicted to be higher in the Upper Grandstand across the site.

My sedimentological and stratigraphic interpretations of the Nanushuk Formation played an important part in the evolving reservoir model and simulations for Umiat field. Umiat Field was originally estimated to contain 70 million barrels of recoverable oil (Molenaar, 1982), while recent industry assessments estimated 250 million barrels of recoverable oil (Watt et al., 2010). The UAF Umiat group used the sandstone thicknesses of the Lower and Upper Grandstand from Chapter 1 to revise the reservoir model to 1.52 of billion barrels of original oil in place (OOIP), but this model also included sandstones of the Shale Barrier which I determined to be impermeable (Levi-Johnson, 2010). The latest reservoir model used the refined facies-controlled horizontal and vertical permeability characteristics and reservoir geometries to further revise the model, and put final estimates of oil in place at 12-15% of the 1.2 billion barrels in place, or 180-225 million barrels of recoverable oil (Kohshour et al., 2013).

The geometry of the permeable sandstones has major implications for drilling techniques at Umiat. The laterally continuous nature of the Lower and Upper Grandstand reservoir units make them good targets for horizontal drilling techniques (Hanks et al., in press), and also help determine well spacing. Several new vertical and horizontal wells have been drilled or planned at Umiat since my conclusions were first reported to the U.S. Department of Energy. A new well, Umiat No. 18, penetrated a 100 ft.-thick pay zone in the Lower Grandstand. Unfortunately for Linc Energy, the new operator of Umiat field, the drilling operations experienced similar ice-related complications as earlier attempts (Lidji, 2013). The company also recovered 300 ft. of core in 2013, which will eventually be analyzed at a research facility. The successful recovery of oil-saturated core from the Lower Grandstand indicates that my assessment of the geometry and permeability characteristics of the reservoir interval were accurate.

5.2 $^{40}Ar/^{39}Ar$ Dating and Geochemistry of Cretaceous Bentonites

In Chapter 3 I investigated the geochronology and geochemistry of bentonite deposits in the Nanushuk, Seabee, Tuluvak, and Schrader Bluff formations. Radiometric ages are potentially valuable because they can be used to better constrain evolution of the Colville foreland basin throughout the Albian-Cenomanian, an age range that covers 21 million years. Age constraints are particularly important with extensive, time-transgressive progradational systems like the Nanushuk Formation.

The results presented in the Chapter 3 reinforce that $^{40}Ar/^{39}Ar$ dating of mineral phases preserved in bentonites is a promising technique, but one fraught with complications related to mixing and sorting of volcanic ash in sedimentary environments, sample size, sample composition, argon loss. Successful $^{40}Ar/^{39}Ar$ dates from the project include the first publishable radioisotopic age (102.4 ± 1.0 Ma) from the Nanushuk Formation, but many of the results were less promising. The only other geologically reasonable ages were from the base of the Seabee Formation (98.2 ± 0.8 Ma) and several samples in the Tuluvak Formation (94.4 ± 0.9 Ma; 96.6 ± 1.4 Ma; and 96.2 ± 2.0 Ma).

Unfortunately there were insufficient dates to address regional stratigraphic questions. The $^{40}Ar/^{39}Ar$ technique itself was very effective in returning precise ages, but the rate of recovery of acceptable, geologically realistic ages was less than 50%. This could be improved with more technical mineral separation procedures that would eliminate the dating of non-K bearing phases. K-bearing phases were sparse in most of the samples, and several mineral phases were improperly identified in the geochronology lab. Other samples had dates outside the range of geologically realistic ages for the formations in which they were found.

The inaccurate, older than expected ages do not represent the depositional age of the bentonite deposits, and raised the question of excess argon and contamination by detrital material or xenoliths in the mineral separates. The ages of both accurate and inaccurate dates fall conspicuously in the range of volcanic activity in the Okhotsk-Chukokta

volcanic belt (OCVB) in eastern Siberia, highlighting a possible source of the volcanic ash and xenoliths. When compared using igneous classification diagrams, all of the bentonites are from continental arc sources, and six bentonites from the Umiat wells show a trend of increasingly felsic composition from the Albian-Cenomanian. The continental arc source also compares favorably to the OCVB system, which includes a wide range of continental arc rocks of various compositions (Tikhomirov et al., 2012). These results, though not the primary goal of Chapter 3, show that the combination of $^{40}Ar/^{39}Ar$ dating and bentonite geochemistry could be used to further pinpoint the age and source of Cretaceous volcanogenic deposits on the North Slope.

5.3 Nanushuk Formation Facies and Shoreline Trajectories

In Chapter 4 I set out to identify the potential factors affecting the stacked distribution of wave (lower) and river influence (upper) in the Nanushuk Formation, specifically in the central Brooks Range foothills. This dichotomy was first recognized in the Umiat wells, and described Chapter 2. For Chapter 4 I looked at additional wells from the central Brooks Range foothills (Gubik No. 1, Grandstand No. 1, Square Lake No. 1, and Wolf Creek No. 3) to test my hypothesis that wave-influence was related to open ocean conditions during shelf progradation, while river-influence occurred when the shoreline of Nanushuk Formation was further back on the shelf.

To better deal with the regional nature of the subsurface interpretations I developed a broad classification scheme (marine-distributive and river-distributive) for the Nanushuk Formation based on dominant sediment dispersal mechanisms, as opposed to localized depositional environments. Marine-distributive systems occur where waves, tides, or currents are the dominant sediment distributary mechanism, and and where much of the sediment is deposited and reworked away from shore. In river-distributive systems, which include river-dominated deltas, autocyclic fluvial processes disperse sediment, which may be further reworked by fluvial processes on the delta or alluvial plain.

Once facies and depositional systems were identified, I applied models from previous shoreline trajectory studies to the distribution and stacking patterns of facies observed in the regional wells. I identified accretionary transgressive shoreline trajectories in wave-influenced deltas and shoreface deposits in the lower Nanushuk and normal regressive trajectories in deltaic deposits in the upper Nanushuk pointed to the affects of relative sea level and shelf bathymetry on local accommodation. The trajectories suggest that aggradation of Nanushuk and Torok formation sediments occurred in balance with high accommodation in the Colville foreland basin, and may have helped maintain the characteristic steep, north-south oriented clinoforms found in the central portion of the basin.

5.4 Additional Considerations

It is also important for me to reiterate that the core repository at the Alaska Geologic Materials Center (GMC) is a remarkable and underutilized resource for the study of the Colville foreland basin. Though field studies are preferable for identifying architectural elements and lateral relationships, core analysis is undervalued, especially considering the abundant, publicly available data resources and federal reports on the drilling efforts in the National Petroleum Reserve–Alaska. Core analyses and in-depth study of published work made this project possible, as each chapter in this dissertation made use of new core descriptions or physical rock samples from the GMC collections. I encourage future workers to take advantage of research opportunities at the GMC, especially geology students in the University of Alaska system.

5.5 References

Collins, F.R., 1958, Test Wells, Umiat Area Alaska: U.S. Geological Survey Professional Paper 305-B, p. 71-206.

Fox, J.E., Lambert, P.W., Pitman, J.K., and Wu, C.H., 1979, A study of reservoir characteristics of the Nanushuk and Colville Groups, Umiat Test Well 11, National Petroleum Reserve in Alaska: U.S. Geological Survey Circular 820, 47 p.

Hanks, C., Shimer, G., Koshour, I.O., Ahmadi, M., McCarthy, P., and Dandekar, A., 2013, Integrated reservoir characterization and simulation of a shallow, light oil, low temperature reservoir: Umiat Field, National Petroleum Reserve, Alaska: Accepted Manuscript, American Association of Petroleum Geologists Bulletin.

Kohshour, I.O., Ahmadi, M., and Hanks, C., 2013, Uncertainty assessment in geologic modeling and sensitivity analysis of static and dynamic models in Umiat: A frozen shallow oil accumulation in National Petroleum Reserve Alaska: Society of Petroleum Engineers Conference Paper, SPE Western Regional and AAPG Pacific Section Meeting, April 19-25, Moneterey, CA, DOI: 10.2118/165341-MS.

Levi-Johnson, O., 2010, Petrophysical property modeling of Umiat field, a frozen reservoir: M.S. thesis, University of Alaska Fairbanks, 129 p.

Lidji, E., 2013, Winter work done: Mechanical problem jeopardizes Umiat flow test; Linc plans that for 2014: Petroleum News, v. 18, no. 19.

Molenaar, C.M., 1982, Umiat Field, an oil accumulation in a thrust-faulted anticline, North Slope of Alaska, *in,* R.B. Powers, ed., Geologic Studies of the Cordilleran Thrust Belt: Rocky Mountain Association of Geologists, v. 2, p. 537-548.

Tikhomirov, P.L., Kalinina, E.A., Moriguti, T., Makishima, A., Kobayashi, K., Cherpanova, I.Yu., and Nakamura, E., 2012, The Cretaceous Okhotsk-Chukotka Volcanic Belt (NE Russia): Geology, geochronology, magma output ranges, and implications on the genesis of silicic LIPs: Journal of Volcanology and Geothermal Research, v., 221-222, p. 14-32.

Watt, J.S., Huckabay, A., and Landt, M.R., 2010, Umiat: A North Slope giant primed for oil development: Oil and Gas Journal, January 11, p., 30-38.

Appendix

Guide to Supplemental Materials

A. Online Data Sources

Online data was a crucial component of this project. Much of the data is from federal or state repositories. Other data came from collaborative compilations. The supplemental document summarizes each source, including its internet URL, and includes some navigational tips.

B. Stratigraphic Sections

Stratigraphic sections from wells are difficult to represent in a text due to the exceptional length of exploratory wells. It is impossible to illustrate several thousand feet of section on an 8.5 x 11 inch page with any detail. We present selected sections in all three chapters. The supplemental file is a compilation of full sections in digital (.PDF) format, and is the size of a poster.

C. Air Permeameter Data

Air permeameter data (Chapter 2) was collected during several trips to the Geologic Materials Center in Eagle River, Alaska. Not all of the data was used because the instrument did not seal properly during many tests. The tables included in the supplemental materials contain all available data.

D. $^{40}Ar/^{39}Ar$ Data

This data for this supplemental file includes all instrumental results from the $^{40}Ar/^{39}Ar$ dating process.